AD-A139 870 ONE-DIMENSIONAL MODEL HINDCASTS OF COLD ANOMALIES IN THE NORTH PACIFIC OCEAN(U) NAVAL POSTGRADUATE SCHOOL MONTEREY CA G L STRINGER DEC 83 1/2

UNCLASSIFIED F/G 8/10 NL

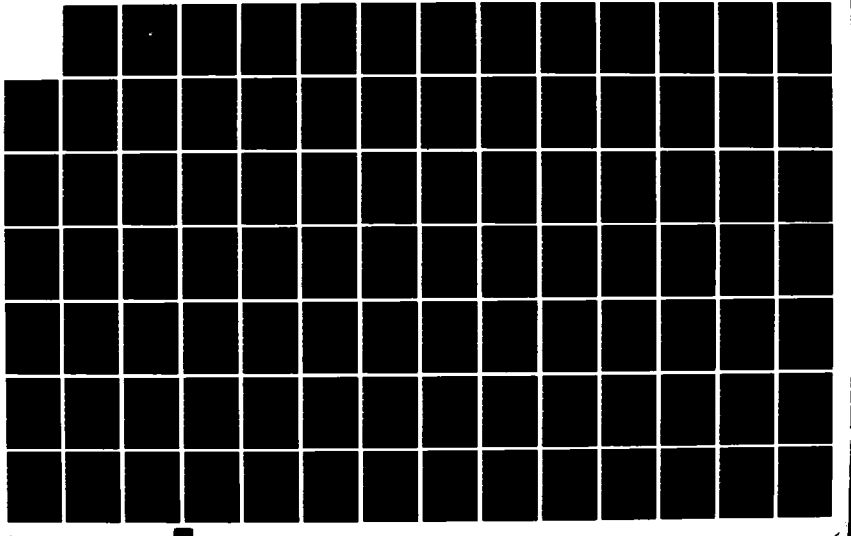

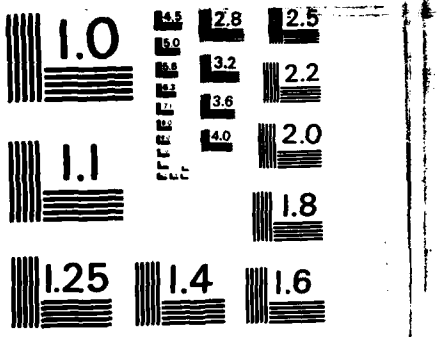

MICROCOPY RESOLUTION TEST CHART
NATIONAL BUREAU OF STANDARDS-1963-A

NAVAL POSTGRADUATE SCHOOL
Monterey, California

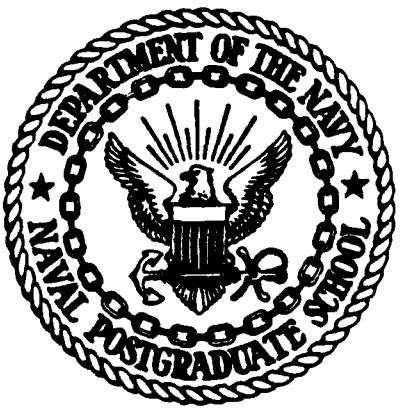

THESIS

ONE-DIMENSIONAL MODEL HINDCASTS OF
COLD ANOMALIES IN THE NORTH PACIFIC OCEAN

by

Gary L. Stringer

December 1983

Thesis Advisor: R. L. Elsberry

Approved for public release; distribution unlimited.

UNCLASSIFIED

SECURITY CLASSIFICATION OF THIS PAGE (When Data Entered)

REPORT DOCUMENTATION PAGE		READ INSTRUCTIONS BEFORE COMPLETING FORM
1. REPORT NUMBER	2. GOVT ACCESSION NO. ADA139870	3. RECIPIENT'S CATALOG NUMBER
4. TITLE (and Subtitle) One-Dimensional Model Hindcasts of Cold Anomalies in the North Pacific Ocean		5. TYPE OF REPORT & PERIOD COVERED Master's Thesis; December 1983
		6. PERFORMING ORG. REPORT NUMBER
7. AUTHOR(s) Gary L. Stringer		8. CONTRACT OR GRANT NUMBER(s)
9. PERFORMING ORGANIZATION NAME AND ADDRESS Naval Postgraduate School Monterey, California 93943		10. PROGRAM ELEMENT, PROJECT, TASK AREA & WORK UNIT NUMBERS
11. CONTROLLING OFFICE NAME AND ADDRESS Naval Postgraduate School Monterey, California 93943		12. REPORT DATE December 1983
		13. NUMBER OF PAGES 136
14. MONITORING AGENCY NAME & ADDRESS(if different from Controlling Office)		15. SECURITY CLASS. (of this report) Unclassified
		15a. DECLASSIFICATION/DOWNGRADING SCHEDULE

16. DISTRIBUTION STATEMENT (of this Report)

Approved for public release; distribution unlimited.

17. DISTRIBUTION STATEMENT (of the abstract entered in Block 20, if different from Report)

18. SUPPLEMENTARY NOTES

19. KEY WORDS (Continue on reverse side if necessary and identify by block number)

North Pacific Ocean
Cold Anomalies
One-Dimensional Model Hindcasts
TRANSPAC

20. ABSTRACT (Continue on reverse side if necessary and identify by block number)

Two cases of pronounced, long-term cold anomalies from the North Pacific Ocean Experiment TRANSPAC monthly analyses during 1976-79 are studied. The first case developed after October 1977 and persisted to June 1978. Two periods of amplification of the anomaly are identified. The second anomaly was the most extreme cold anomaly in the four-year sample. The relationships between local atmospheric

DD FORM 1 JAN 73 1473 EDITION OF 1 NOV 65 IS OBSOLETE
S/N 0102-LF-014-6601

UNCLASSIFIED
SECURITY CLASSIFICATION OF THIS PAGE (When Data Entered)

(20. ABSTRACT Continued)

forcing, and the development, existence and decay of the anomalies are examined with the Garwood ocean mixed layer model. In the first case, the fall deepening period was hindcast very well. However, the period of spring transition and seasonal warming were not well predicted. It is deduced that the most likely cause of the errors is inaccurate atmospheric forcing. In the second case, the model predictions are very sensitive to the surface heat flux. This anomaly cannot be satisfactorily simulated with the Garwood model. This appears to be due to large uncertainties in the surface heat flux fields in the summer.

Approved for public release; distribution unlimited.

One-Dimensional Model Hindcasts of Cold Anomalies in the North Pacific Ocean

by

Gary L. Stringer
Lieutenant Commander, United States Navy
B.S., University of Washington, 1975

Submitted in partial fulfillment of the
requirements for the degree of

MASTER OF SCIENCE IN METEOROLOGY AND OCEANOGRAPHY

from the

NAVAL POSTGRADUATE SCHOOL
December 1983

Author: Gary L. Stringer

Approved by: Russell L Elsberry
Thesis Advisor

Second Reader

Chairman, Department of Meteorology

Dean of Science and Engineering

ABSTRACT

Two cases of pronounced, long-term cold anomalies from the North Pacific Ocean Experiment TRANSPAC monthly analyses during 1976-79 are studied. The first case developed after October 1977 and persisted to June 1978. Two periods of amplification of the anomaly are identified. The second anomaly was the most extreme cold anomaly in the four-year sample. The relationships between local atmospheric forcing, and the development, existence and decay of the anomalies are examined with the Garwood ocean mixed layer model. In the first case, the fall deepening period was hindcast very well. However, the period of spring transition and seasonal warming were not well predicted. It is deduced that the most likely cause of the errors is inaccurate atmospheric forcing. In the second case, the model predictions are very sensitive to the surface heat flux. This anomaly cannot be satisfactorily simulated with the Garwood model. This appears to be due to large uncertainties in the surface heat flux fields in the summer.

TABLE OF CONTENTS

LIST OF TABLES

LIST OF FIGURES

ACKNOWLEDGEMENTS

The author would like to thank Drs. Warren White and Buzz Bernstein for providing the TRANSPAC analyses of ocean thermal structure. The data archiving division of Fleet Numerical Oceanography Center provided the atmospheric forcing fields. Appreciation is due to Dr. Roland Garwood who provided the ocean mixed layer prediction model. Miss Arlene Bird deserves thanks for her assistance in computer programming. A special thank you goes to Mr. Pat Gallacher for interpolating the FNOC atmospheric forcing fields, providing valuable comments and assistance during the study and for his review of the manuscript. The computing was done at the W.R. Church Computer Center.

The author would like to express his sincerest gratitude and appreciation to Dr. Russ Elsberry for the time and effort he has spent assisting in the defining and analysis of this study, and in the preparation of this thesis.

Finally, and most importantly, I want to give my heartfilled love and thanks to my wife, Linne; without her support and encouragement this thesis would not have been possible.

I. INTRODUCTION

A. PURPOSE AND HYPOTHESIS

The purpose of this study is to test the applicability of the Garwood (1977) one-dimensional bulk mixed layer model for hindcasting the cold ocean thermal anomalies found in the Anomaly Dynamics Study (ADS) domain. Elsberry (1983) describes numerous cold anomalies and selects several anomalies that are particularly suitable for testing ocean prediction models. Two of these cold anomalies were chosen for this study. The ability to predict departures from climatology provides a useful test of a model's capabilities relative to either a persistence or a climatological (zero anomaly) forecast. The study of anomalies also lends insight into the large-scale variability of the ocean thermal structure. A second purpose of this study is to demonstrate the usefulness of the corrections derived by Elsberry et al. (1982) to Fleet Numerical Oceanography Center (FNOC) surface heat flux estimates in North Pacific Ocean predictions. These corrections are necessary to offset a systematic bias in the FNOC heat fluxes which was discovered in the prediction experiments of Elsberry et al. (1979), Budd (1980) and Steiner (1981).

The seasonal variation in heat content of the upper ocean, away from the major current systems, is primarily

determined by the net heat flux across the ocean-atmosphere interface. This heat is distributed in the vertical almost exclusively by turbulent mixing. During and after the formation of the seasonal thermocline, the gradual increase in the solar flux tends to be offset by upward surface heat fluxes and increases in entrainment mixing associated with strong atmospheric storms. That is, a decrease in sea-surface temperature is found during periods of higher wind speeds (Elsberry and Garwood, 1978). These higher wind events occur less frequently during the spring and summer. The balance between periods of net warming and net cooling is in favor of increasing sea-surface temperature from the spring transition until early autumn. After this time, the net surface cooling and entrainment mixing associated with strong storms reverses the balance, and the sea-surface temperature decreases. Superposed on these seasonal trends are periods with above or below normal temperatures.

Anomalous sea-surface temperatures can be caused by anomalous solar radiation and surface heat fluxes or by anomalous entrainment heat flux at the mixed layer base generated by wind stirring and convective overturning (Elsberry and Garwood, 1978) and by horizontal advection, Ekman pumping and upwelling. The basic hypothesis of this study is that near-surface cold temperature anomalies in the North Pacific Ocean during 1976-1978 were primarily generated by local vertical mixing processes.

B. STUDY DESCRIPTION

An objective of the North Pacific Ocean Experiment (NORPAX) was the study of the interaction between large-scale ocean temperature anomalies and weather. One observational component of NORPAX was a ship-of-opportunity expendable bathythermograph (XBT) program (TRANSPAC) designed to observe the ocean thermal structure on space scales of thousands of kilometers (White and Bernstein, 1979). The TRANSPAC analyses provide the initial and verifying temperature profiles that are required to validate ocean prediction models (Elsberry and Garwood, 1980). Because all of the TRANSPAC observations made within a particular month are used in the objective analysis, this defines the time and space scales for the initialization and verification of the model.

The NORPAX ADS area (Fig. 1) is the oceanic region examined in this study. The ADS region is bounded by 30°N-50°N and 130°W-160°E and encompasses midlatitude regions that contain large-scale thermal anomalies. This region also has strong atmospheric variability. In this study, two cold anomalies are examined. The first is a large-scale, long-duration event that began in the fall of 1977, and extended into the spring of 1978 in the vicinity of 36°N, 150°W. The second anomaly is a shallow, large-scale, rapid transition event occurring in the summer of 1976 in the vicinity of 40°N, 165°E. These two anomalies provide an

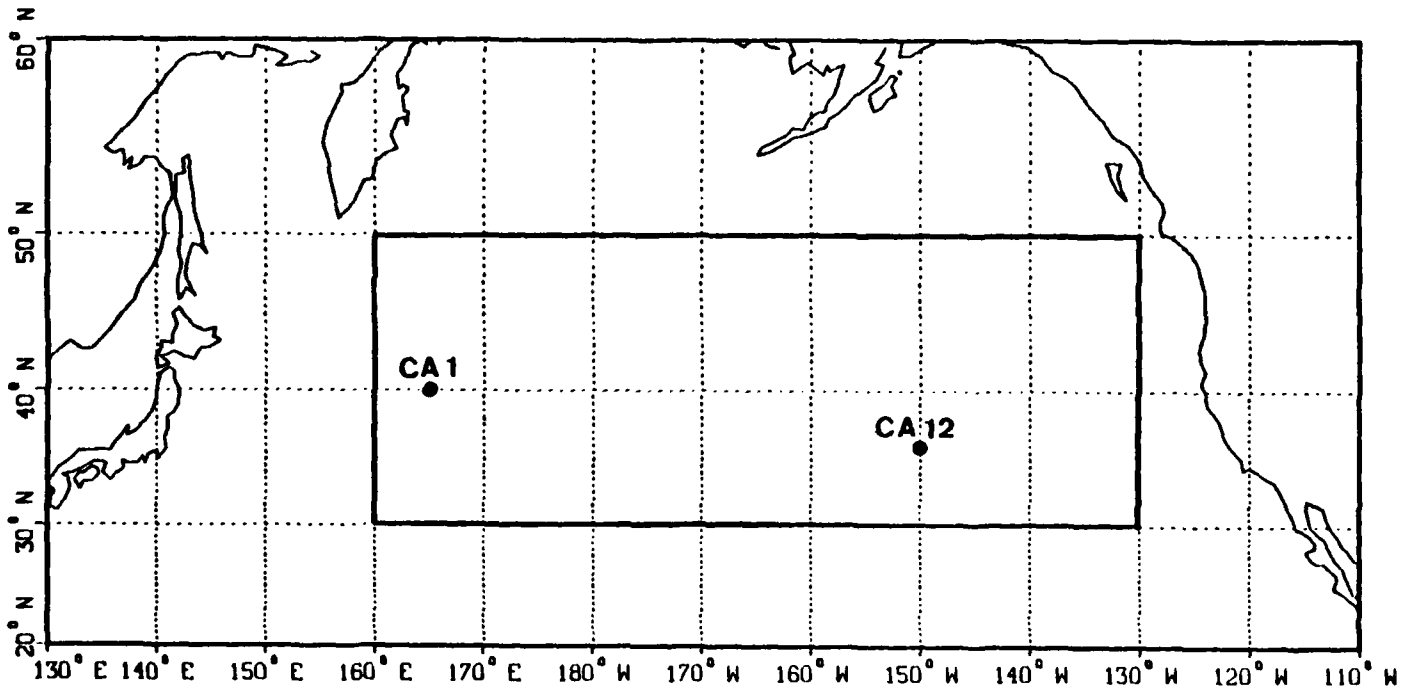

Figure 1. Anomaly Dynamics Study region. Points at 36°N, 150°W and 40°N, 165°E mark the location of maximum intensity for the two anomalies examined.

opportunity to test the Garwood model and the vertical mixing hypothesis.

C. DEFINITIONS

Several terms that will be used throughout this thesis are defined and discussed in this section.

1. Spring Transition

The transition from a winter mixed layer regime to a summer regime occurs during the spring, when the occurrence and magnitude of storms (and thus high wind speeds) are diminishing and the net daily insolation is increasing. The increase of absorption of solar radiation in the near-surface layers promotes stability.

Tully and Giovando (1963) noted that the spring transition appeared to be rapid. Elsberry and Garwood (1978) combined an oceanic model simulation and observations to demonstrate that the spring transition can occur during a single daytime heating cycle. Budd (1980) reported that the spring transition usually occurred within a 36-hour period; however, the time period for transition was longer for steady wind conditions. The key synoptic feature initiating the transition is an extended period of light winds coinciding with a period of net downward heat flux (Elsberry and Raney, 1978). A layer of warmer (less dense) water near the surface is established during the diurnal heating cycle. If the mechanical generation of turbulent kinetic energy is sufficiently small, the layer will remain intact

through the night. A repetition of this cycle through the next several days can lead to the formation of the seasonal thermocline.

A set of criteria based on the mixed layer depth and temperature was used to determine when the ocean boundary layer changed from a winter to a summer regime (similar to Budd, 1980). The transition period was defined as the first period of sustained shallow mixed layer depths (<40 m) that followed a period of greater than 80 m depths. Occasionally the predicted and/or analyzed depths may later exceed 80 m for a short period a week or more after the establishment of the stable layer. Consequently, the transition period was specified as that period which also coincided with a significant increase in mixed layer temperature. As the TRANSPAC temperature analyses were available monthly, only an approximate time frame can be given for the spring transition.

2. Mixed Layer Depth

There is no consensus method for determining the mixed layer depth of a vertical temperature profile. Various definitions have been applied in different studies depending on the requirements (operational or research) and profile resolution. In this study, the mixed layer depth has been defined to be that depth at which the vertical temperature gradient exceeds 0.10°C/5m. For regions with a very slight

negative gradient above a marked thermocline and for which the criteria of 0.1°C decrease in 5 m was too stringent, the mixed layer depth was manually determined from the vertical temperature profile. This was done to reduce any bias in mixed layer depth due to definition as found by Steiner (1981).

In the Garwood model, a minimum mixed layer depth of 5 m was set. This is consistent with the analyses, as the wake turbulence of a ship from which an XBT was launched would destroy an shallow (<5 m) surface layer(s), and thus these layers would not be present in the analyses. The maximum model mixed layer depth was set at 190 m to prevent the model vertical profiles from becoming isothermal.

II. DATA SOURCES AND PROCEDURES

A. DATA SOURCES

This study is based on data between January 1976 and December 1979 from two separate sources. The FNOC atmospheric forcing and TRANSPAC temperature analyses are over the ADS domain bounded by 30°N, 50°N, 130°W and 160°E. The grid resolution is 2° latitude by 5° longitude.

Atmospheric forcing data (wind speed and direction, solar heat flux and total surface heat flux) were obtained from the archived FNOC northern hemispheric atmospheric analyses and short-term predictions. The wind components were available at six-hour intervals, and the solar and total surface heat (latent plus sensible plus back radiation minus solar) flux values at 12-hour intervals. The Garwood model requires atmospheric forcing fields on hourly time scales to resolve the oceanic response to the diurnal heating cycle. Garwood (1977) found that this diurnal component can modulate the seasonal trend. A complete description of the procedures and programs for editing and interpolating the forcing fields to one-hour intervals is in Gallacher (1979).

The TRANSPAC data sources and analysis procedures are described in White and Bernstein (1979). XBT observations were made by ship-of-opportunity personnel along ship

tracks between Japan and the west coast of the United States. Due to ships tending to avoid rough weather there is a seasonal and a "fair weather" bias in the data. During the summer, the ship tracks are farther north and there is good data coverage over the domain. However, the northern part of the domain is not well sampled during the winter. It was found that the northwest and the southwest corners of the grid were not well sampled (Elsberry, 1983). Consequently, these areas are excluded in this study and will appear as cross-hatched areas on all appropriate figures.

The XBT profiles have been objectively analyzed at depths of 0, 30, 60, 90, 120, 150 and 200 m. These objectively analyzed fields produced by White and Bernstein (1979) are not vertically coupled. Since the analyzed temperature profiles are available monthly, they are taken to be representative of the "observed" temperature profile on the 15th of the month. To assure a continuous record, wherever minor data gaps existed along the edge or in the interior of the ADS grid, time and space interpolations were made at 0, 60, 120 and 200 m (Elsberry, 1983). Since data gaps were not removed in the analysis at the other analyses levels, only the analyses at 0, 60 and 120 m were used to describe the horizontal temperature anomaly structure. The horizontally edited values at the above levels, plus objectively analyzed values (if present) at 30, 90 and 150 m, were then vertically interpolated to a

5 m spacing between 0 and 200 m. These gridded monthly oceanic temperature fields were used to initialize the model simulations and to verify the model output.

The following comments should be kept in mind during subsequent discussions of the analyses over the entire domain. Due to the sparse ocean data, differences between the Garwood model predictions and the TRANSPAC observations of less than 0.5°C are probably not significant (Budd, 1980). The baseline study conducted by White and Bernstein (1979) indicated that the region west of 175°W was dominated by strong mesoscale (300 km) baroclinic eddies or waves, whereas east of 175°W the larger scale variability dominated. The temporal and spatial data coverage and the 2° latitude by 5° longitude grid interval are inadequate to resolve eddies in the region west of the dateline and in the California current. Furthermore, the analyses in regions north of 45°N and south of 35°N are less reliable due to the seasonal variation in data coverage (Elsberry, 1983).

B. MEAN AND ANOMALY FIELDS

The monthly mean temperature (climatological) fields used in this study are an average of the TRANSPAC monthly objectively analyzed fields over the four years, 1976-1979. These mean temperature fields are based only on the TRANSPAC vertical temperature profiles, and do not include any other source of temperature observations. The advantage of the

four-year mean is that the analysis method is consistent in both the mean and the anomaly fields (Elsberry, 1983). The disadvantage is that the anomaly fields will differ from those generated using the long-term NORPAX mean fields (Barnett and Ott, 1976). This is particularly true because two of the four winter periods (1976 and 1977) include extreme conditions in the Central Pacific (White and Bernstein, 1979; Elsberry et al., 1979; White et al., 1980; Haney, 1980; Budd, 1980). Thus cold anomalies during these winters have a smaller magnitude in this study than in the NORPAX fields. Elsberry (1983) found that there is an overall trend toward a warm bias in the four-year surface TRANSPAC mean fields relative to the long-term Barnett and Ott (1976) fields.

The anomaly fields were formed by subtracting the four-year mean (climatological) fields from the analyzed fields at 0, 60 and 120 m. The resulting horizontal anomaly fields are taken to be the anomalous conditions on the 15th of the month.

C. PREDICTION MODEL

The Garwood (1977) ocean mixed layer model is a second order closure bulk model. Since the model is one-dimensional, no advection or Ekman dynamics are included. A more complete description of the Garwood model is contained in the Appendix.

The Garwood model is initialized with the initial (TRANSPAC objectively analyzed) temperature profile fields for the 15th of the month. The model is used to predict the evolution of the oceanic thermal structure over the ADS area due to local surface forcing. The model predicts vertical temperature profiles in 5 m increments to 200 m over the entire grid every hour. For this study, the model output consists of the vertical temperature profiles averaged over 5 days centered on the 15th of each month, and the mixed layer temperature at the time of maximum mixed layer depth for each day.

The model anomaly fields were formed by subtracting the four-year mean (climatological) fields from the model predicted fields at 0, 60 and 120 m. The resulting horizontal model anomaly fields are taken to be representative of the conditions on the 15th of the month.

III. LARGE-SCALE LONG-DURATION CASE

A. COLD ANOMALY 12 DESCRIPTION

The cold anomaly (CA) described below was designated and described by Elsberry (1983) as CA 12. CA 12 is a large-scale, long-duration event which persisted for approximately eight months and encompassed a vast region of the ADS grid.

The entire domain had above average temperatures during October 1977 (Fig. 2A). For orientation purposes, the ultimate location of maximum intensity or central point (36°N, 150°W) for CA 12 is marked as a dot on the applicable figures. Starting in November 1977 (Fig. 2B), CA 12 began to develop at the surface in the northeast region. The temperature decreases in this region are noteworthy relative to the climatological cooling during this period. In the northeast region, which changed from a warm to cold anomaly between October and November 1977, the surface temperature decrease was greater than 1.5 times the climatological decrease (Fig. 3). The cold anomaly continued into December 1977 (Fig. 4); however, the temperature decrease was almost the same as climatology. At this time, the majority of the region had below normal temperatures and the anomaly had penetrated 60 m (Fig. 4). From December 1977 to January 1978 (Fig. 5), the rate of temperature decrease (Fig. 6) slowed to half that of climatology

in the northeast region, whereas the rate increased to 1.5 times climatology in the southeast region as the anomaly expanded southward.

The anomaly continued to increase in amplitude and spatial extent between January and March 1978. Temperature decreases became more erratic over the area during this period. The vertical structure of CA 12 during January 1978 and March 1978 is shown in Figs. 5 and 7. The cold anomaly penetrated to 120 m in January 1978. A warm anomaly, extending to 120 m, was found along the eastern boundary in January 1978. This resulted in an anomaly pattern with a north-south orientation. During February (not shown) and March 1978 this warm anomaly extended westward in the vicinity of 44°N, 140°W. Thus CA 12 had a maximum amplitude in the southeast region. During March 1978, CA 12 reached maximum intensity (-1.91 °C at 36°N, 150°W) and areal extent. The western anomaly pattern in the vicinity of 38°N, 170°E in March 1978 was due to the formation of CA 18 (Elsberry, 1983) which persisted throughout the remainder of the existence of CA 12.

The vertical structure for April through June 1978 is shown in Figs. 8 to 10. The anomaly amplitude diminished from March to April 1978. During this period, the temperature in the vicinity of the central point increased at a rate (not shown) of 1.5 times the climatological rate as this area underwent spring transition. However, the

temperature in the eastern portion of the region remained below normal through June 1978 (Figs. 8-10). Through that time, the anomaly center was maintained but the pattern changed shape. From April to May 1978 the surface features of the anomaly became more diffuse, but the anomaly amplitude at 60 m showed little change. The most rapid surface temperature increase took place during these two months (Fig. 11); it was associated with the very late spring transition throughout the remainder of this region (Elsberry, 1983). In the region of CA 12, the temperature increase during May to June 1978 was much the same as the expected climatological increase (Fig. 12). However, the region of CA 18 increased in temperature at twice the climatological rate. In May 1978 the surface signature of CA 12 was absent, although there was a 10° longitude westward displacement of minimum temperatures at 60 and 120 m. By June 1978 (Fig. 10), the cold anomaly 12 became diffuse at 60 and 120 m, but interestingly, it intensified again at the surface. In June 1978, there was substantial vertical tilt between the surface and 60 m but not between 60 and 120 m. After July 1978 (not shown), the region was generally cold throughout the remainder of the year and periods with above normal temperatures did not persist (Elsberry, 1983).

In summary, CA 12 was a long-duration, large-scale event with multiple periods of amplification followed by sustaining periods. The location and minimum temperature

for CA 12 each month is given in Table 1. CA 12 formed between October and November 1977 at about 44°N, 145°W and was only sustained by the expected cooling during the southward expansion in December 1977. In January 1978 the anomaly progressively expanded southward. The anomaly reached its maximum amplitude and areal extent in March 1978. By April 1978, the anomaly reached its southern most location (32°N, 155°W) and had started to diminish in size and amplitude, although portions of the regions remained colder than climatology for several months. In May 1978, the surface signature of the anomaly disappeared. In June 1978, CA 12 was displaced northward to about 38°N, 155°W and the signature of the anomaly had all but disappeared at depth and had reappeared at the surface. This cold anomaly was clearly a major climatolgoical event.

These changes in the analyzed strength of CA 12 (Table 1) could be due to several effects: (1) atmospheric forcing pulses due to localized atmospheric effects; (2) oceanic response to seasonal climatic changes; (3) anomaly-anomaly interactions; and (4) advection effects resulting from Ekman and/or Sverdrup mass transport. An effect of the above physical mechanisms is that CA 12 could be interpreted as being composed of several consecutive cold anomalies that have monthly life spans and appear in a region that is anomalously cold. It is not possible to separate completely the above effects with the available data.

TABLE 1

Comparison of analyzed CA 12 and model MA 12 development for each month. The locations and temperatures given are the location of the lowest temperature in CA 12 and MA 12 for each month.

		ANALYSIS		MODEL	
Month	Year	Location	Temperature	Location	Temperature
Nov	1977	44°N,145°W	-1.63°C	46°N,140°W	-2.51°C
Dec	1977	40°N,145°W	-1.61°C	(1) 46°N,140°W	-1.69°C
				(2) 30°N,155°W	-1.48°C
Jan	1978	38°N,145°W	-1.36°C	(1) 46°N,140°W	-1.99°C
				(2) 34°N,155°W	-2.14°C
Feb	1978	34°N,145°W	-1.76°C	34°N,150°W	-2.23°C
Mar	1978	36°N,150°W	-1.91°C	34°N,150°W	-2.15°C
Apr	1978	32°N,155°W	-1.85°C	30°N,155°W	-3.10°C
May	1978	34°N,150°W*	-1.31°C	30°N,150°W	-2.65°C
Jun	1978	38°N,155°W	-1.65°C	36°N,150°W	-3.79°C

* at 60 m

There may be some tilt present in the vertical structure of the anomalies. These tilts will not be examined here because the objective analysis of the temperature field is done independently at each level, and the horizontal resolution of these analyses is not appropriate. The next section describes the model hindcast of CA 12.

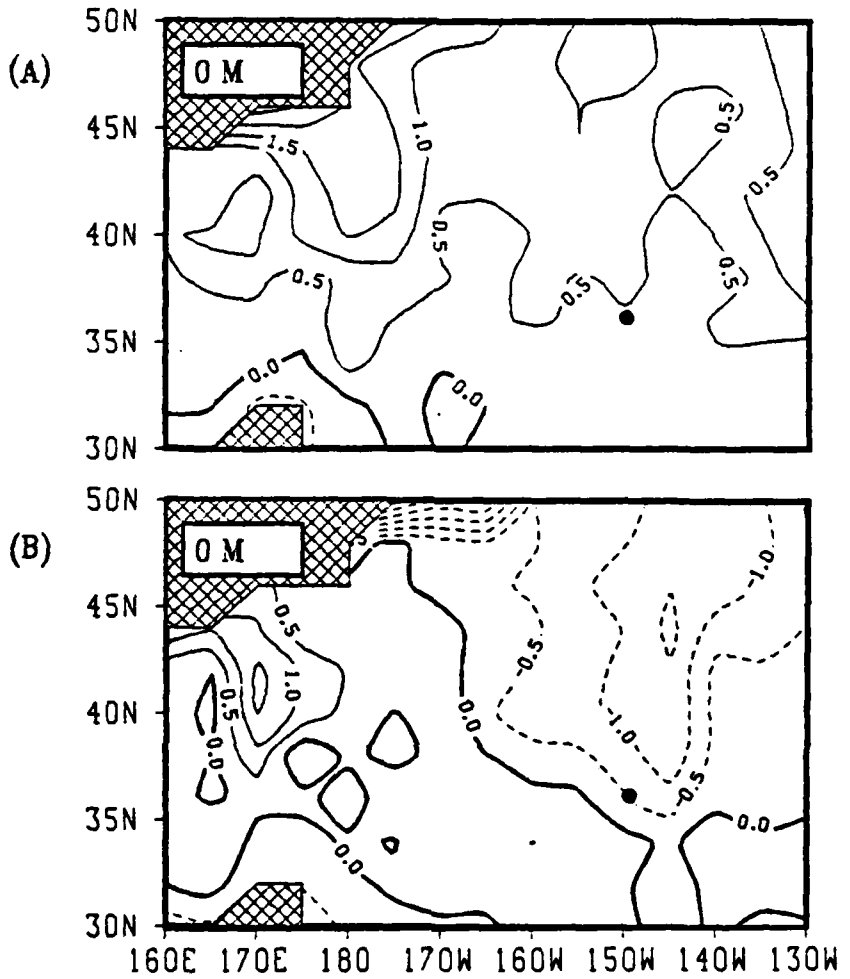

Figure 2. Temperature (°C) anomaly CA 12 at surface during (A) October 1977 and (B) November 1977. The horizontal temperature analysis for each month is centered on the 15th of that month. Negative (dashed) lines represent regions with temperatures less than climatology, zero (heavy solid) same as climatology and positive (light solid) temperatures greater than climatology. The interval is 0.5 °C. Cross hatched areas have insufficient data for analysis. Dot marks the ultimate location of maximum intensity or central point (36°N, 150°W) for CA 12.

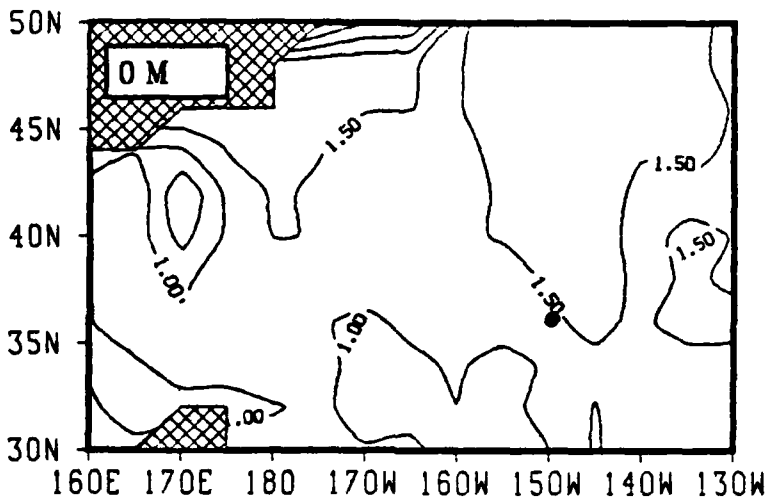

Figure 3. The ratio of change in analyzed temperatures (°C) from 15 October to 15 November 1977 to the climatological temperature change for the same period. Values greater than 1.0 during this period indicate above-average temperature decreases.

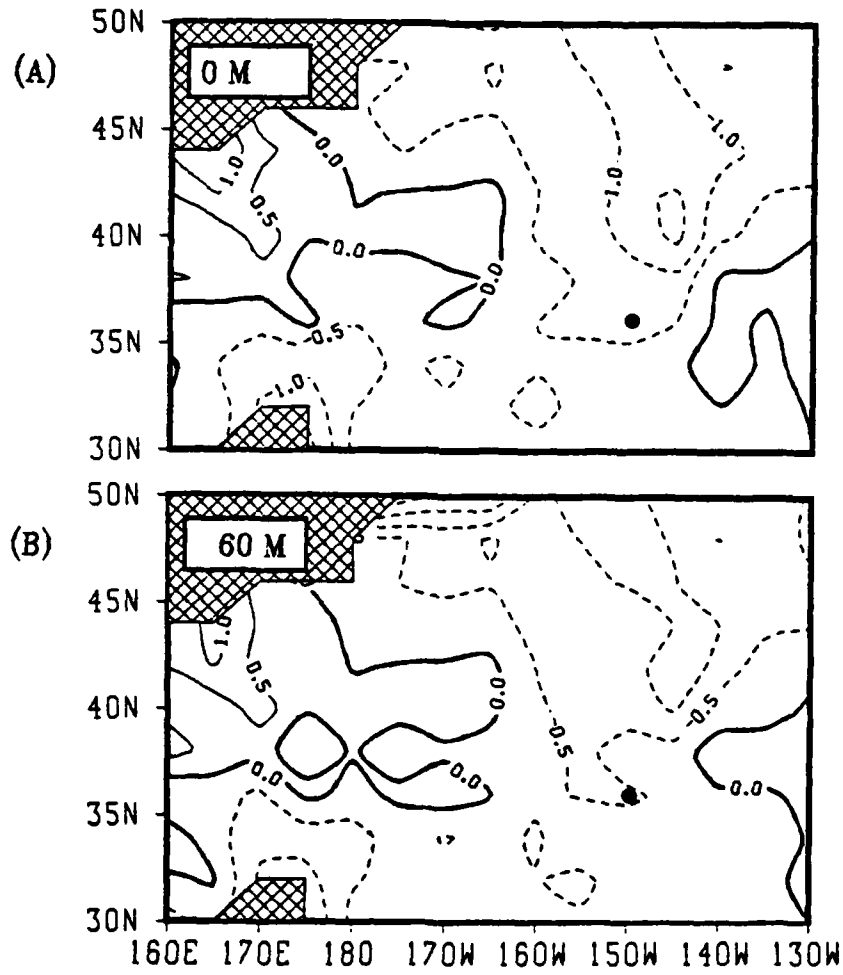

Figure 4. Temperature (°C) anomaly CA 12 during December 1977 at (A) surface and (B) 60 m.

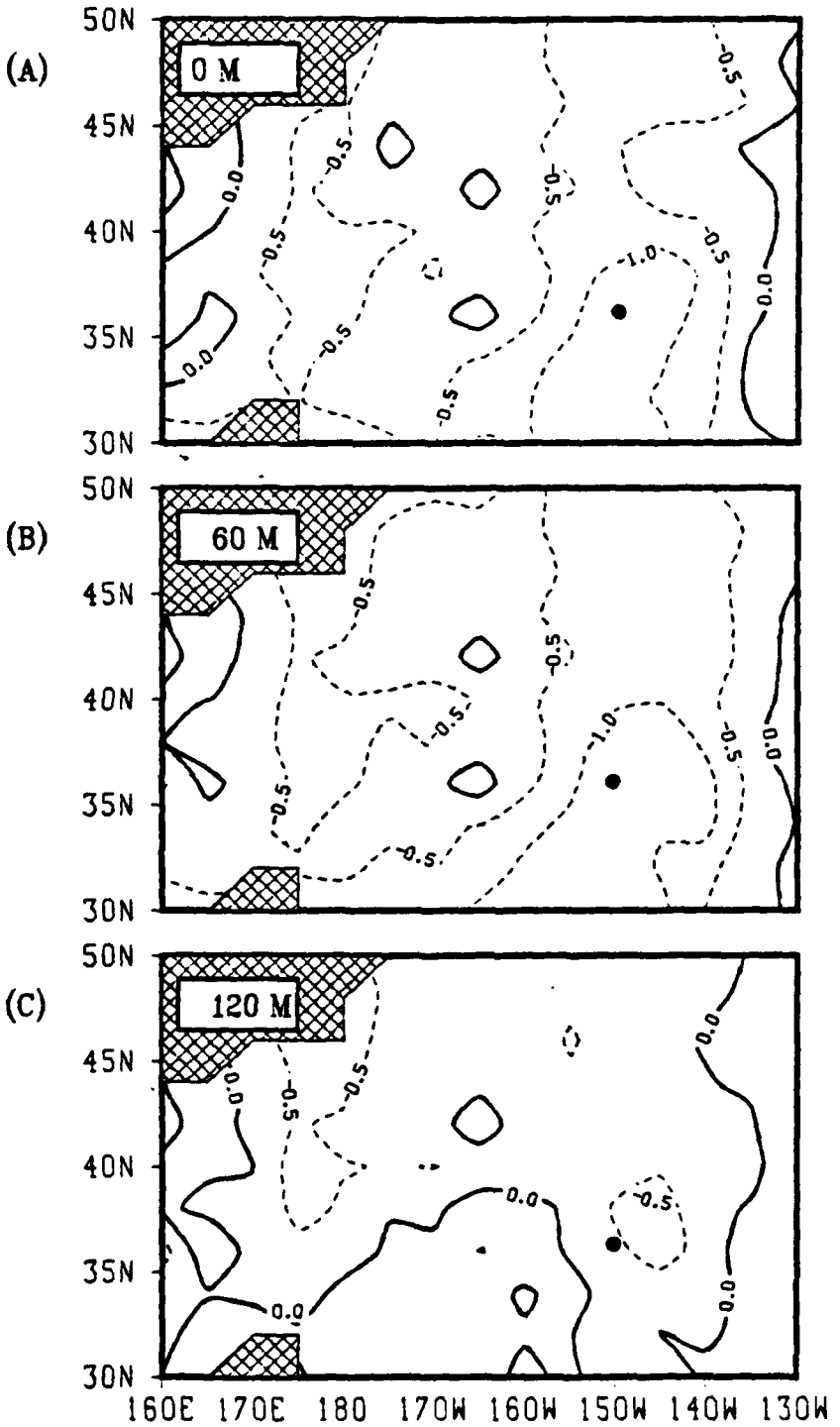

Figure 5. Temperature (°C) anomaly CA 12 during January 1978 at (A) surface, (B) 60 m and (C) 120 m.

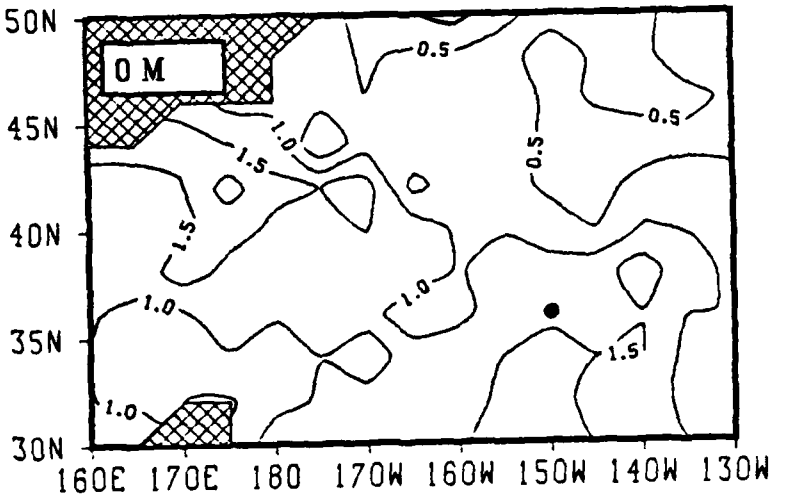

Figure 6. Similar to Fig. 3 except for the period from 15 December 1977 to 15 January 1978.

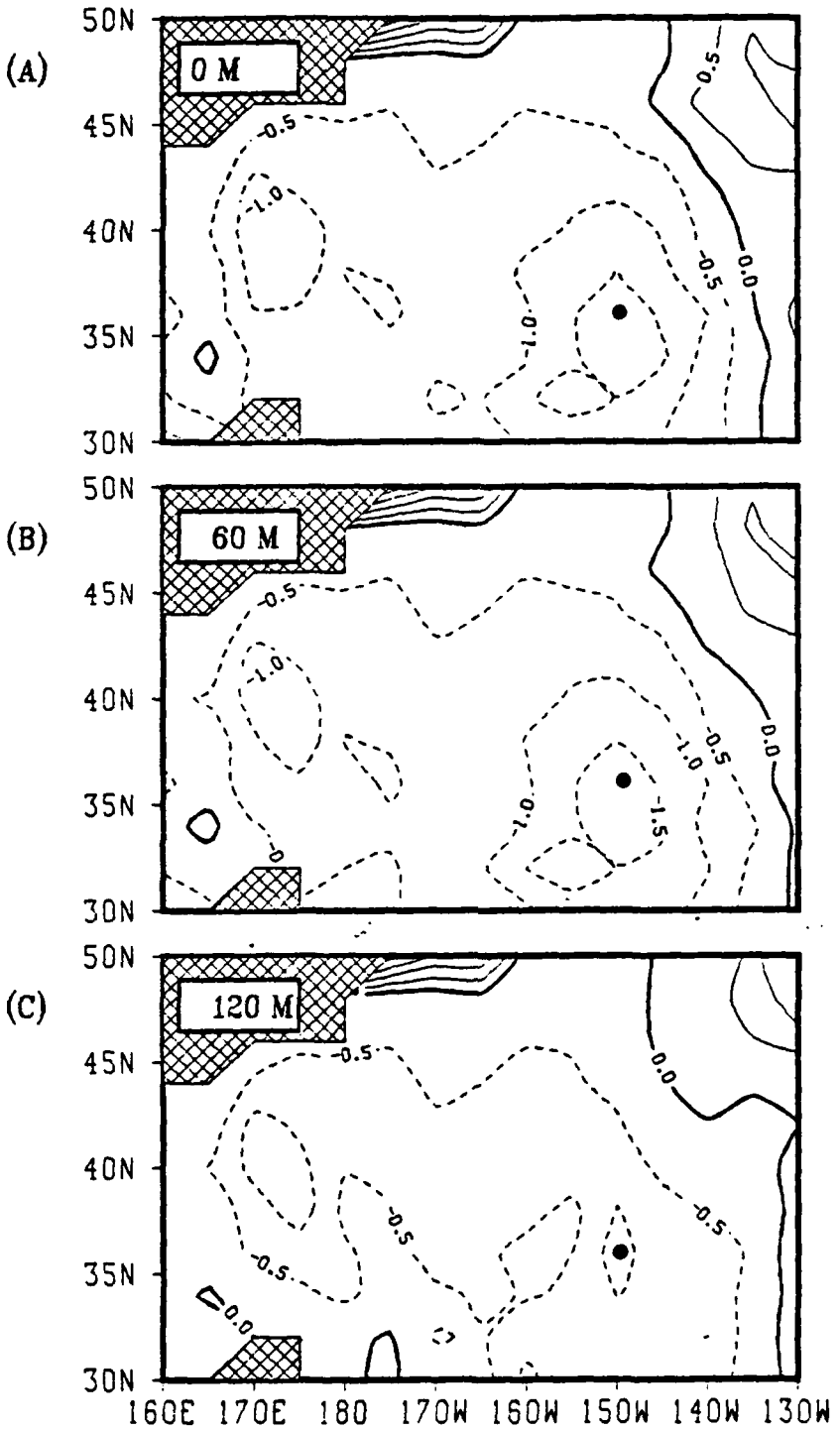

Figure 7. Similar to Fig. 5 except for March 1978.

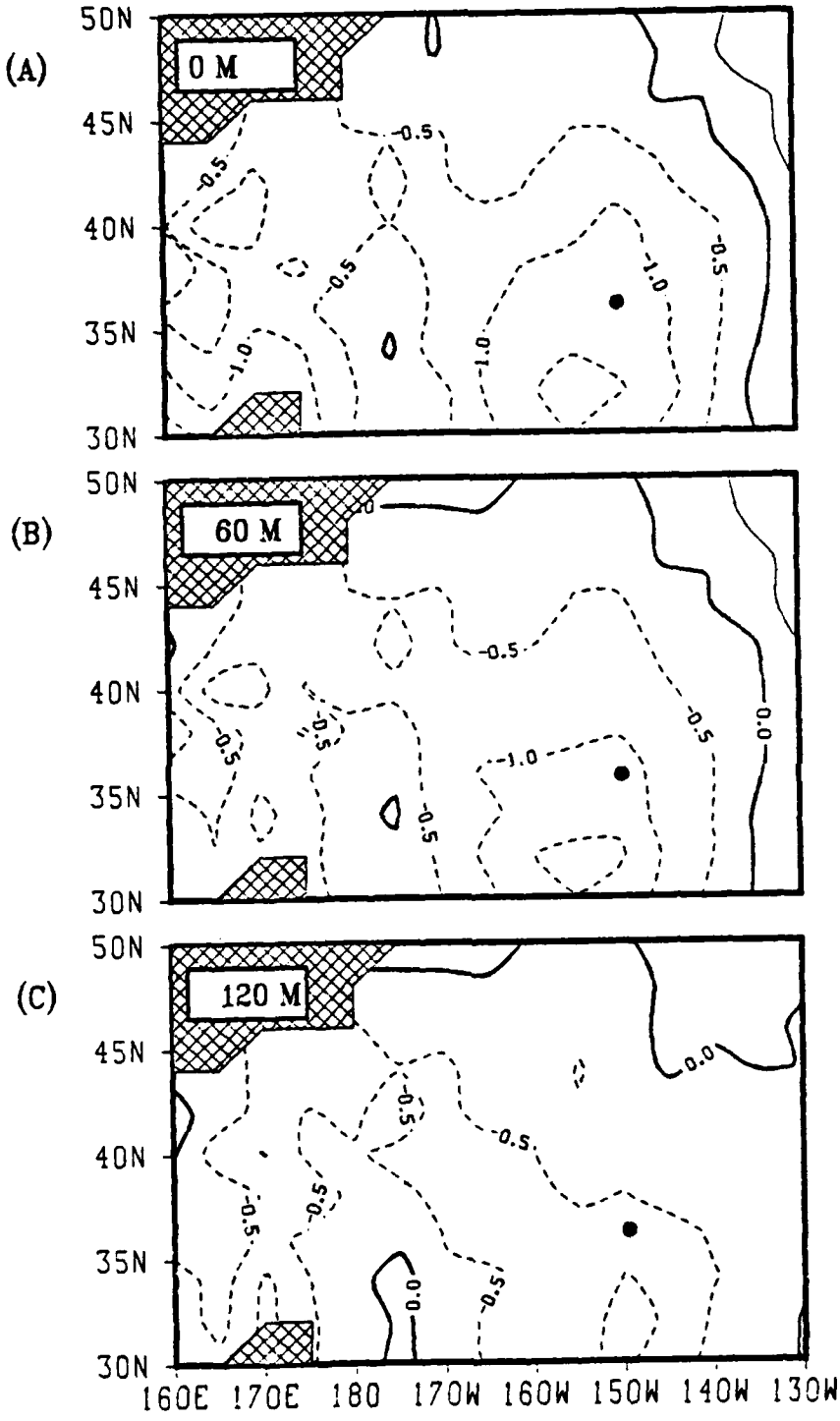

Figure 8. Similar to Fig. 5 except for April 1978.

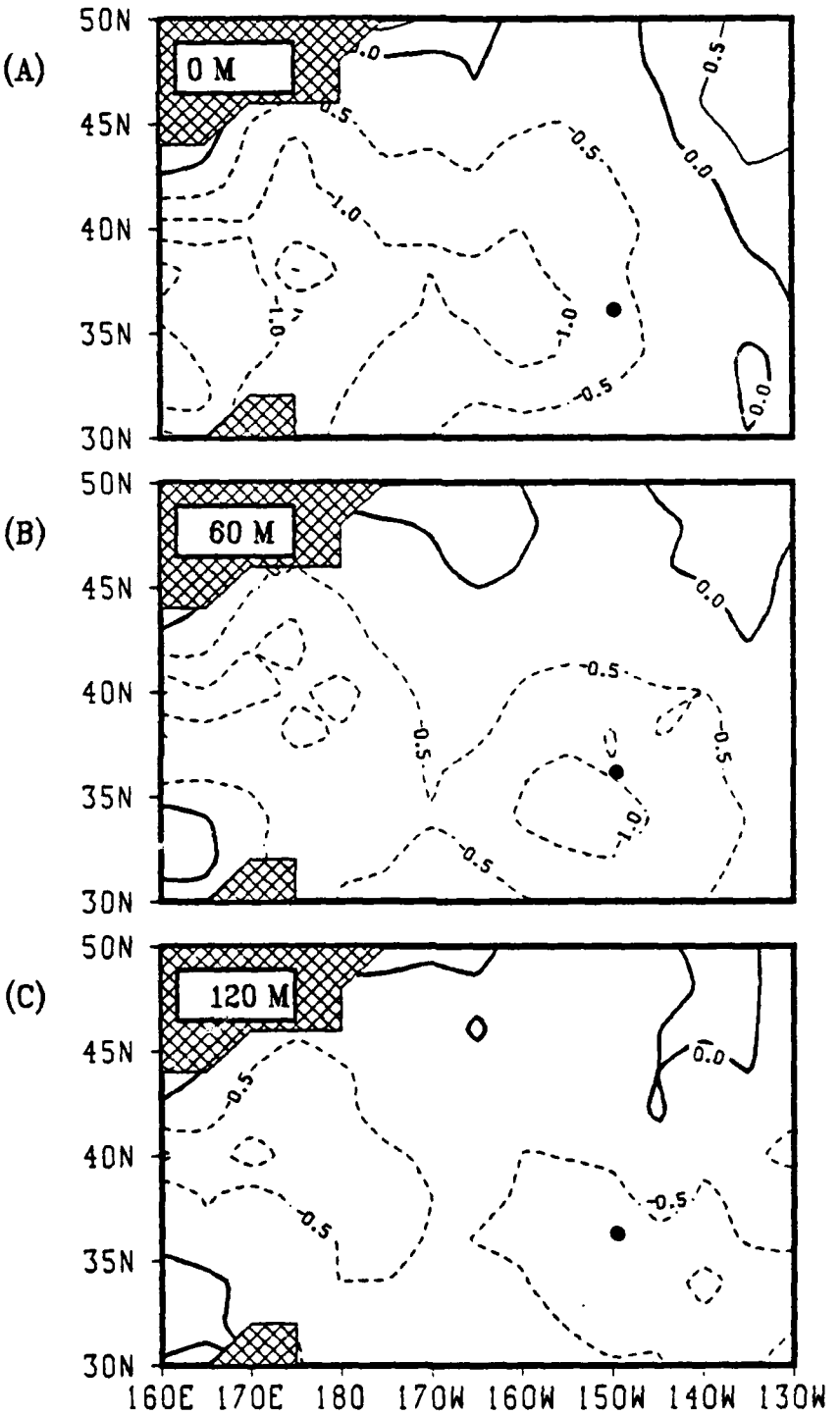

Figure 9. Similar to Fig. 5 except for May 1978.

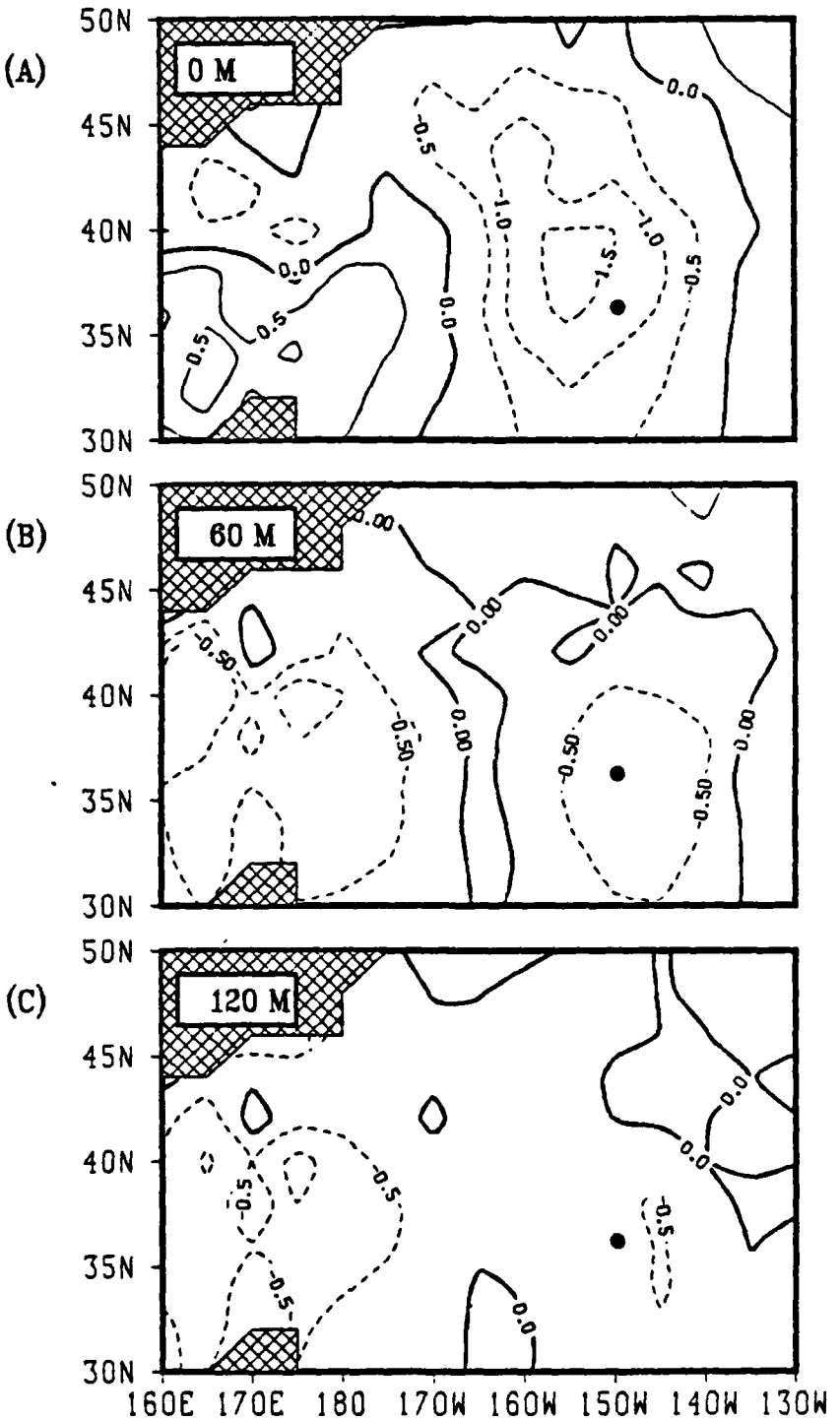

Figure 10. Similar to Fig. 5 except for June 1978.

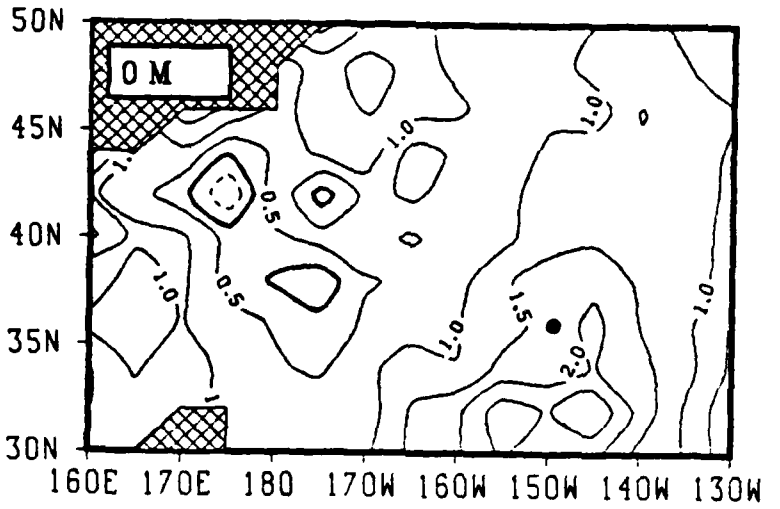

Figure 11. Similar to Fig. 3 except from 15 April to 15 May 1978. Values greater than 1.0 indicate greater temperature changes than the normal monthly change. Negative (dashed) values indicate temperature decrease during a period in which seasonal warming is taking place.

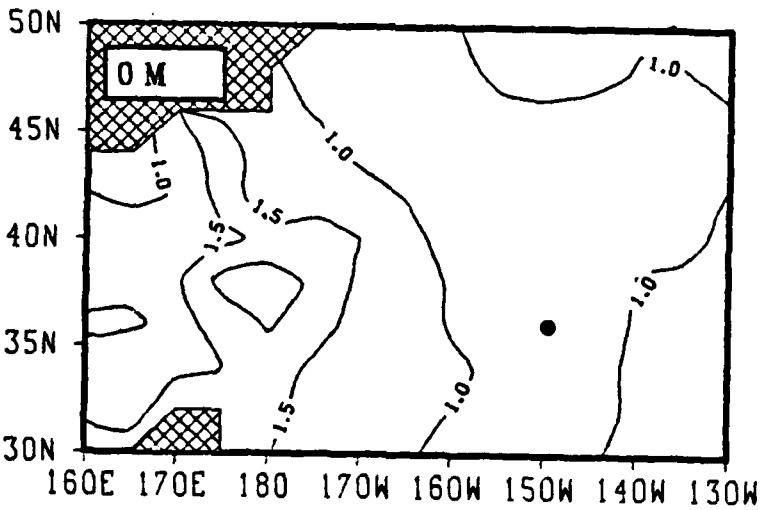

Figure 12. Similar to Fig. 3 except from 15 May to 15 June 1978.

B. MODEL HINDCAST

The Garwood model was initialized with the ocean temperature analysis from 15 October 1977 and integrated through 18 June 1978 to cover the life span of CA 12. As may be seen in Fig. 13, the model does a rather remarkable job in predicting the mixed layer temperature through March 1978 during the deepening and maintenance phases of the anomaly at the central point (36.0°N, 150.0°W). From April through June 1978 however, the model-predicted mixed layer temperatures remained too low.

Recall that the model was initialized with the October 1977 fields which showed the region covered by above average temperatures (Fig. 2A). By November 1977 (Fig. 14), the model developed a cold anomaly on the surface in the northeast region. The model anomaly (MA) underwent rapid temperature decreases (Fig. 15) from October to November 1977 as did CA 12. In the northeast region, the analyzed surface temperature decrease was greater than 1.5 times the climatological decrease (Fig. 3), while the model surface temperature decrease was greater than twice the climatological decrease (Fig. 15). From November to December 1977, the model sustained the anomaly by a cooling rate much the same as climatology. By this time the majority of the region had below normal temperatures. The model-derived anomaly penetrates to 60 m at the central point in December 1977 (Fig. 16), which is one month earlier than analyzed

(Figs. 4 and 5). That is, the model decreases in mixed layer temperature (and increases in depth) are slightly larger than observed in CA 12 from October to November 1977. The model anomaly in the northeast (MA 12N) at 46°N, 140°W is in the locality where CA 12 first appeared. MA 12N remains in the same location for three months, and disappears as a separate center by February 1978.

In December 1978, another cold model anomaly (MA 12) center appears on the surface in the southeast (-1.48°C at 30°N, 155°W). Both centers (MA 12 and MA 12N) are considered to be part of the model's representation of CA 12. As the southeast center (MA 12) development after December 1978 closely parallels that of CA 12, the discussion below will focus on MA 12. From December 1977 to January 1978 (Fig. 17), the predicted rate of temperature decrease (Fig. 18) slowed to that of climatology in the northeast region, but stayed at 1.5 times climatology in the southeast region as the anomaly expanded southward. This general pattern is consistent with the analyzed changes in the eastern half of the domain (Fig. 6).

The vertical structure for January and March 1978 can be seen in Figs. 17 and 19. The model predictions are noisy at 60 and 120 m, although the features of CA 12 are still very discernable. The model prediction takes on a weak north-south orientation similar to the analyses. The warm anomaly along the eastern boundary is not predicted in

January 1978 except at 120 m, where it is correctly oriented north-south but has a larger areal extent. By March 1978 (Fig. 19), this warm anomaly at 120 m has moved eastward to along the eastern boundary of the ADS area, where it remains through June 1978. Since this warm anomaly has a large areal extent in the eastern region at 120 m, MA 12 does not penetrate to 120 m in the vicinity of 36°N, 150°W until February 1978 (not shown), which is one month later than analyzed.

The model does a fairly good job in hindcasting the marked changes in shape of the vertical thermal structure for the central point of CA 12. The model mixed layer temperatures (MLT's) are in close agreement, albeit on the cold side, with those analyzed through March 1978. The analyzed and predicted vertical temperature profiles for October through December 1977 can be seen in Fig. 20A and 20B and those for January through March 1978 in Fig. 21A and 21B. The October 1977 profiles are, of course, identical as this is the initial time. The predicted mixed layer temperatures (MLT's) for November and December 1977 were nearly the same as analyzed, while the remainder of the vertical profiles approximated the analyses. One exception is the higher thermoclime temperatures analyzed during November 1977 only. It is during the period from January to March 1978 that the model predictions come the closest to hindcasting correctly the vertical temperature profiles

at the central point down to 200 m. The mixed layer depth is also largest during this period. The model MLT's for January through March 1978 are less than 0.5°C lower than the analyzed MLT and the thermal structure below the mixed layer is in fair agreement with the analyses.

The analyzed spring transition at the central point occurred between March and April 1978 using the criteria described in Chapter I, Section C1. Determination of the mixed layer depth for both the model and analyzed profiles was made using the criteria described in Chapter I, Section C2. The analyzed March 1978 vertical temperature profile (Fig. 21A) appears to have a mixed layer depth (MLD) of about 80 m, although the temperature gradient below this level is quite small. By April 1978 (Fig. 22A), the analyzed MLD has shallowed to about 40 m and the MLT has increased by 1.0°C. Using the same criteria as for the analyzed spring transition, the model spring transition does not occur until between April and May 1978. As may be seen in Fig. 22B, the model MLD in April 1978 is 150 m. By May 1978, the model MLD has shallow-d to about 5 m and the model MLT has increased by 1.0°C. Using the daily maximum model MLD and corresponding MLT from Fig. 13, the predicted spring transition would be during the latter half of April 1978.

Throughout the spring, the model mixed layer temperature remained too low (Fig. 13). In the southwest region, the

model predictions continued to decrease in temperature from March to April 1978, whereas the region actually had undergone spring transition and the cold anomaly was diminishing. The model-derived vertical structure for April through June 1978 can be seen in Figs. 23 to 25. It is during April 1978 that MA 12 reaches maximum intensity (-3.10°C at 30°N, 155°W) and areal extent. The model anomaly center in April 1978 is southwest of the analyzed central point. Between April and May 1978, the surface temperature in the model began to increase at a rate (Fig. 26) close to twice the climatological rate, which is consistent with the analyzed changes (Fig. 11). This rapid increase in temerature did not persist long enough for the model mixed layer temperature to increase to the analyzed temperatures. In May 1978 (Fig. 24), the predicted anomaly is quite intense rather than having somewhat diffuse surface features, as was analyzed. The model prediction does maintain the eastern portion at below normal temperatures through June 1978. From May to June 1978, the predicted rate of temperature increase (Fig. 27) is less than that of climatology, and is approximately equal to the analyzed rate of temperature increase (Fig. 12) in the region of CA 12. By June 1978, at the central point, the model-derived anomaly is still quite prominent, -1.79°C, at 60 m, whereas at 120 m the anomaly has diminished to only

-0.65°C. The model correctly predicts the intensification of the surface anomaly at the central point in June 1978 (Fig. 25); however, the model anomaly is twice as intense as analyzed.

In summary, the Garwood model does a very notable job in hindcasting CA 12 as it developed during the autumn of 1977 and reached the maximum amplitude and area extent during the winter of 1978. The mixed layer temperature and depth, and corresponding vertical temperature profiles at the center of the anomaly, are fairly close to those analyzed. The model spring transition is late compared to the analyzed spring transition, and the model mixed layer temperatures remain too low. A summary of the locations and minimum temperatures during the life spans of both CA 12 and MA 12 is provided in Table 1 (Chapter III, Section 3B). It is very satisfying to see numerous similarities during the life span of the cold anomaly. The model hindcast of CA 12 is slightly on the cold side as seen in Fig. 13. These results show that CA 12 can be accounted for the most part by local atmospheric forcing.

It is interesting to look at other grid points around the central point of CA 12. One grid point examined is located to the northeast of CA 12 near the persistent warm anomaly along the eastern boundary of the ADS area. The model predictions there are not as good, as the model does

not hindcast the warm anomaly along the eastern boundary. At 38°N, 135°W (Fig. 28), the model mixed layer temperature is also consistently too low throughout the integration. However, the monthly trends of temperature change are well simulated. At the northwest edge of the anomaly (40°N, 160°W), themodel prediction (Fig. 29) is much better than at the central point of CA 12. Thus, the temperature changes in the central area of the ADS region appear to be explained by one-dimensional processes. Furthermore, the anomalous thermal structure appears to be generated by local atmospheric forcing. The hindcast for 34°N, 160°W (Fig. 30) is also quite good. At this location, the model captures the trend during the autumn-winter temperature decrease and also does a good job in the spring, except for April 1978. In April, the model mixed layer temperature is significantly colder than the analyzed monthly mixed layer temperature.

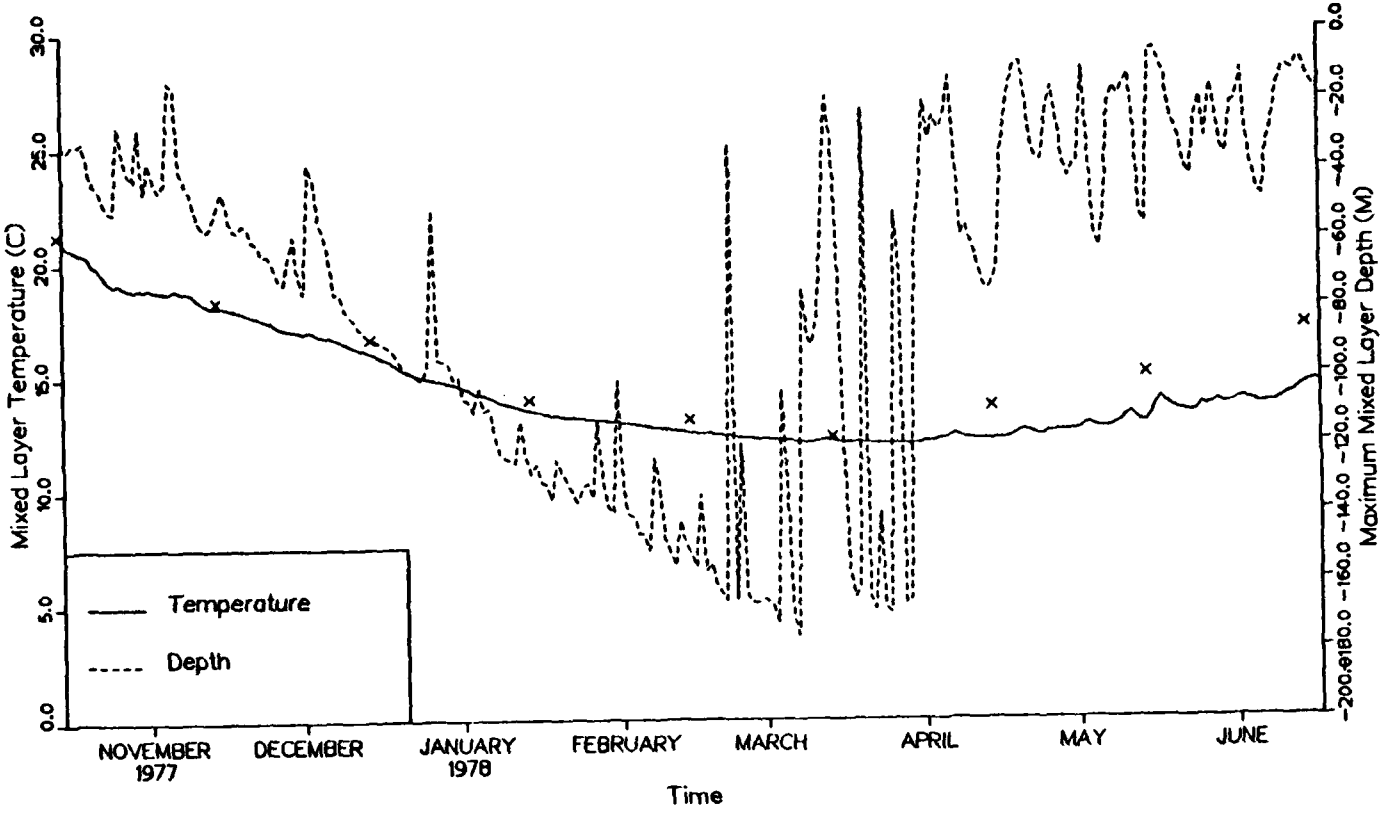

Figure 13. Daily maximum model mixed layer depth and corresponding model mixed layer temperature (MLT) compared to objectively analyzed MLT (denoted by x on the 15th of each month) at the center of cold anomaly 12, 36.0°N, 150.0°W from 15 October 1977 to 18 June 1978.

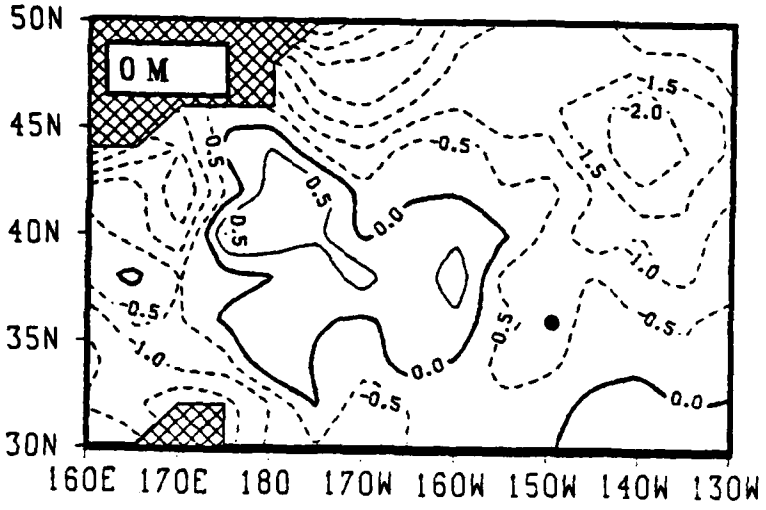

Figure 14. Model temperature (°C) anomaly MA 12 at surface during November 1977.

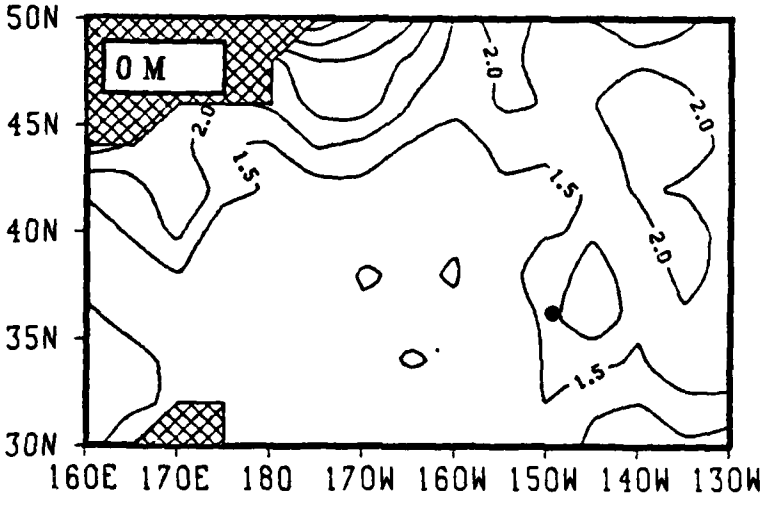

Figure 15. The ratio of the change in model temperatures (°C) from 15 October to 15 November 1977 to the climatological temperature change for the same period. Values greater than 1.0 during this period indicate above-average temperature decreases.

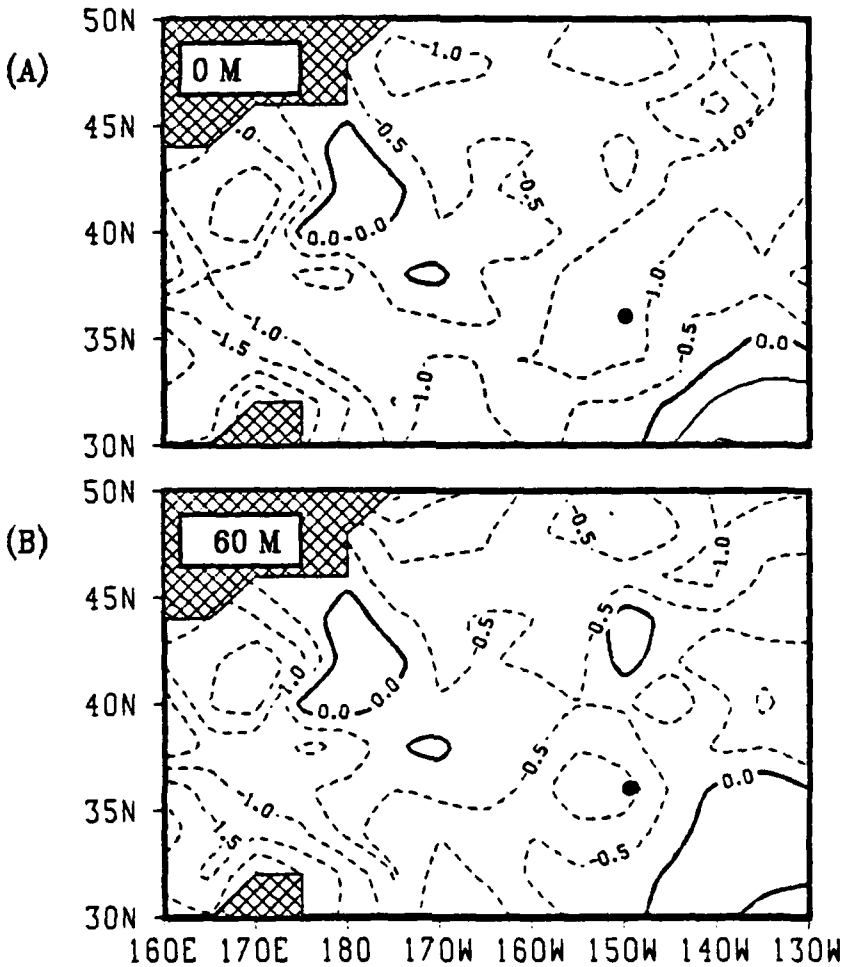

Figure 16. Model temperature (°C) anomaly MA 12 during December 1977 at (A) surface and (B) 60 m.

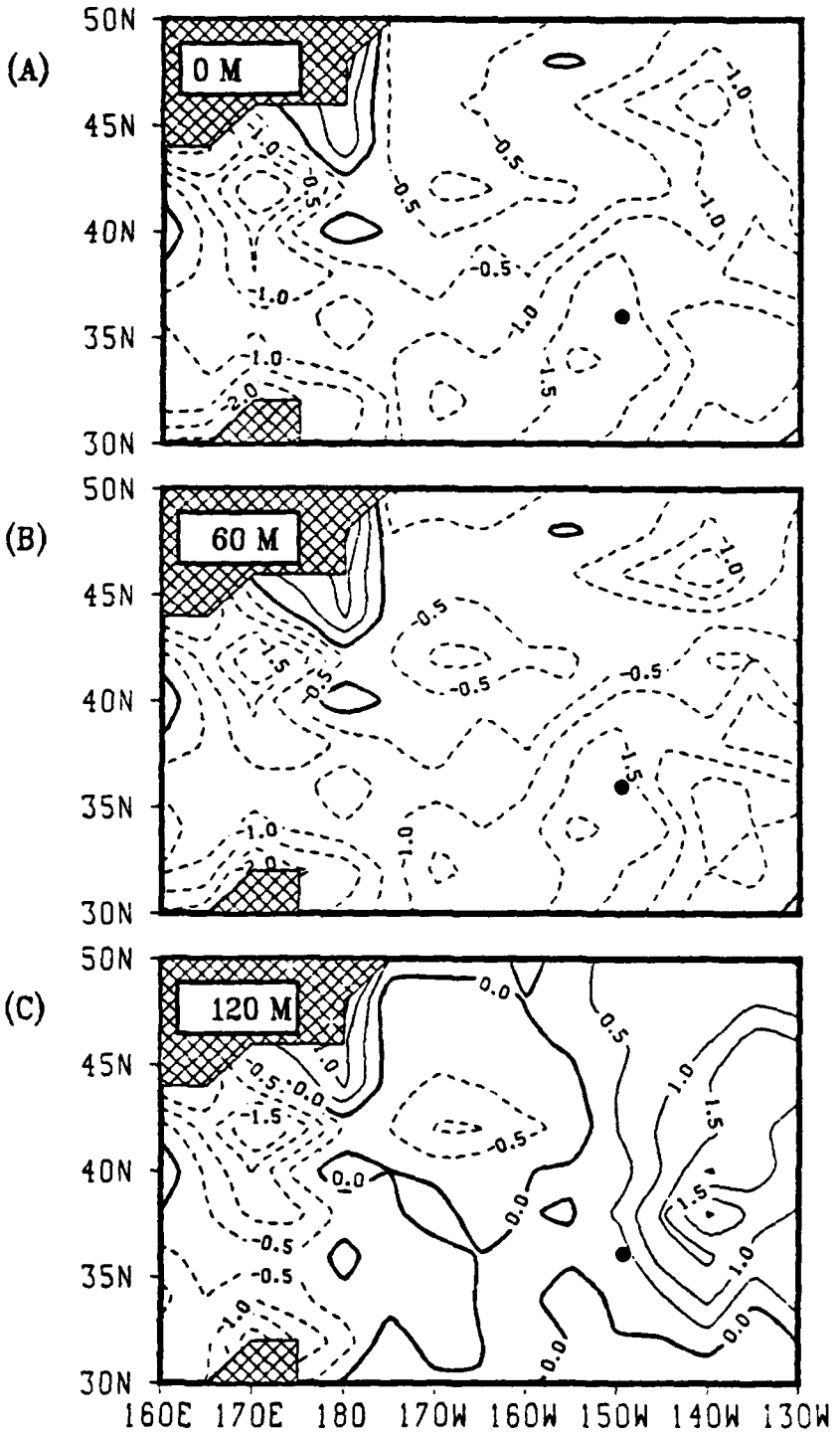

Figure 17. Model temperature (°C) anomaly MA 12 during January 1978 at (A) surface, (B) 60 m and (C) 120 m.

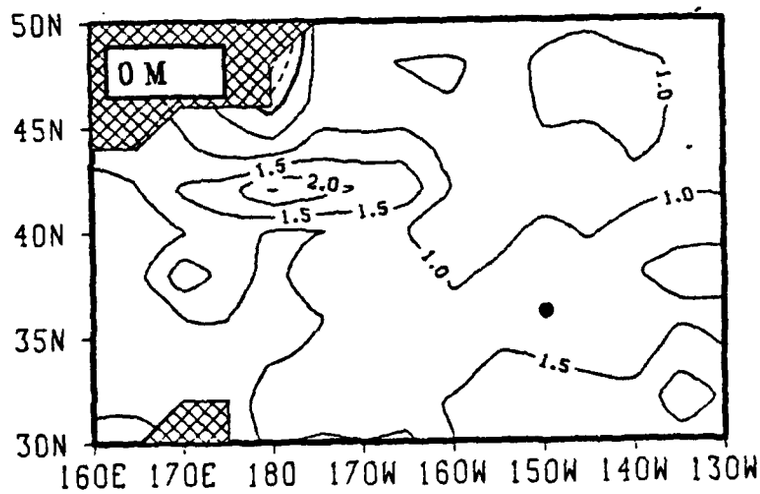

Figure 18. Similar to Fig. 15 except from 15 December 1977 to 15 January 1978. Values greater than 1.0 indicate greater temperature changes than the normal monthly decrease. Negative (dashed) values indicate a temperature increase during a period in which seasonal cooling is expected.

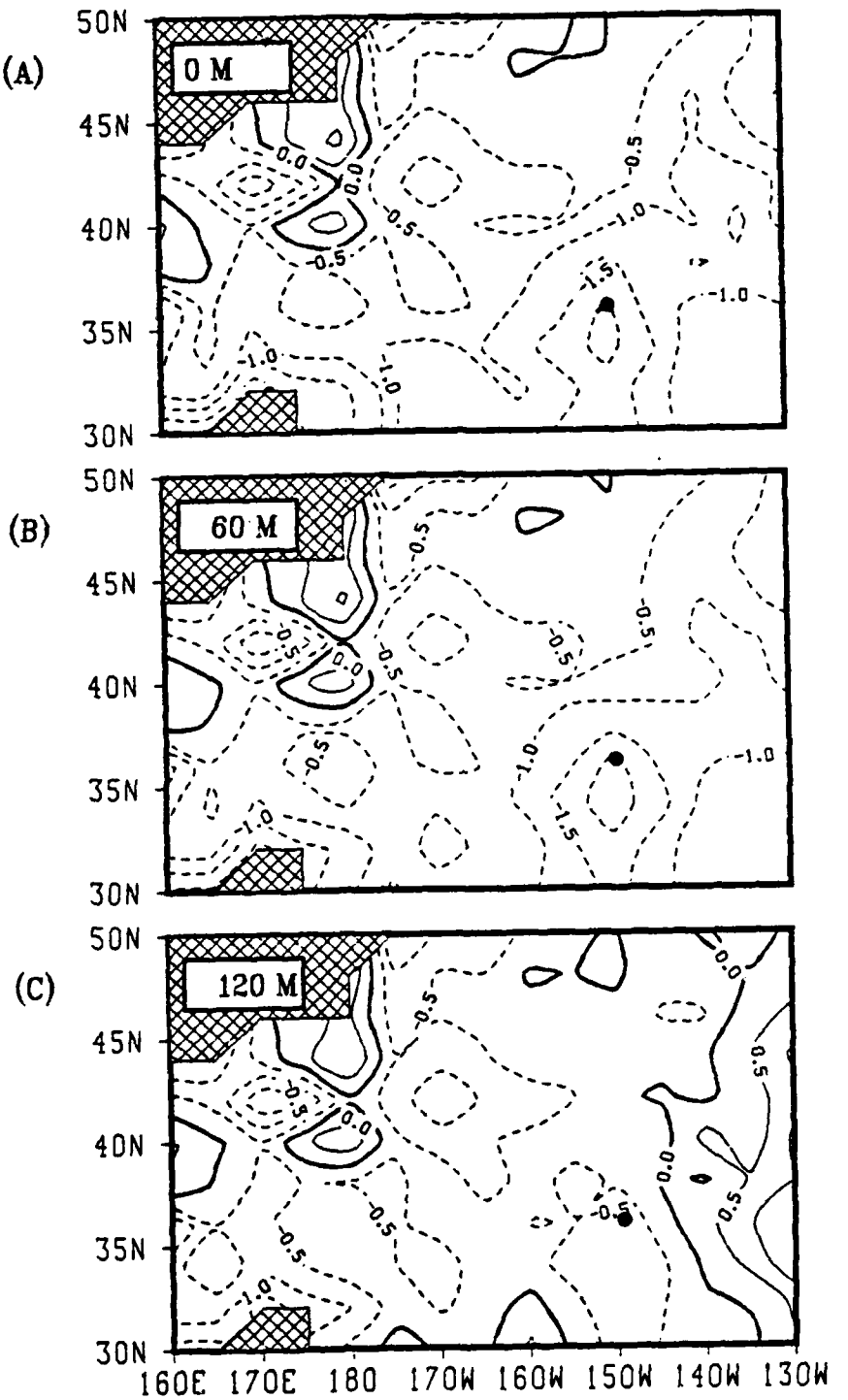

Figure 19. Similar to Fig. 17 except for March 1978.

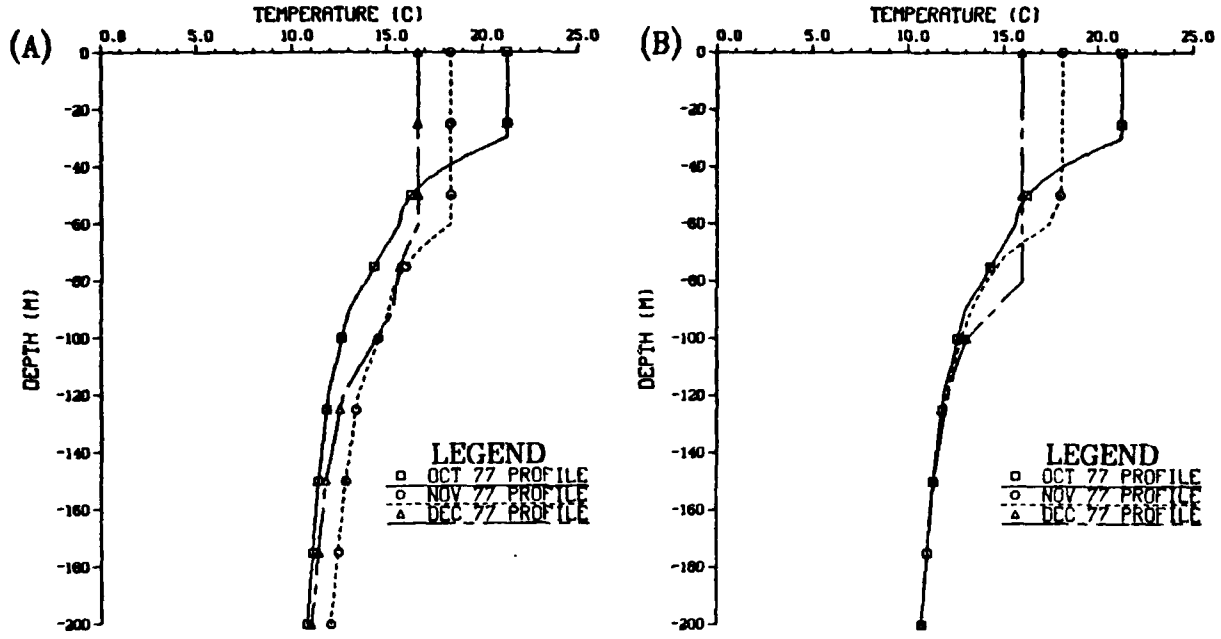

Figure 20. (A) Objectively analyzed monthly vertical temperature (°C) profiles centered on the 15th of the month for October (squares), November (circles) and December (triangles) 1977. (B) Model monthly vertical temperature (°C) profiles averaged over five days centered on the 15th of each month for October (squares), November (circles) and December (triangles) 1977.

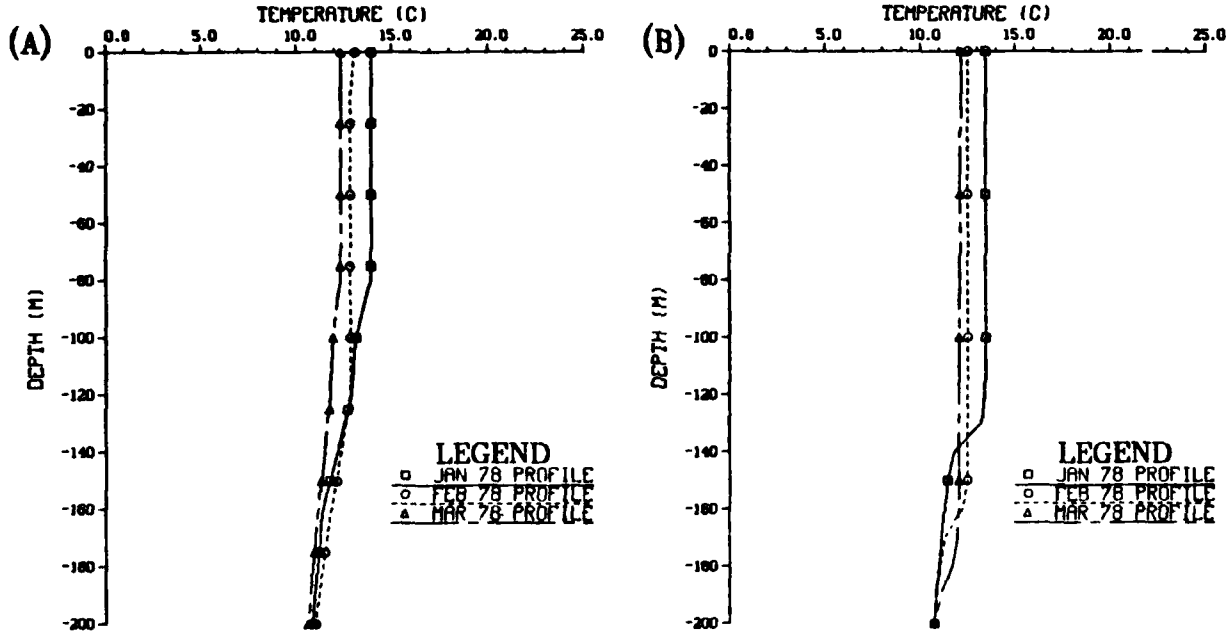

Figure 21. Similar to Fig. 20 except for January (squares), February (circles) and March (triangles) 1978.

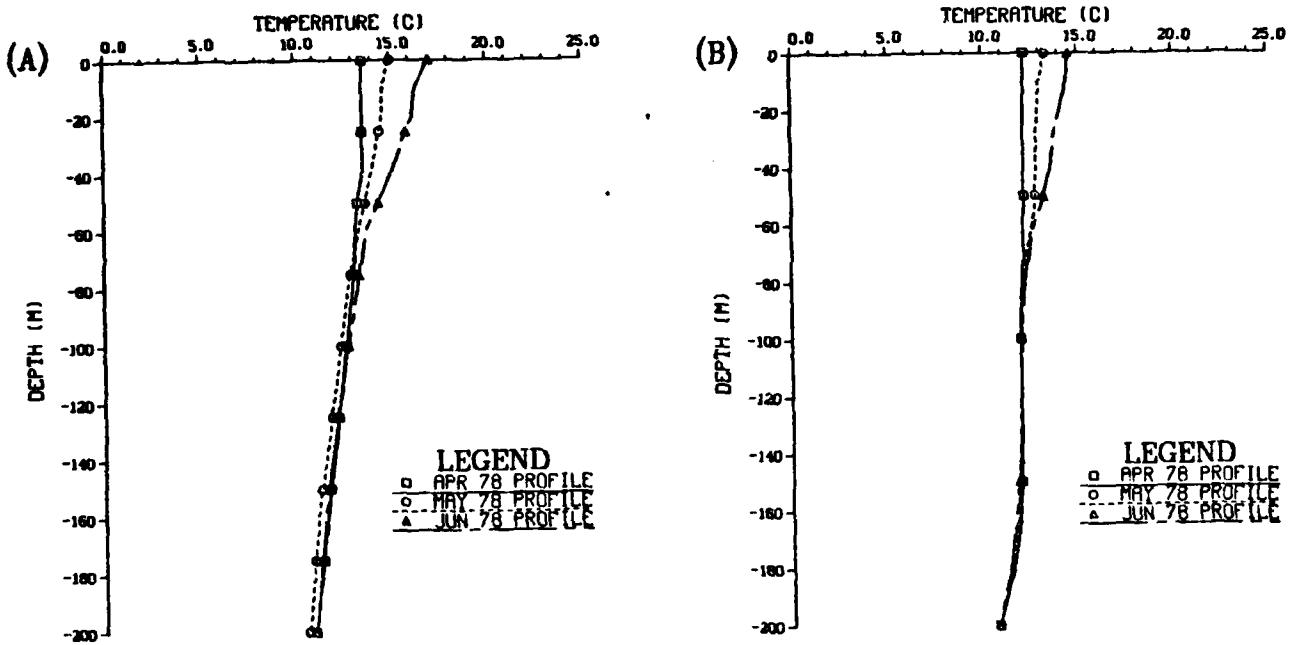

Figure 22. Similar to Fig. 20 except for April (squares), May (circles) and June (triangles) 1978.

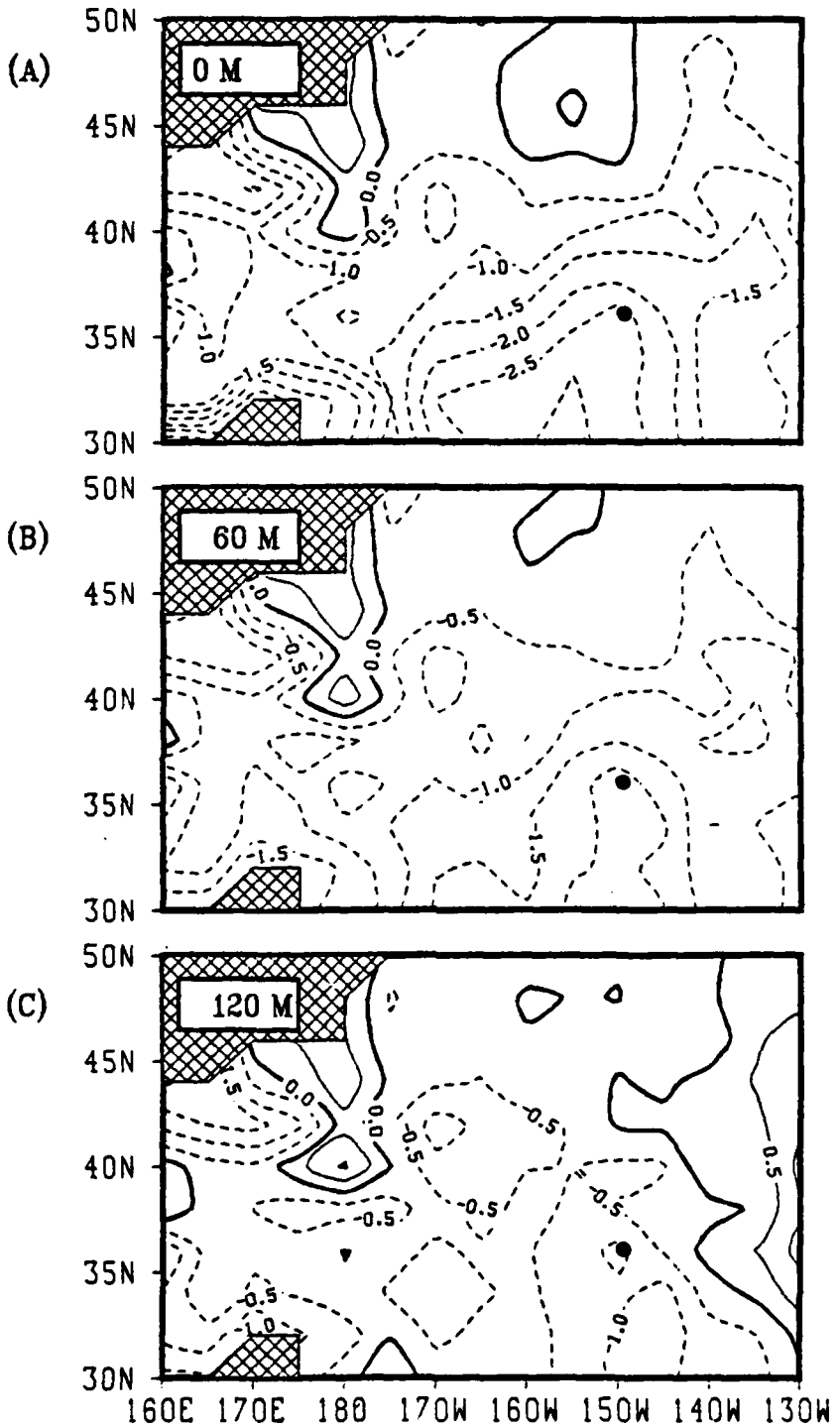

Figure 23. Similar to Fig. 17 except for April 1978.

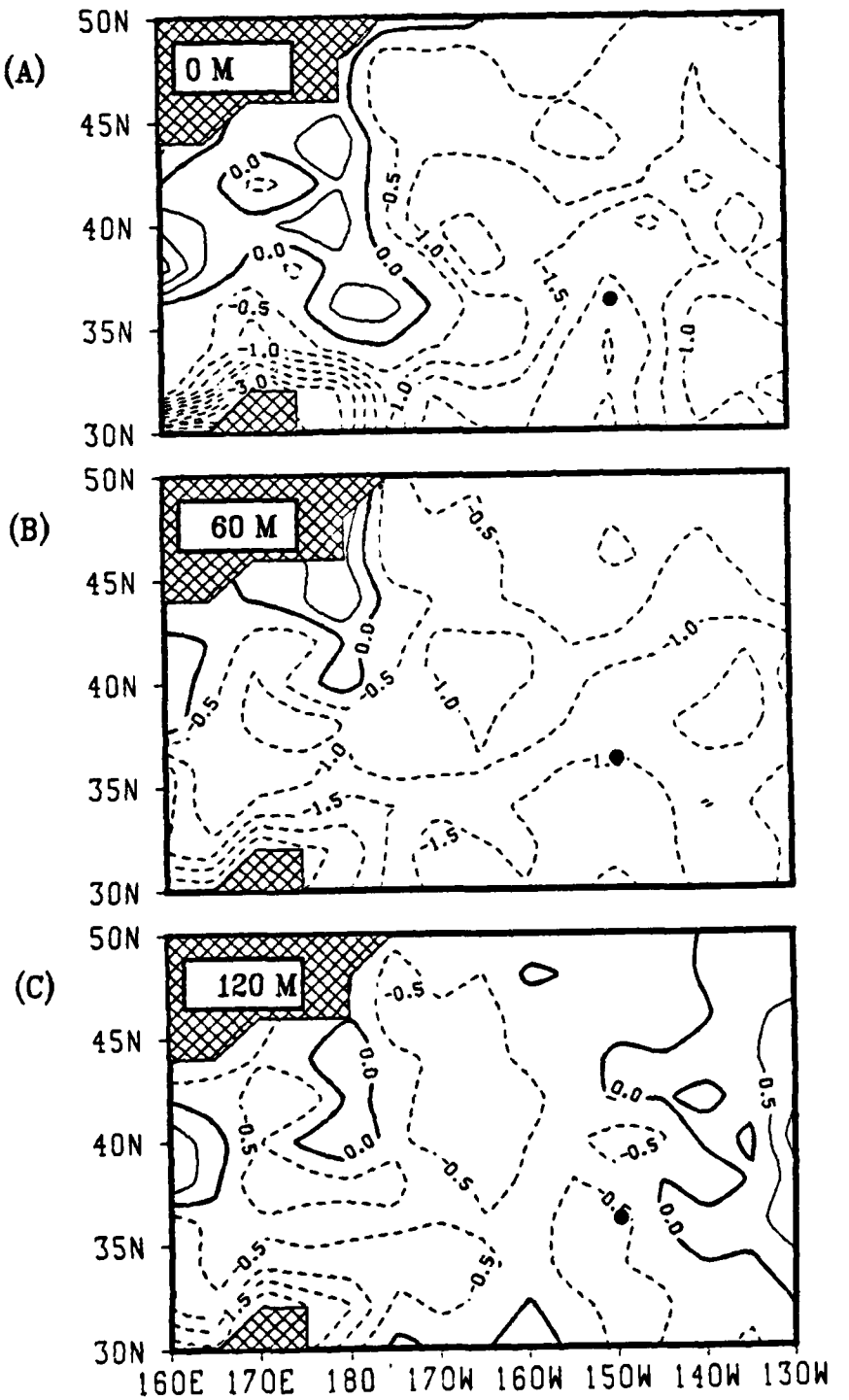

Figure 24. Similar to Fig. 17 except for May 1978.

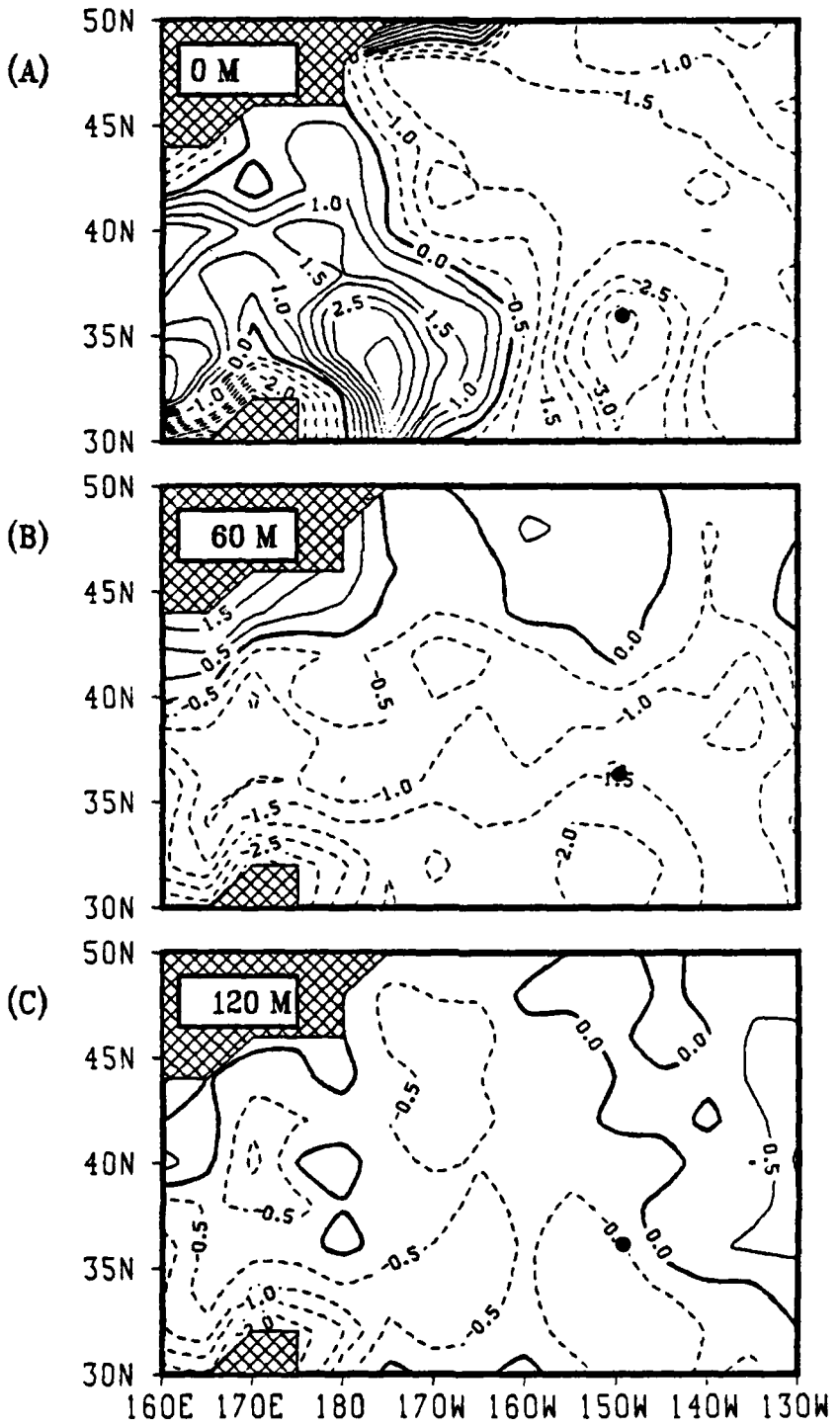

Figure 25. Similar to Fig. 17 except for June 1978.

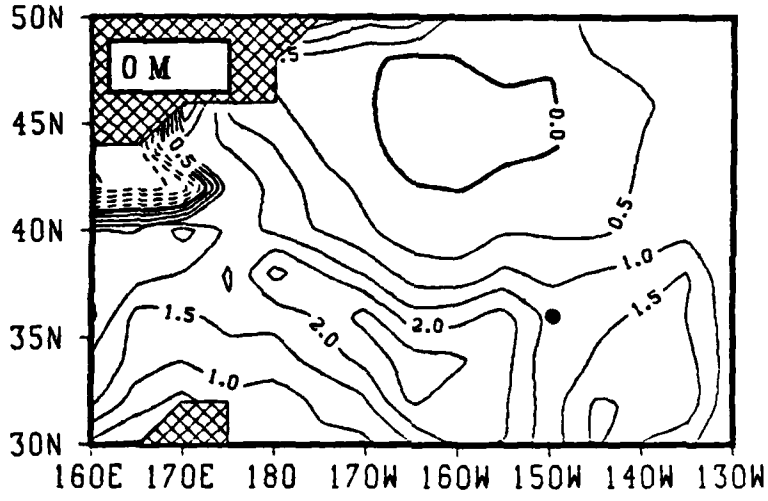

Figure 26. Similar to Fig. 15 except from 15 April to 15 May 1978.

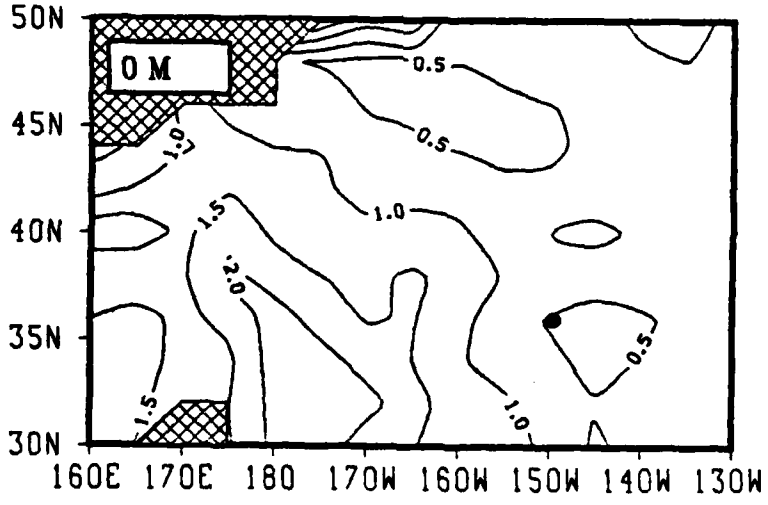

Figure 27. Similar to Fig. 15 except from 15 May to 15 June 1978.

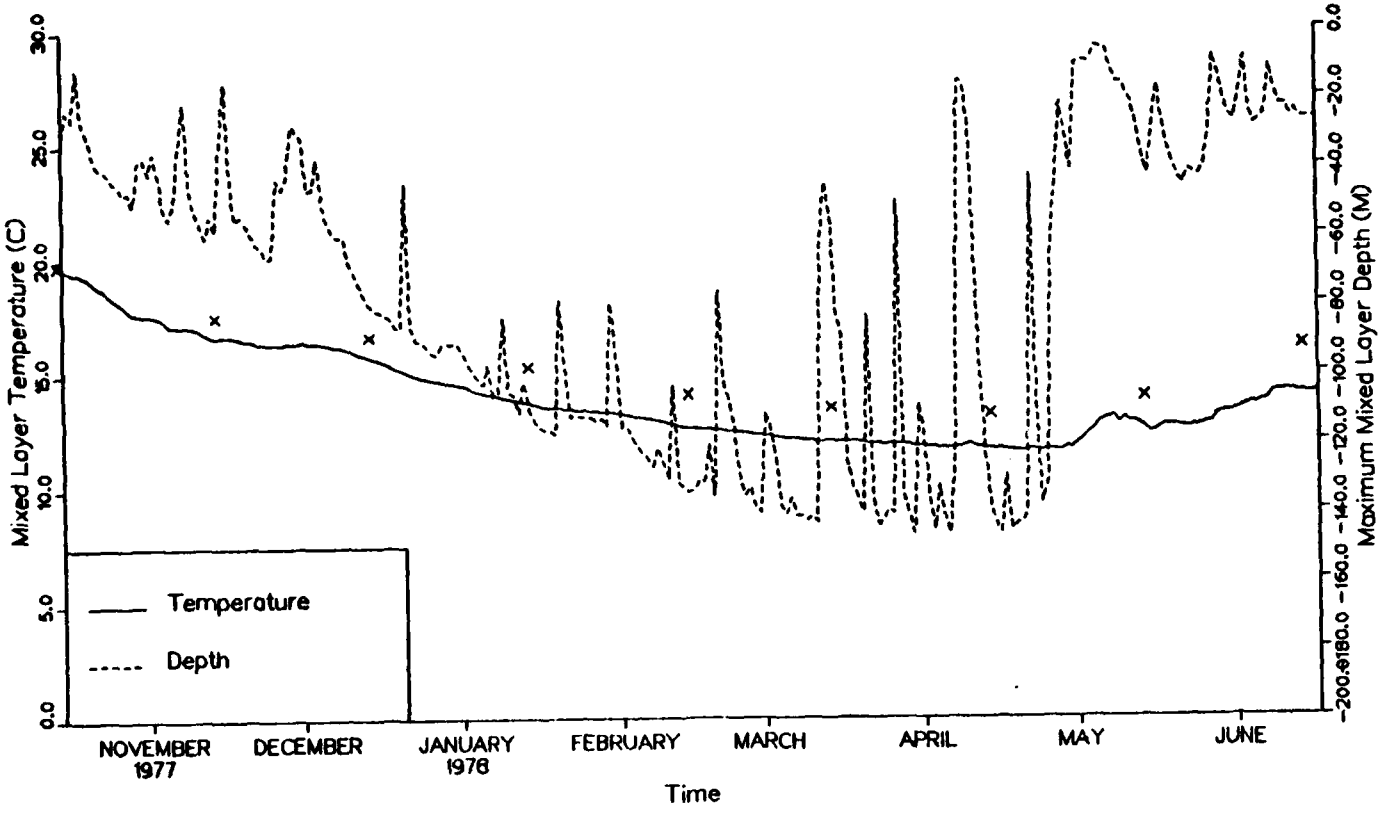

Figure 28. Similar to Fig. 13 except at grid point 38.0°N, 135.0°W.

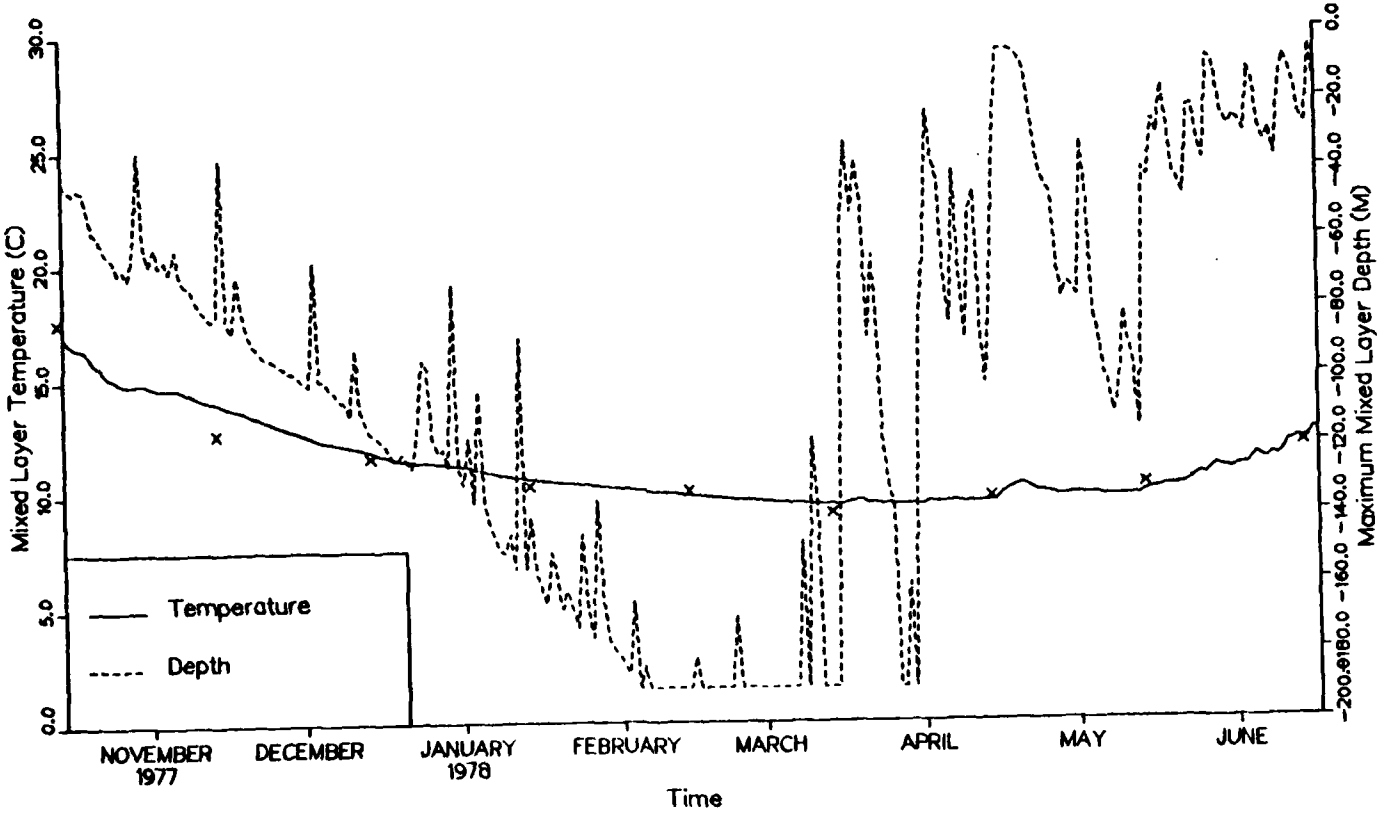

Figure 29. Similar to Fig. 13 except at grid point 40.0°N, 160.0°W.

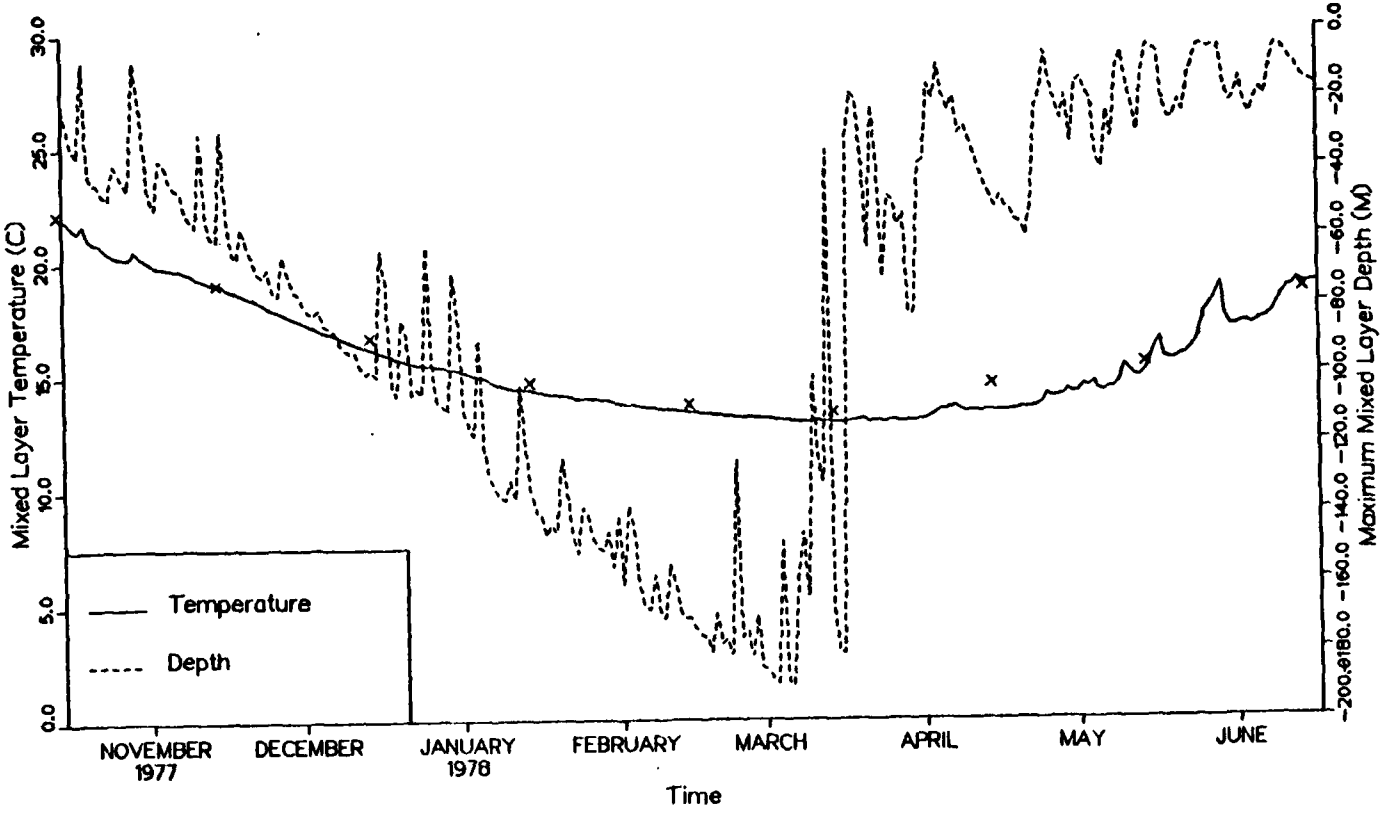

Figure 30. Similar to Fig. 13 except at grid point 34.0°N, 160.0°W.

C. ERROR DISCUSSION

A later (earlier) than normal mixed layer spring transition is expected to be related to the development of lower (higher) than normal sea-surface temperatures. This relationship held rather well for the 19-year sample at Ocean Weather Station "P" (50°N, 145°W) (Elsberry and Garwood, 1978) and also during 1976 and 1977 in the ADS region (Budd, 1980). If the timing of spring transition is not correct (for example, due to incorrect forcing), the model predictions after that time will be in error.

One may observe these errors in the heat content of the model vertical temperature profile. The difference in heat content relative to 200 m between analyzed and model profiles, ΔQ, is given by:

$$\Delta Q = \rho_o C_p \left[\int_{-200}^{0} (T_{anal}(z) - T_{anal}(200))\, dz - \int_{-200}^{0} (T_{mod}(z) - T_{mod}(200)\, dz \right], \quad (1)$$

where ρ_o is the density, C_p is the specific heat and z is the depth below the surface. The relative error in the heat content relative to 200 m is given by:

$$\text{relative error} = \frac{\Delta Q}{\rho_o C_p \int_{-200}^{0} (T_{anal}(z) - T_{anal}(200))\, dz}. \quad (2)$$

Trapezoidal integration is used in the determination of the heat content. The heat content is calculated relative to the 200 m temperature with the intent of removing some of the change in heat content due to vertical displacements of the thermocline and also due to horizontal effects. To remove completely the change in heat content due to vertical displacements, one should integrate with respect to an isotherm in the thermocline. However the analyses have insufficient resolution to allow such an integration. Another motivating factor for calculations relative to 200 m was that the calculations to determine the correction fields to the surface heat flux fields were also relative to this depth (Elsberry et al., 1982).

Values for the analyzed and model hindcast heat content relative to 200 m from November 1977 to June 1978 are given in Table 2. Also shown in Table 2 are the differences in heat content for each month and the relative error in the heat content between analyzed and model profiles. The model heat content is derived from the temperature profiles averaged over five days centered on the 15th of each month. Using averaging periods of 10 and 20 days showed little change in the heat content of the averaged model temperature profiles relative to 200 m. Thus all of the model profiles used in this study are based on the five-day averaging period.

TABLE 2

Analyzed and model hindcast heat content (x104 cal/cm^2) relative to 200 m at 36.0°N, 150.0°W, their difference, and the relative error in heat content above 200 m between analyzed and hindcast temperature profiles.

Month	Year	Analyzed	Hindcast	Difference	Relative Error
Nov	1977	6.33	6.64	-0.31	-0.049
Dec	1977	6.33	5.79	0.56	0.086
Jan	1978	4.09	3.95	0.14	0.036
Feb	1978	2.97	3.01	-0.04	-0.013
Mar	1978	2.38	2.48	-0.10	-0.043
Apr	1978	3.24	2.45	0.79	0.244
May	1978	3.88	2.89	0.99	0.255
Jun	1978	4.47	3.43	1.04	0.233

The relative errors in Table 2 show a seasonal trend. During winter, the mixed layer is deep and the relative error is small. During summer, the mixed layer is shallow and the relative error is increased over five-fold. This is not surprising. When the mixed layer is shallow and warm during the summer, there is a greater possibility that the model profile below the mixed layer will be in error, since it is essentially unchanged once the mixed layer shallows.

The relative error is a function of (1) analysis error; (2) model parameterizations; (3) model forcing; and (4) model physical processes. Each of these areas will be examined in more detail in the next four sections.

1. Analysis Error

The number and distribution of ship XBT reports that are included in the objective analysis (White and Bernstein, 1979) determine the accuracy of the fields. One problem appears to be a "fair weather bias" because ships tend to avoid bad weather. During the winter, the ship tracks are further south, and consequently the analysis in the northern portions of the ADS grid is extrapolated from data in the southern portions. Another problem is that merchant ships do not transit the region at equally spaced time intervals. There is no assurance that the reports will be well distributed in space or in time. A candidate for a varied temporal distribution of XBT reports is the month of April 1978. Since CA 12 is in the southern portion of the ADS grid, where the monthly mean wind fields indicate persistent anticyclonic flow, it is unlikely that ships would avoid the region due to bad weather. As seen in Fig. 13, the model mixed layer depth has shallowed to about 25 m at the beginning of April 1978, however, it is predicted to deepen again to about 70 m in the middle of the month and then shallow to approximately 10 m in late April. If ship observations were taken at the beginning and end of the month when the mixed layer was warm and shallow, this would result in an erroneous analysis of MLT. As noted in Fig. 30, a comparison of the observed and model MLT's to the southwest of the central point also shows that the model MLT was lower than the observed MLT for April 1978.

2. Model Parameterizations

There are four constants that are critical to the parameterization of the physical processes in the Garwood model. These constants, m_3, p_3, r and γ, must be evaluated empirically (a more complete description of these constants and the parameterizations is contained in the Appendix). The model parameters m_3 and p_3 are important in predicting the seasonal cycle of sea-surface temperature. The values of these constants were empirically determined by Gallacher et al. (1983) for the ADS region using data between January 1976 to December 1978.

The model constants r (fraction of solar flux absorbed in first meter) and γ (absorption coefficient) determine the predicted vertical distribution of heat in the water column, and are functions of the turbidity of the water. These parameters are most important during the spring and summer when the mixed layer depth is small. To determine the model sensitivity to r and γ, the model was rerun from 15 February to 18 June 1978 with r decreased from 0.5 to 0.4 and γ increased from 0.001 to 0.002. These values will lead to more heat being absorbed into the surface layers of the column. However, the new mixed layer temperature prediction was not a significant improvement on the model results shown in Fig. 13. This was not surprising since the model constants have already been adjusted to be as consistent as possible with the atmospheric forcing

(Gallacher et al., 1983). Thus, some other reasons/ processes are responsible for the analysis-model differences in the spring.

3. Model Forcing

It is necessary to first determine if the errors are due to an initial value problem associated, in this case, with the long integration period. That is, the accumulated errors in the model forcing or in model constants could have led to incorrect profiles prior to the spring period. To test the contribution from this source of error, the model was initialized with the 15 February 1978 analysis. The daily maximum mixed layer depth and corresponding temperature plots when the model was initialized in February 1978 were very nearly the same as in Fig. 13. The relative errors in Table 3 for this experiment are similar to those in Table 2, which shows that there is minimal improvement by initializing the model in February 1978. To determine if the model could produce the correct trend after the spring transition had occurred, the model was also initialized with the 15 April 1978 analysis. Even in this case, the model did not predict the correct trend in the mixed layer temperature, and the predicted June 1978 sea-surface temperatures continued to be too low.

Since the errors were not due to an initial value problem, the actual model forcing from October 1977 through June 1978 was examined. As the model predictions were good

through March 1978, it is assumed that the forcing through that time were reasonably correct. Earlier studies (Elsberry et al., 1979; Budd, 1980; Steinder, 1981) found that the monthly integrated FNOC surface heating did not have a sufficiently large seasonal amplitude. There was also a persistent bias toward excessive heat loss to the atmosphere especially along the southern boundary of the domain. Elsberry et al. (1982) calculated bimonthly heat flux correction fields to be added to the FNOC surface heat flux fields to reduce this excessive upward flux. There was a downward heat flux correction of about 4 $cal/cm^2/h$ applied during April-May (Elsberry et al., 1982). The fraction of the correction fields that should be attributed to the solar heat flux was not determined by Elsberry et al. (1982), as previous studies (Elsberry et al., 1979; Budd, 1980; Steiner, 1981) indicated that the solar heat flux fields were reasonably correct. The resulting heat fluxes were used in the model forcing for this study.

As mentioned earlier, the model predicted inadequate ocean warming in the spring. This suggests that the most likely cause of the observed errors is inaccurate atmospheric forcing. It is important to point out that the predictions during the spring are very sensitive to the magnitude of the downward surface heat flux. There is a delicate balance between the heat flux tending to form a

stable and shallow layer near the surface and the wind mixing tending to erode the stable layer to re-establish a mixed layer characteristic of winter. Once the shallow mixed layer is formed, the greater the downward flux, the more rapid the warming, and the less likely that wind mixing will erode the layer. Thus, the magnitude of the heating has a double effect in the spring transition period. As discussed earlier, this was the period when the relative errors in heat content relative to 200 m began increasing dramatically.

Budd (1980) found that the time changes in fluxes of solar radiation and total heat flux were apparently of much less importance than variations in wind speed during the change of the mixed layer from a winter to a summer regime. Thus the effect of errors, even small ones, in wind speed forcing are enhanced during the period of spring transition. It is not possible to determine corrections to the FNOC wind fields as no indpendent wind reports are available. However, one would expect the FNOC analyses to be biased toward lower wind speeds, due to the fair weather bias. Since the model mixed layer depth is too deep, the FNOC winds would have to be too high, which is unlikely.

To illustrate the sensitivity of the model predictions during this period, an additional downward heat flux was added to the surface heat flux correction determined by Elsberry et al. (1982). Several model runs with additional

downward heat flux were made. These runs were initialized in February 1978 to reduce computer time. It was found that to predict correctly the trend from March to June 1978 (Fig. 31), an additional downward heat flux of about 5 cal/cm^2/h had to be added each time step from 15 March to 18 June 1978. With the additional heat, the relative errors in heat content dropped dramatically (Table 3) and the spring transition occurred during the same period as the analysis. The resulting horizontal structure features for March and April 1978 (Figs. 32 and 33) were closer to the analyzed structure (Figs. 7 and 8) of CA 12 than the original model predictions (Figs. 19 and 23). The additional heat also created a small warm anomaly along the eastern boundary of the ADS region in March 1978. By April 1978, this warm anomaly covered a larger section of the northeast than was analyzed, but the anomaly features are still closer than the original predictions to the analyzed features. The improvement of the model features, the presence of a warm model anomaly along the eastern boundary and the reduction in relative errors suggests that the most likely cause of the errors at the central point for March and April 1978 is inaccurate atmospheric forcing. However, the downward surface heat flux of 5 cal/cm^2/h did not improve the horizontal temperature anomaly structure for May and June 1978 (not shown). Those fields had much too strong thermal anomalies which did not

resemble the analyzed horizontal structure, although the relative errors in heat content were decreased substantially (Table 3). This suggests that a correction of about 5 cal/cm^2/h of heat should be added, but not entirely as surface heat flux. It is also possible that some other reasons or processes are responsible for the analysis-model differences found in May and June 1978.

TABLE 3

Relative error in model hindcast heat content relative to 200 m at the central point 36.0°N, 150.0°W when the model was initialized on 15 February 1978 (column labeled Hindcast) and when an additional 5 cal/cm^2/h was added to the downward surface heat flux from 15 March to 18 June (last column)

Month	Year	Hindcast	Hindcast + 5 cal/cm^2/h
Mar	1978	-0.021	-0.026
Apr	1978	0.255	0.133
May	1978	0.260	0.062
Jun	1978	0.236	-0.033

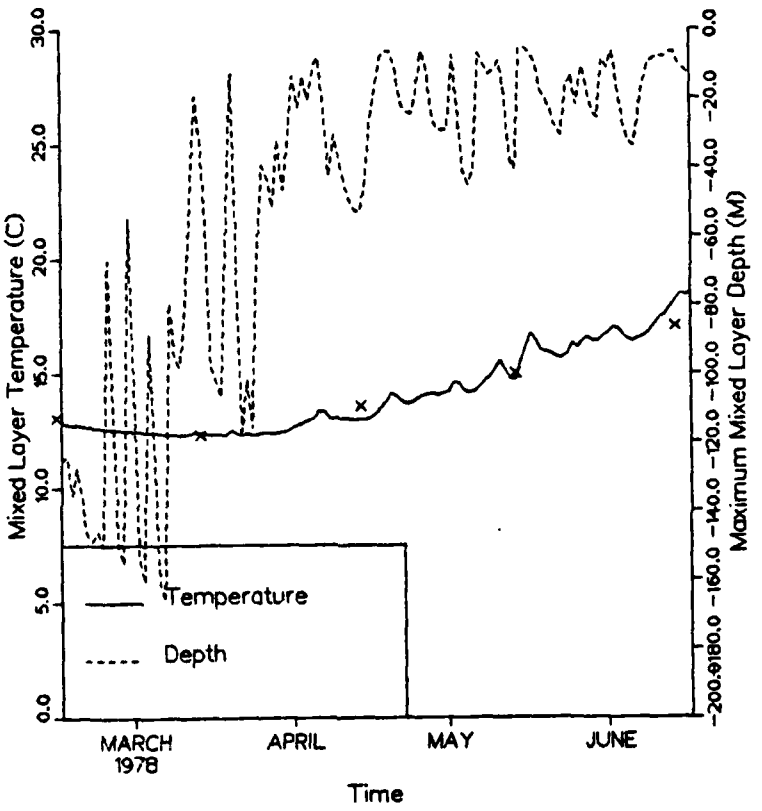

Figure 31. Daily maximum model mixed layer depth and corresponding model mixed layer temperature at the central point of cold anomaly 12, 36.0°N, 150.0°W. The model was initialized on February 1978 and 5 cal/cm^2/h was added each time step to the downward surface heat flux from 15 March to 18 June 1978. The objectively analyzed MLT are denoted by x on the 15th of each month.

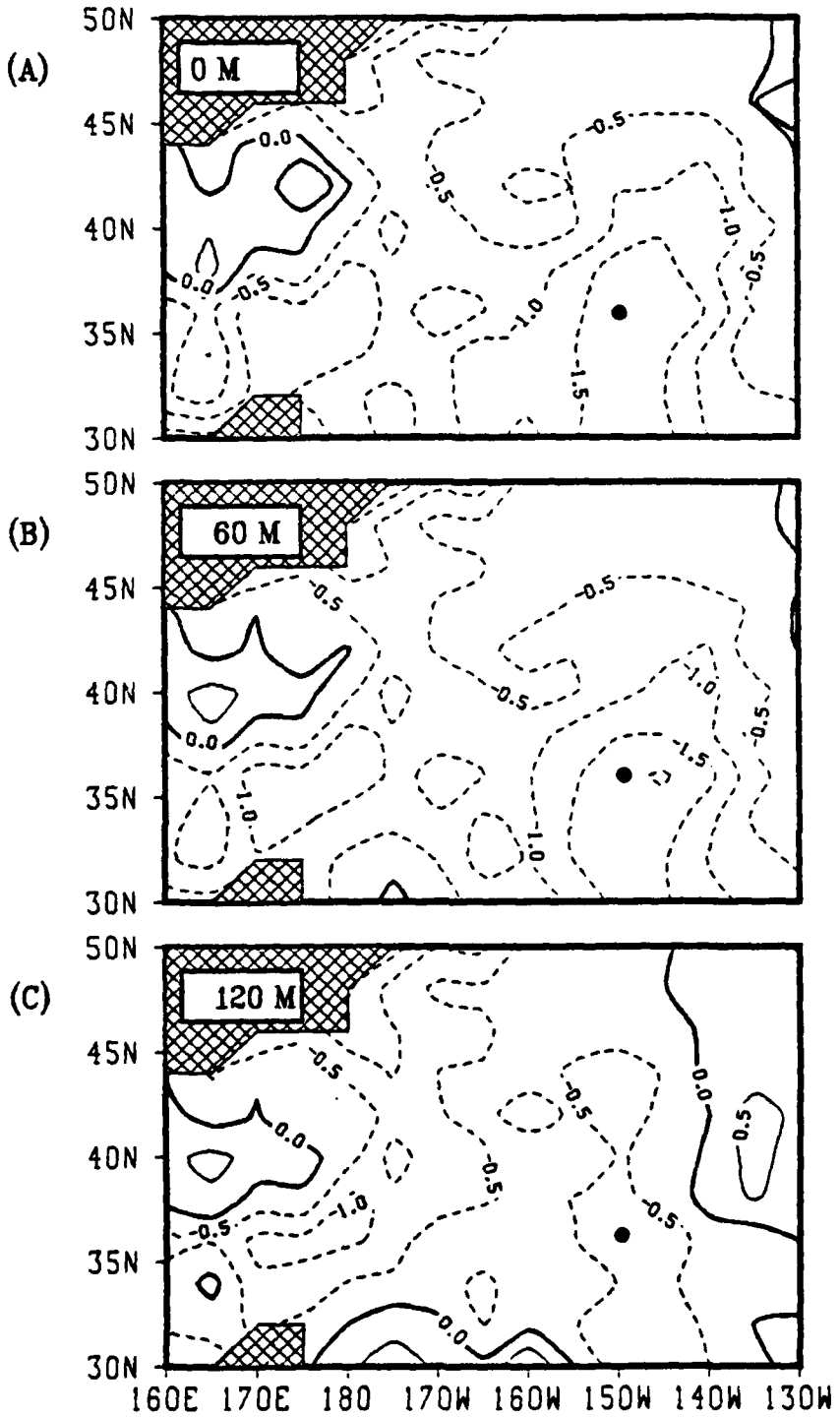

Figure 32. Predicted temperatures (°C) during March 1978 at (A) surface, (B) 60 m and (C) 120 m from the model initialized on 15 February 1978 and integrated with the addition of 5 cal/cm^2/h each time step to the downward surface heat flux from 15 March to 18 June 1978.

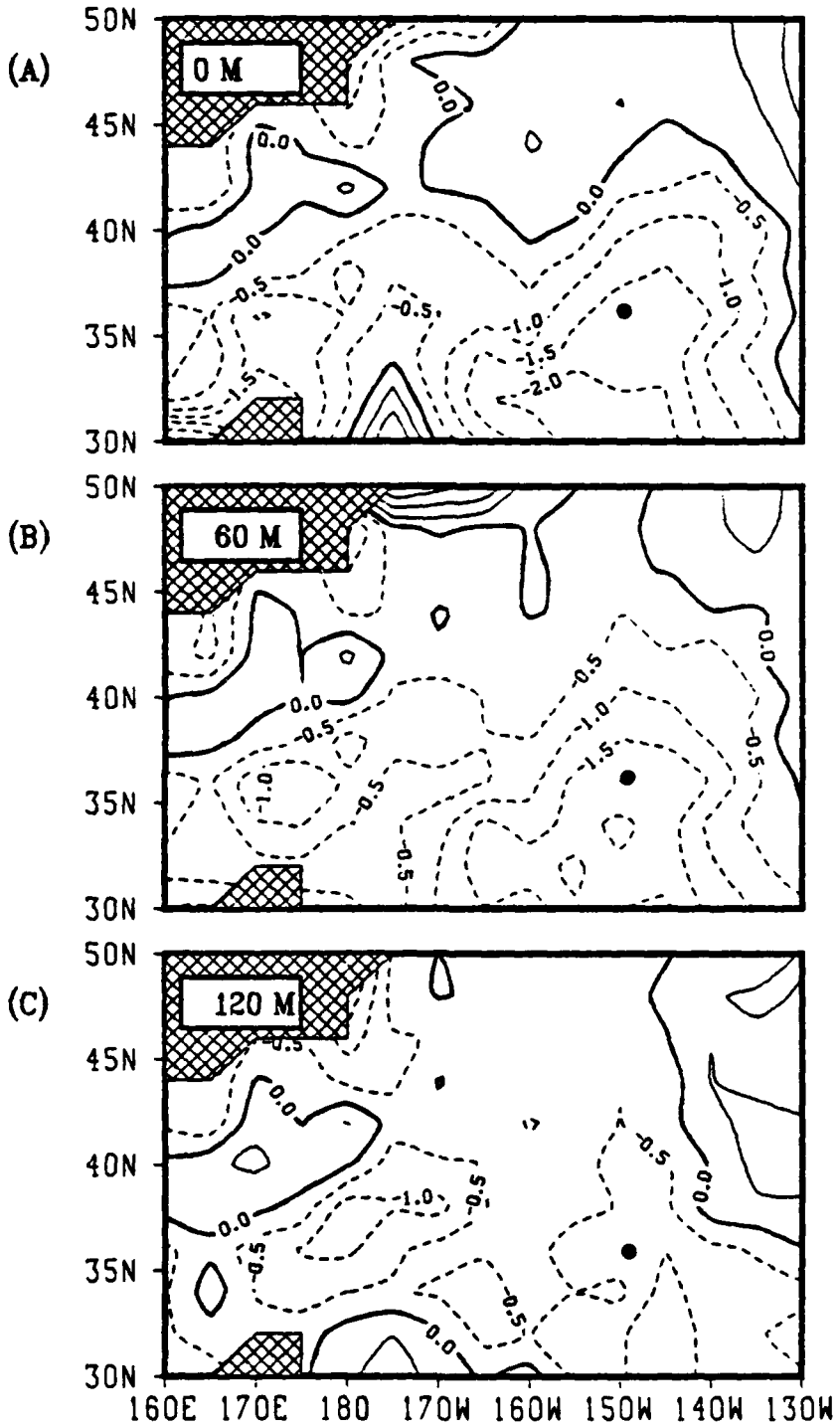

Figure 33. Similar to Fig. 32 except for April 1978.

4. Model Physical Processes

This one-dimensional version of the Garwood model does not treat advective effects. Of the physical processes not included in the model, horizontal advection is the most likely to contribute to the erroneous prediction during the spring of 1978. To examine this effect it is necessary to describe the synoptic situation during the spring. The monthly mean streamfunction fields, calculated from the FNOC winds over the ADS grid, were used to examine the interannual variability in the monthly mean surface pressure fields. The streamfunction is generally proportional to and parallel to the isobars.

During March of 1976, 1977 and 1978 a large anticyclone was centered near 35°N, 135°W and covered most of the eastern North Pacific south of 45°N. This general anticyclonic pattern continued through April with the cell weakening in both 1976 and 1977, but intensifying in 1978. In the northern portions of the ADS area during March and April the winds were generally westerly. During May, the anticyclone was replaced by a cyclonic pattern, except in 1978. The anticyclone was anomalously weak over the southeast of the region (centered approximately 34°N, 145°W) during May 1978. In June of all three years, the eastern Pacific subtropical anticyclone was re-established over the eastern half of the ADS grid.

Two arguments can be given to explain why the model temperatures were too low in May and June 1978. The first

argument concentrates on the atmospheric effects of the anomalous anticyclonic circulation over the eastern part of the ADS area during May 1978. With an anticyclonic circulation, there would be an increased downward solar heat flux due to the clear skies and light winds. Neither of these conditions is conducive to turbulent mixing in the ocean, so that an increase in downward solar heat flux may account for the errors in the spring.

The second argument examines the anomalous surface Ekman and Sverdrup mass transport. The anticyclonic winds during May 1978 are southeasterly over the region of the central point. This is expected to produce a surface Ekman mass transport of warmer water towards the northeast (since the depth-integrated Ekman mass transport is 90° to the right of the wind stress) into CA 12. To balance this convergence and subsequent downwelling caused by Ekman pumping under the atmospheric anticyclone, there must be a geostrophic mass transport such that the total Sverdrup mass transport balances the negative curl of the wind stress. The balancing mass transport is southward bringing colder water into the region of CA 12. There is not sufficient data to say which mass transport is dominant. The observed vertical temperature profiles below the mixed layer for April, May and June 1978 (Fig. 22A) do show that there was warm advection in April, cold advection in May followed again by warm advection in June.

In summary, the synoptic scale flow over the region of CA 12 during April and May 1978 was more anticyclonic than during 1976 or 1977. During March and June the synoptic scale flow over the region of CA 12 was anticyclonic all three years. Either an additional downward heat flux or an Ekman transport of warm water would be consistent with the synoptic conditions. It is not possible to determine which effect is more important due to lack of data.

IV. LARGE-SCALE RAPID TRANSITION CASE

A. COLD ANOMALY 1 DESCRIPTION

The cold anomaly described below was designated and described by Elsberry (1983) as CA 1. CA 1 is a shallow, large-scale, rapid transition event that persisted for approximately seven months. It was the most intense cold anomaly detected in the ADS region during 1976-1979 (Elsberry, 1983).

This cold anomaly is especially dramatic as it occurred after at least six months (the first available map is January 1976) of above-normal temperatures at all depths (Elsberry, 1983). The conditions on the surface during June 1976 (Fig. 34) show that the majority of the ADS region had above-normal temperatures due to a large-scale, warm anomaly centered 36°N, 160°W. For orientation purposes, the ultimate location of maximum intensity or central point (40°N, 165°E) for CA 1 is marked as a dot on the figures. The rate of temperature increase (Fig. 35) from June to July 1976 (Fig. 36) along the western boundary was less than 0.5 times the expected climatological rate. This gave rise to CA 1, which during July 1976 (Fig. 36) included two centers at 42°N, 165°E and 36°N, 165°E with temperatures of -2.47PC and -2.18°C respectively. The southern center appeared to be relatively deep as it penetrated to at least 120 m, but this center did not persist. The eastern anomaly

pattern in the vicinity of 42°N, 140°W in July 1976 (Fig. 36) was designated CA 2 by Elsberry (1983). This anomaly persisted throughout most of the life of CA 1. The very slow rate of temperature increase relative to climatology (Fig. 37) continued into August 1976 (Fig. 38). It was during August 1976 that CA 1 reached maximum intensity (-4.41°C at 40°N, 165°E) and areal extent. At this time CA 1 eradicated the surface signature of a warm anomaly which was located near 42°N, 175°E during July 1976. Even though this cold anomaly is very intense, it is interesting that it was a very shallow feature. As may be seen in Fig. 38, CA 2 also reached maximum intensity (-1.76°C at 42°N, 140°W) and areal extent during August 1976.

Summer warming continued erratically from August to September 1976 (Fig. 39) over the region of CA 1, whereas a cooling trend would have been expected based on climatology. By September 1976 (Fig. 39), CA 1 began to diminish. The northern section of CA 1 was sustained, although the center of -2.32°C was displaced to 42°N, 170°E. The southern section diminished during September 1976, perhaps in response to the arrival of an intense warm anomaly at 60 m and below.

The expected fall cooling occurred between September and October 1976 (Fig. 40) over the entire grid as the rates of temperature decrease (Fig. 41) were of the same order as climatology. During October 1976 (Fig. 40), CA 1

took on a two-cell appearance with centers at 42°N, 180° and 38°N, 165°E and with temperature anomalies of -1.81°C and -1.35°C respectively. The western center extended below 120 m. Between these two centers was a strong warm anomaly at 60 m. From October to November 1976 (Fig. 42), the rate of temperature decrease (Fig. 43) over the entire grid was again much the same as climatology. Thus the anomaly is simply being maintained during September to November rather than being significantly strengthened or diminished. In November 1976 (Fig. 42), CA 1 increased in intensity with depth and extended through 120 m. By December 1976, CA 1 was greatly diminished and had a two-cell appearance through 60 m, with the strongest signature at 120 m (Fig. 44). Above-normal temperatures were present over much of the ADS region in December 1976 (Fig. 44), as the rates of temperature decrease (not shown) were slightly less than climatology. The cold anomaly was not discernible after December 1976.

CA 1 often had a two-cell appearance (Table 4). These changes in the analyzed strength of CA 1 may be the result of the physical mechanisms described in Chapter 3, Section A. In November 1976 at 36°N, 165°E and in December 1976 at 36°N, 160°E, the strength of the anomaly increases with depth. There are several explanations for the decrease in anomalous temperature with depth. A possible explanation is that there was surface Ekman mass transport of warmer

water into the region. Based on the monthly mean stream-function fields for 1976, 1977 and 1978, there was anomalous westerly flow over the region of CA 1 in November and December 1976. This flow would not result in the transport of warmer surface water into the region by surface Ekman mass transport. Instead, it would tend to increase the surface intensity of CA 1. Another possibility is cold advection at depth. However, a complete description of the cause of this anomalous decrease in temperature with depth is not possible due to lack of data and grid resolution.

In summary, CA 1 was a shallow, long-duration, rapid transition event. CA 1 formed between June and July 1976 in the west central section of the ADS domain with two centers of low temperature (Table 4). Anomaly development was rapid over a region in which the temperature increased at a much slower rate than expected from climatology. The cold anomaly reached maximum amplitude and areal extent during August 1976. The intensity of this anomaly was truly remarkable considering that it occurred during the summer. In September 1976, the anomaly started to diminish in size and amplitude. Up through September 1976, the center of lowest temperature tended to be in the vicinity of 41°N, 163°E. As CA 1 diminished, the centers of lowest temperature erratically moved southward. The anomaly persisted above 60 m until October 1976. Portions of the

regions remained colder than climatology through December 1976. The next section describes the model hindcast of CA 1.

TABLE 4

CA 1 development for each month during 1976. The location(s) and temperature(s) are for the lowest temperatures in region of CA 1 for that month.

Month	Location	Temperature
Jul	(1) 42°N, 165°E	-2.47°C
	(2) 36°N, 165°E	-2.18°C
Aug	40°N, 165°E	-4.41°C
Sept	42°N, 170°E	-2.32°C
Oct	(1) 38°N, 165°E	-1.35°C
	(2) 42°N, 180°	-1.81°C
Nov	36°N, 165°E	-0.72°C
Dec	(1) 38°N, 165°E	-1.35°C
	(2) 34°N, 160°E	-0.76°C

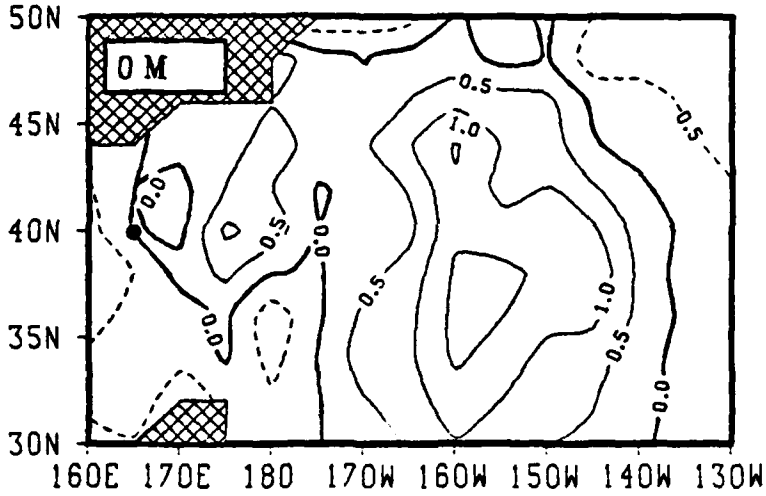

Figure 34. Temperature (°C) anomaly CA 1 at surface during June 1976. The horizontal temperature analysis for each month is centered on the 15th of that month. Negative (dashed) lines represent regions with temperatures less than climatology, zero (heavy solid) same as climatology and positive (light solid) temperatures greater than climatology. The interval is 0.5°C. Cross hatched areas have insufficient data for analysis. Dot marks the ultimate location of maximum intensity of central point (40°N, 165°E) for CA 1.

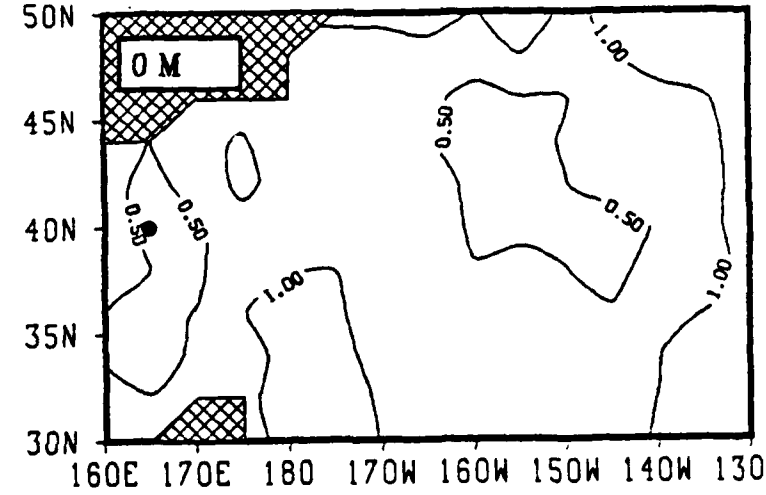

Figure 35. The ratio of change in analyzed temperatures (°C) from 15 June to 15 July 1976 to the same climatological temperature change for the same period. Values greater than 1.0 during this period indicate above-average temperature increases.

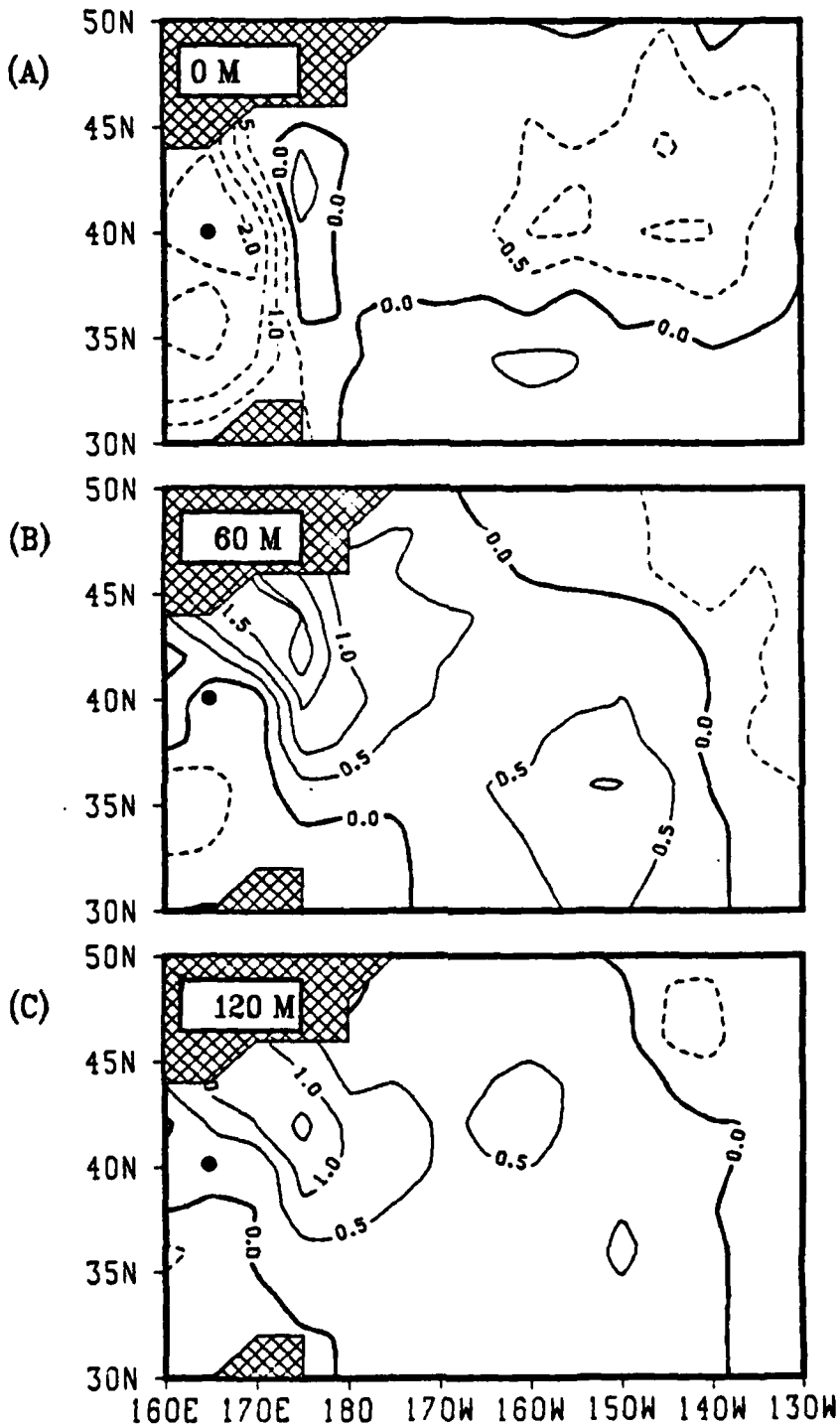

Figure 36. Temperature (°C) anomaly CA 1 during July 1976 at (A) surface (B) 60 m and (C) 120 m.

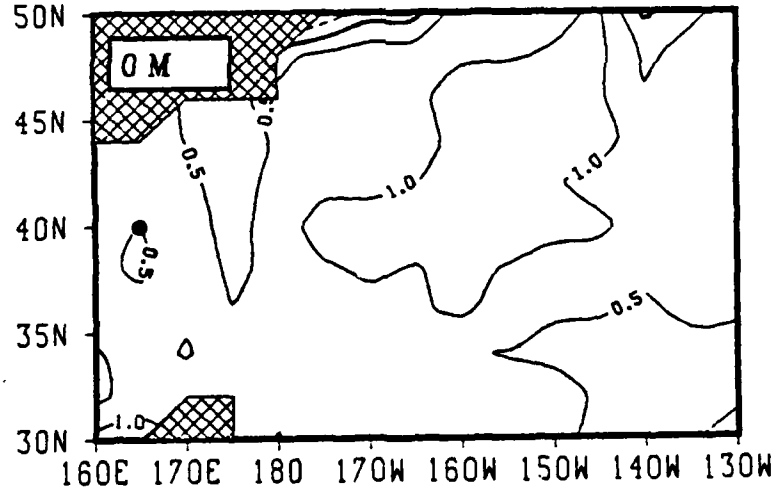

Figure 37. Similar to Fig. 35 except for period from 15 July to 15 August 1976. Values greater than 1.0 indicate greater temperature changes than the normal monthly seasonal increase.

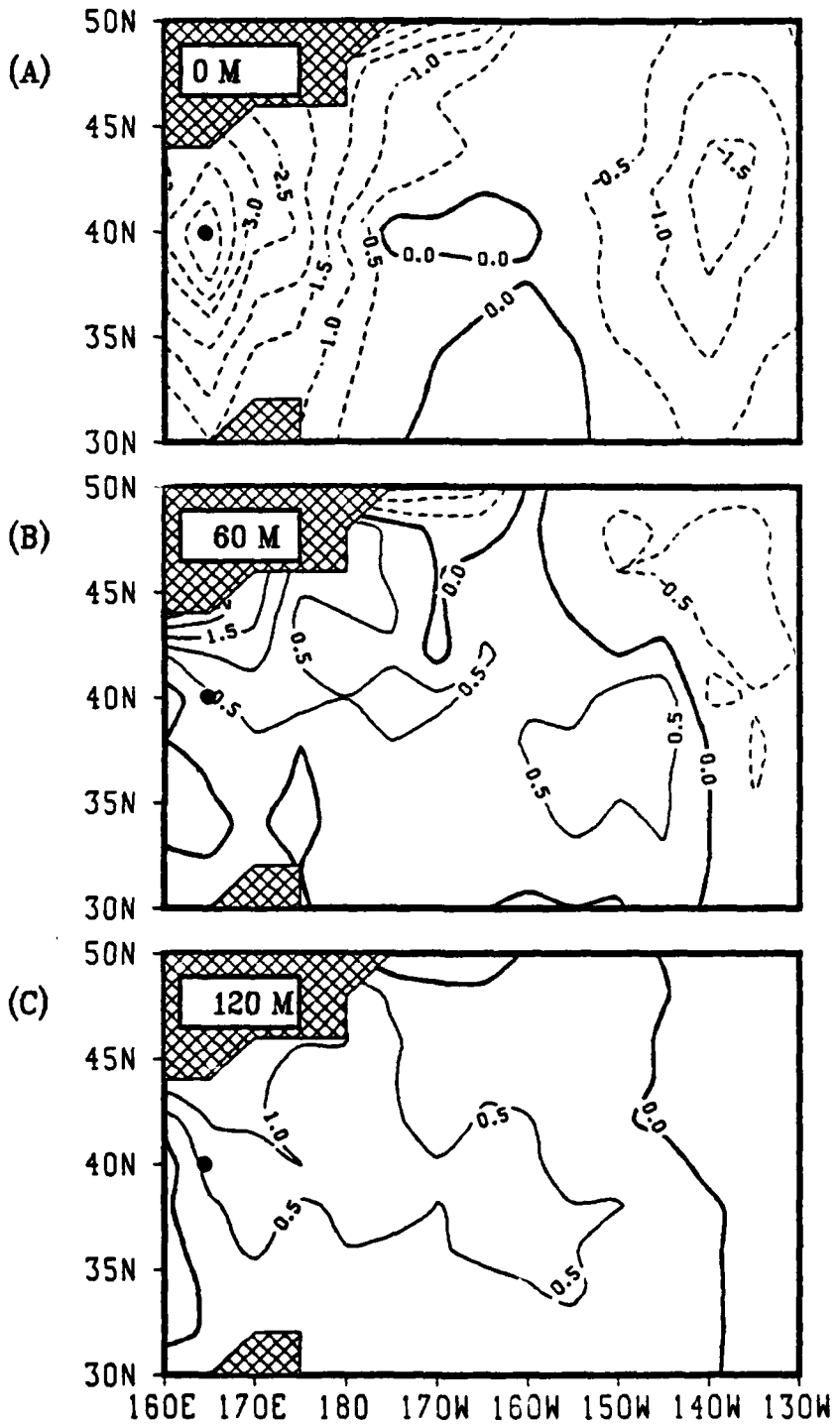

Figure 38. Similar to Fig. 36 except for August 1976.

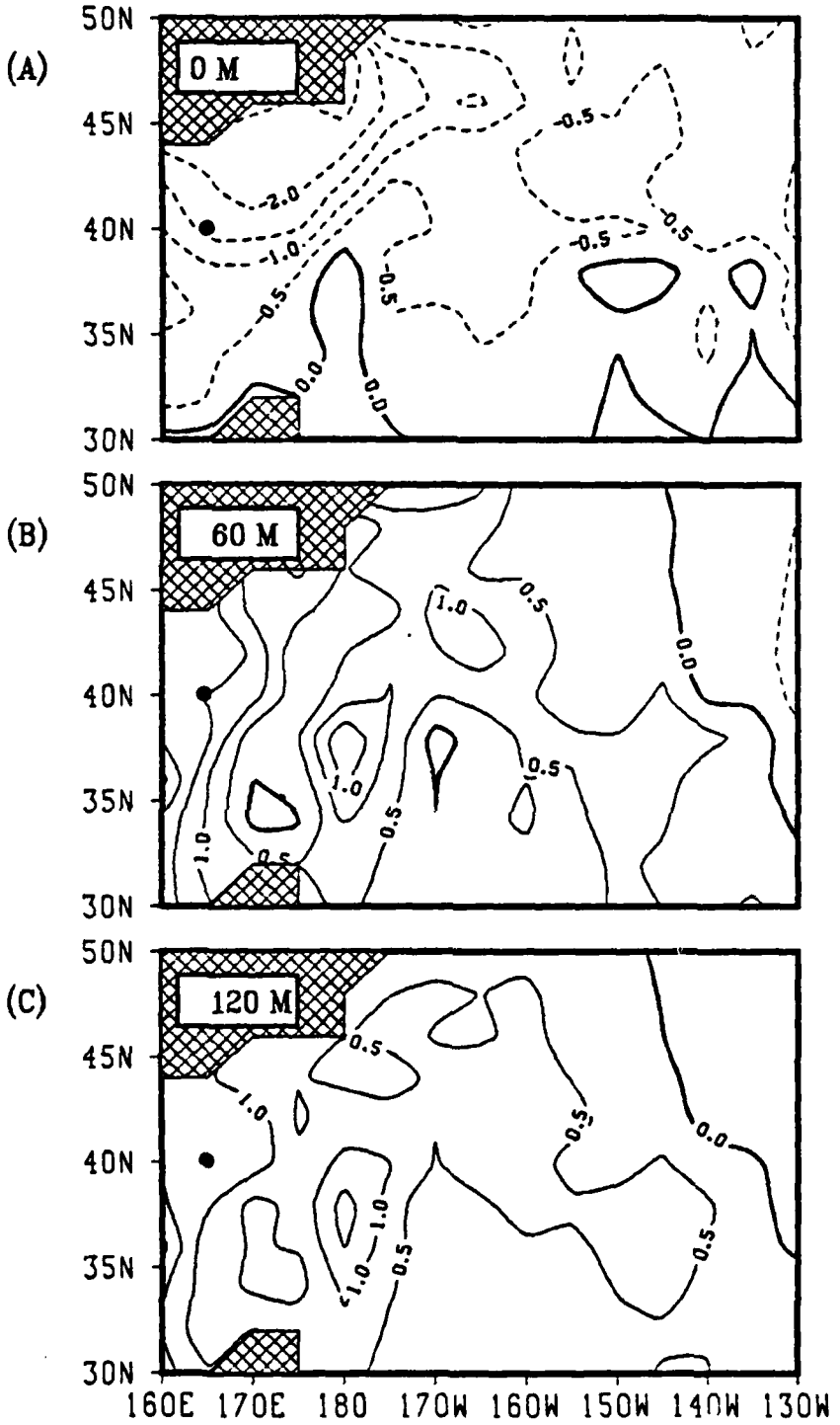

Figure 39. Similar to Fig. 36 except for September 1976.

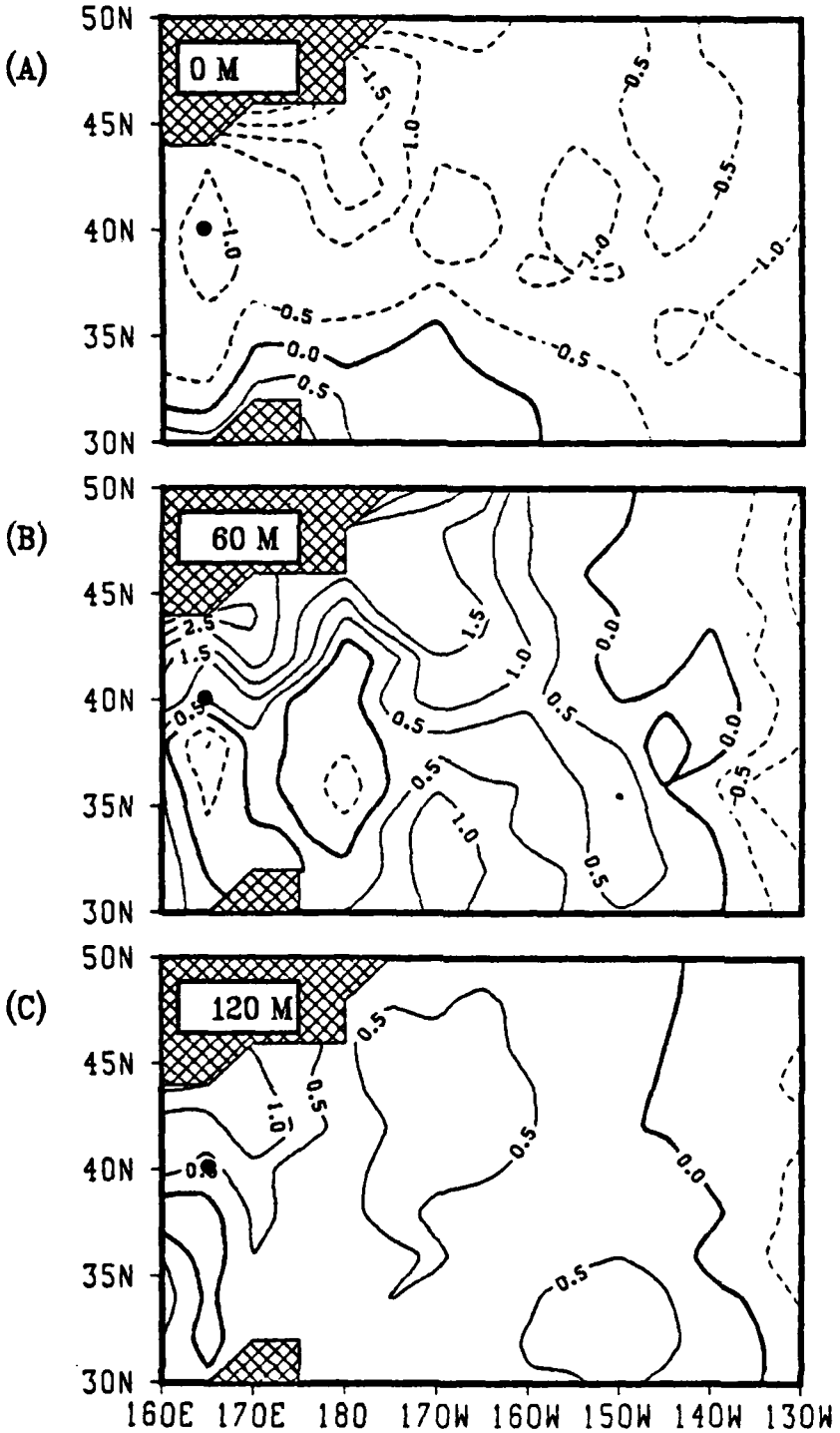

Figure 40. Similar to Fig. 36 except for October 1976.

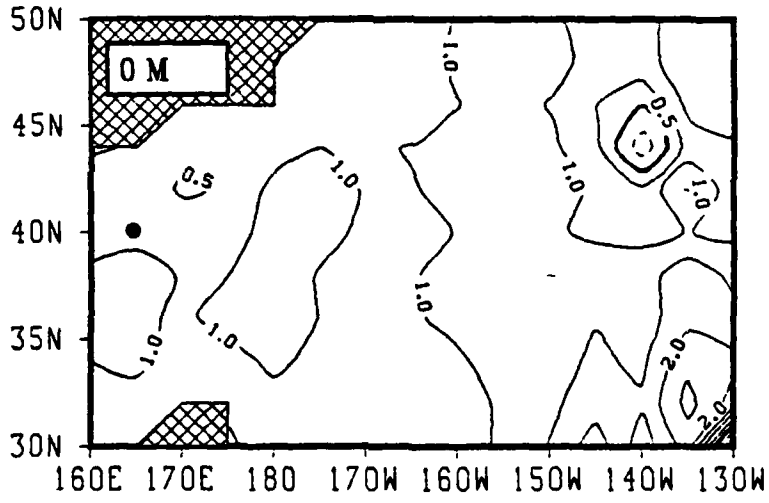

Figure 41. Similar to Fig. 35 except for the period 15 September to 15 October 1976. Values greater than 1.0 indicate greater temperature decreases than the normal monthly change. Negative (dashed) values indicate a temperature increase during a period in which seasonal cooling is taking place; except, in the lower right hand corner where the dashed lines indicate a temperature decrease in an area where climatology is warming.

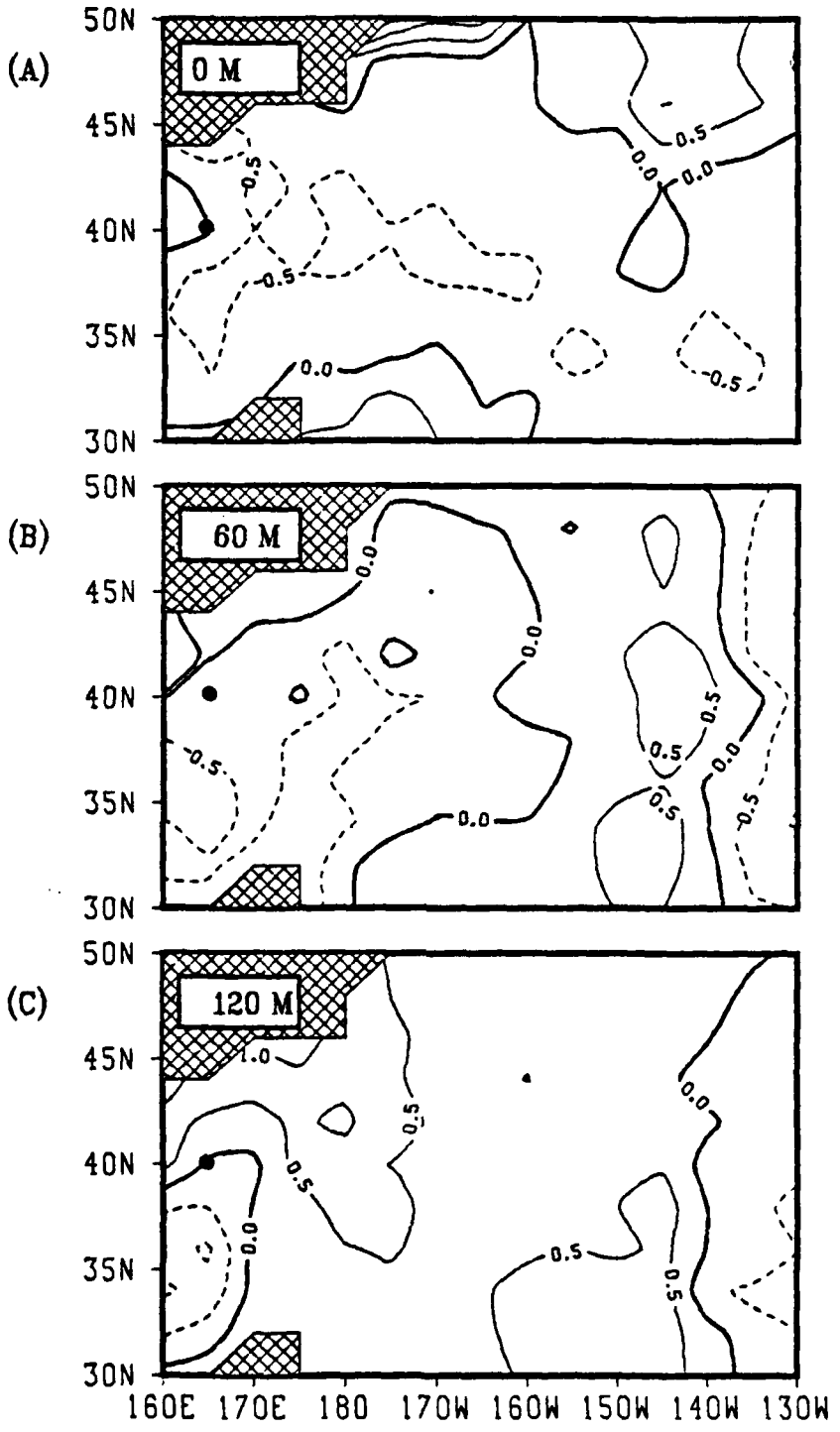

Figure 42. Similar to Fig. 36 except for November 1976.

AD-A139 870 ONE-DIMENSIONAL MODEL HINDCASTS OF COLD ANOMALIES IN THE NORTH PACIFIC OCEAN(U) NAVAL POSTGRADUATE SCHOOL MONTEREY CA G L STRINGER DEC 83 2/2

UNCLASSIFIED F/G 8/10 NL

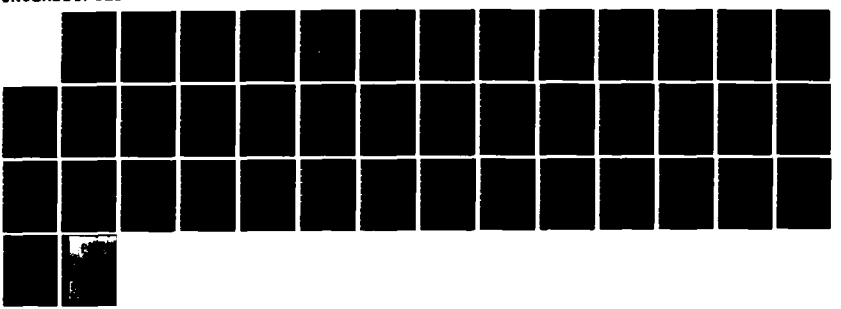

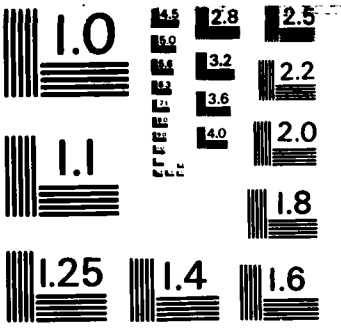

MICROCOPY RESOLUTION TEST CHART
NATIONAL BUREAU OF STANDARDS-1963-A

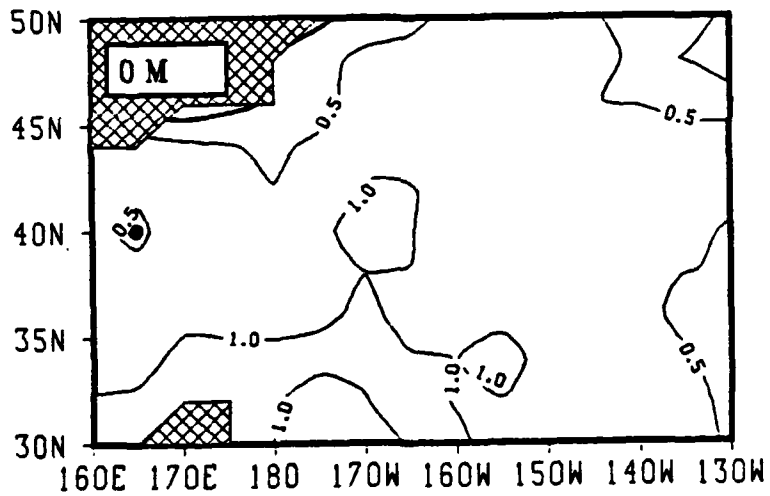

Figure 43. Similar to Fig. 35 except for the period 15 October to 15 November 1976. Values greater than 1.0 indicate greater temperature decreases than the normal monthly seasonal change.

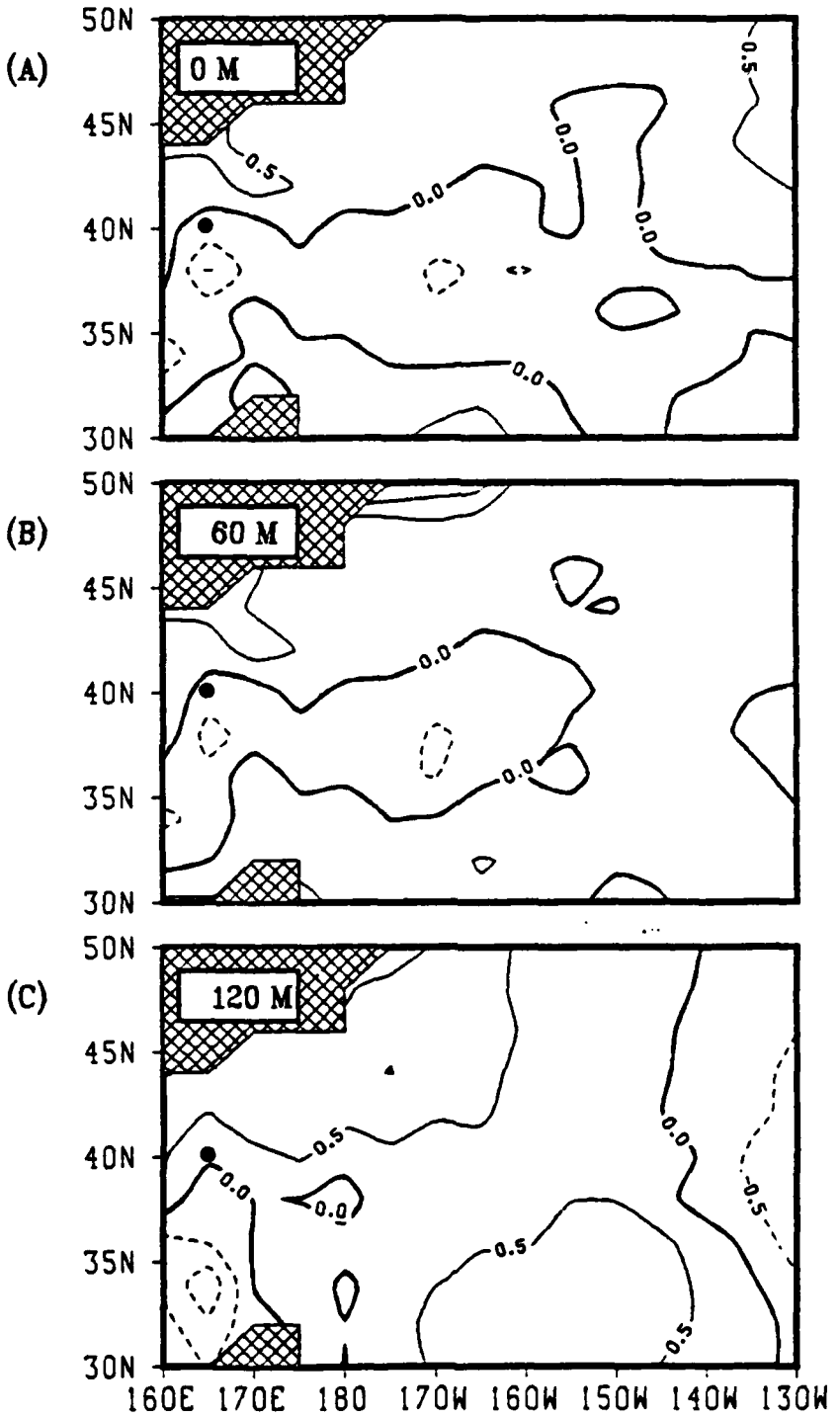

Figure 44. Similar to Fig. 36 except for December 1976.

B. MODEL HINDCAST

The Garwood model was initialized with the TRANSPAC temperature analysis from 15 June 1976 and integrated through 18 December 1976 to cover the life span of CA 1. Instead of hindcasting the extremely intense CA1, the first model prediction created an extremely shallow and warm anomaly. The model results for August 1976 at the surface can be seen in Fig. 45. The daily maximum model mixed layer depth and corresponding mixed layer temperatures (not shown) at the central point (40°N, 165°E) of CA 1 shows that the temperatures are over 15°C higher than analyzed. By December 1976, the mixed layer temperature is about 5°C higher than analyzed. As shown in Fig. 45, these high surface temperatures are part of a zonal surface temperature pattern with temperatures much too high in the regions south of 42°N and too low in the northern regions. The predicted surface temperatures are particularly high to the west of 180° longitude. The next section will investigate the reasons and processes that could produce erroneous results.

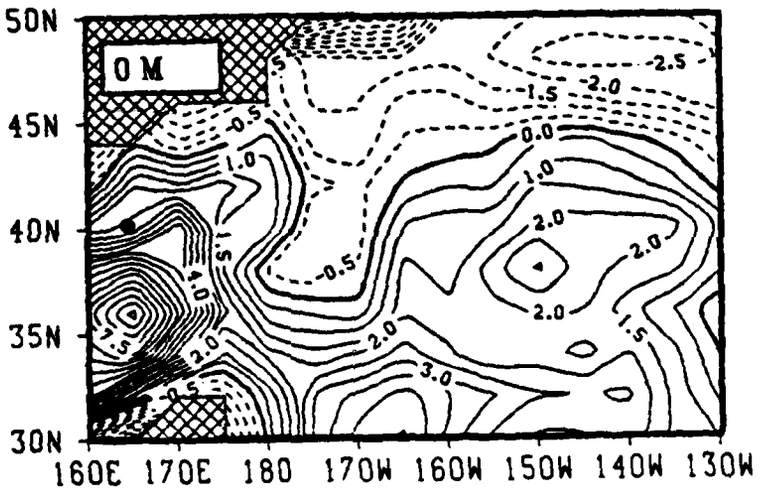

Figure 45. Model temperature (°C) anomaly MA 1 at the surface during August 1976. The model used the surface heat flux correction relative to 200 m as determined by Elsberry et al. (1982).

C. ERROR DISCUSSION

The model anomaly field bore little resemblance to that analyzed, and did not produce a cold anomaly in the region of CA 1. The poor model results could be a function of (1) data quality; (2) model physics; and (3) model forcing. Each of these areas will be examined in more detail in the next three sections.

1. Data Quality

The original objective analysis procedure used by White and Bernstein (1979) generates values at all grid points regardless of whether any observations are present in the vicinity of the grid points. In a data-sparse region, a faulty XBT could significantly degrade the quality of the monthly objectively analyzed values at the surrounding grid points and cause a temperature bias with depth. However, one would expect that the objective analysis technique would tend to eliminate such a bias if other correct profiles are in that region.

CA 1 is the most intense anomaly observed by Elsberry (1983) during 1976-1979 (Fig. 46). CA 1 is about 2.5°C colder than the next coldest anomaly. It is possible that the extreme intensity of CA 1 is due to erroneous data. However, neither the XBT profiles nor the data distribution maps for the life span of CA 1 are available to determine if this factor can explain part of the model discrepancy.

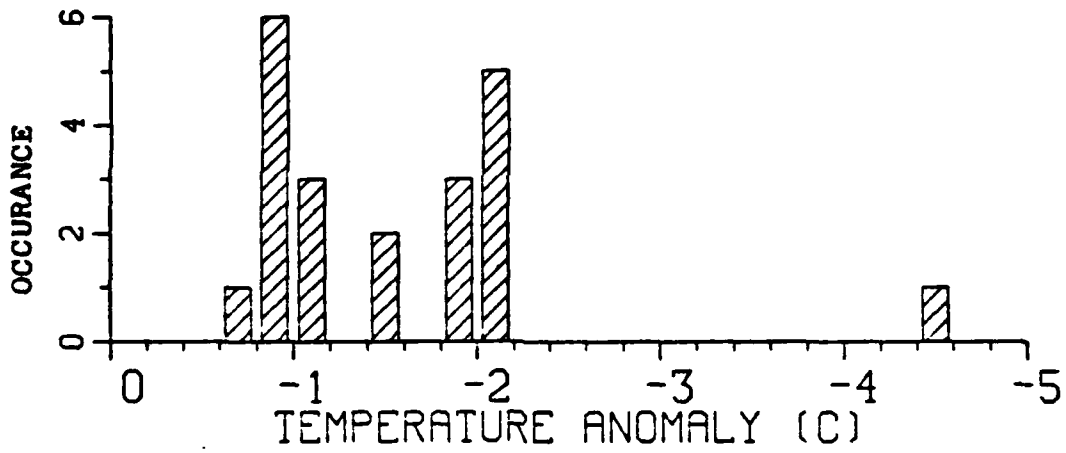

Figure 46. Histogram showing the occurrence of cold anomalies during the period January 1976 to December 1979. CA 1 is on the extreme right in the histogram (from Elsberry, 1983).

2. Model Physics

Because Garwood (1977) found that shear production significantly affected entrainment mixing in relatively limited conditions, the version of the model used here does not contain equations for mean momentum or a term for shear production in the turbulent kinetic energy equation. However, there is some evidence as reported by Price (1981), Kraus (1981) and Martin (1982) for the importance of shear as a mixing mechanism. Martin (1983) suggests that the Garwood model would benefit from the inclusion of shear production due to the mean current, in that augmented shear production should prevent overly shallow mixed layers from persisting. In the Garwood model, the time derivative terms in the entrainment equation are dropped when the layer is shallowing, and the new mixed layer depth is solved for algebraically. The absence of entrainment shear production may account for some of the model tendency toward too high sea-surface temperatures during the spring and summer.

The parameterization of the absorption of solar radiation in the vertical may be another source of error. A discussion of the parameterization of the flux of solar radiation, Q_s, in the Garwood model is provided in the appendix. Fifty percent of the incoming solar radiation is absorbed in the upper meter of the ocean. The fraction that penetrates to greater depths can have a significant effect on the development of the upper ocean thermal

structure. In spring and summer, solar radiation provides a direct means of heating the seasonal thermocline below the mixed layer. During cloudy periods and storms, the reduction of the solar radiation means less heat will be directly absorbed in the mixed layer, which reduces the thermal gradient below the first meter, and allows for deeper mixing. The turbidity of the water also affects the distribution of solar radiation in the vertical. An increase in turbidity (not included in the model) during the spring and summer could increase the sea-surface temperature and the stratification below the mixed layer, while decreasing the mixed layer depth and the warming of the ocean below the mixed layer.

CA 1 might also be caused by the advection of a cold ocean eddy into the region. White and Bernstein (1979) emphasize that the baroclinic eddy activity west of 175°W was considerably greater than to the east, where the large-scale variability dominates. The transition near the Emperor seamount chain between the strong and the weak eddy regions was quite abrupt, of the order of 5-10° of longitude (Bernstein and White, 1977). Eddies south of the Kuroshio extension would be cold, which agrees with the anomalous temperatures in the region of CA 1. The decay of a cold eddy is also consistent with the analyzed temperature structure. That is, a cold core eddy could have arrived in the region of CA 1 between July and August 1976 and as

the eddy decays the region would be increasing in temperature ans still be colder than climatology. The transitional speed of CA 1 can not be determined accurately using the monthly position(s) of maximum intensity (Table 4). The grid size of 2° latitude by 5° longitude is too coarse to describe the evolution of mesoscale events. Using the -2.0°C isotherm in Fig. 37 to define the edge of CA 1 in August 1976 gives a radius of about 650 km. This radius is approximately 13 times the baroclinic Rossby radius of deformation. Thus if CA 1 was a cold eddy, one would expect a large vertical extent. However, this is not seen as CA 1 in August 1976 (Fig. 38) is completely above 60 m. Since the vertical extent is so small and the horizontal scale so large, it is unlikely that CA 1 is one large eddy.

3. Model Forcing

It is necessary to first determine if the errors are due to an initial value problem associated with initializing after the spring transition when the mixed layer is shallow and warm. According to Martin (1983), errors due to model initialization are minimized by initializing during the winter when the mixed layer is deep. After the mixed layer shallows in the spring and the seasonal thermocline begins to form, the model results are fairly independent of the initial conditions. To test the contribution from this source of error, the model was initialized with the 15 February 1976 analysis and integrated through

18 December 1976. The results of this test showed that the errors are not due to an initial value problem as again the mixed layer was too shallow and too warm throughout the integration period, and especially during the summer months.

Since the first model predictions with the bimonthly heat flux correction fields determined by Elsberry et al. (1982) were too warm in the region of CA 1, the model was run without the surface heat flux corrections. The integration period was from 15 June to 18 December 1976. The daily maximum model mixed layer depths and corresponding mixed layer temperatures at the central point (Fig. 47) were substantially improved over the first prediction. The predicted mixed layer temperature anomaly for August 1976 was within 1°C of the -4.41°C value. However, large negative temperature errors occurred in the remainder of the ADS domain. This can be clearly seen in the model hindcast for the surface during August 1976 (Fig. 48). The errors were largest along the southern boundary of the ADS region. Plots (not shown) of daily maximum mixed layer depth and corresponding temperature at 38°N, 160°W and at 42°N, 135°W showed that a seasonal thermocline was not established. These results agree with earlier studies (Elsberry et al., 1979; Budd, 1980; Steiner, 1981) which found that the monthly surface heating from FNOC does not have a sufficiently large seasonal amplitude. These studies also found a persistent bias toward excessive heat loss along the

southern boundary of the domain. Thus a downward surface heat flux correction is definitely needed in the region, even if it is not at the location of CA 1. Consequently, it was decided to examine carefully the June-August surface heat flux correction fields as determined by Elsberry et al. (1982).

For comparison, the model results with the correction field during the summer of 1978 were examined. The model was initialized with the 15 June 1978 analysis and integrated through 18 August 1978 to illustrate the effect of the June-August surface heat flux correction fields. If the model did not predict the anomalous conditions by August, then it would not get the anomalous conditions after August correct either. Model runs were made with and without surface heat flux correction fields. From the model integration without the correction fields, it was very apparent that as for 1976, a downward heat flux correction is needed to correct a bias of excessive upward heat flux over the ADS region. The model integrations with the correction fields predicted mixed layer temperatures that were too cold in 1978 compared to being too warm in 1976. Thus, the model integrations suggest that the corrected heat flux underestimates the heat flux required for June to August 1978, and overestimates that required for 1976 in the region of CA 1.

The analyzed vertical temperature profiles at 40°N, 165°E for June, July and August of 1976, 1977 and 1978 were examined. The evolution of the profiles during two (1977 and 1978) of the three years were very similar, while the period of CA 1 development during 1976 was quite different. The analyzed vertical temperature profiles for August of 1977 and 1978 were characterized by shallow, warm (<5 m, about 24°C) mixed layers. Even though the mixed layer was also shallow in August 1976 (<5 m), the temperature was about 7°C colder.

A comparison of the model forcing without the surface heat flux correction from June to December for the three years showed that 1976 had noticeably less (about 10-20 $cal/cm^2/h$) total upward flux than the other two years over most of the period. This is consistent with the analyzed mixed layer temperature for August 1976 being much lower than during the other two years. There were no dramatic differences in the wind speed or solar radiation fields among the three June-August periods.

In summary, the surface heat flux forcing is definitely a potential error source. Although the heat correction field derived by Elsberry et al. (1982) may be appropriate to the normal large-scale evolution, it is not appropriate to model predictions of the development of CA 1 from June to August 1976. Thus a new surface heat flux correction field for the period June-August 1976 is described in the next section.

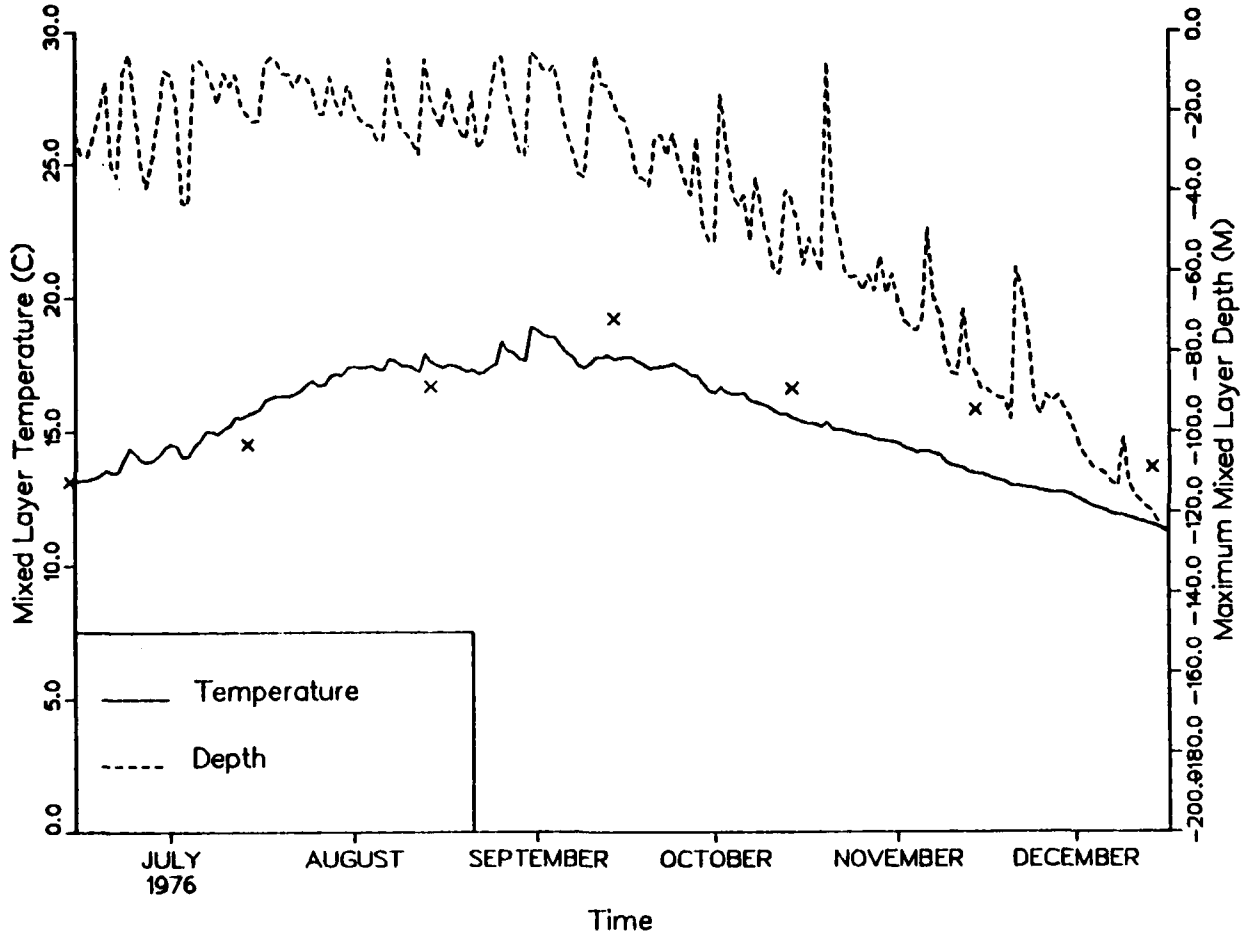

Figure 47. Daily maximum model mixed layer depth and corresponding model mixed layer temperature (MLT) resulting from no surface heat flux corrections being applied compared to objectively analyzed MLT (denoted by x on the 15th of each month) at the center of CA 1 40.0°N, 165.0°E from 15 June to 18 December 1976.

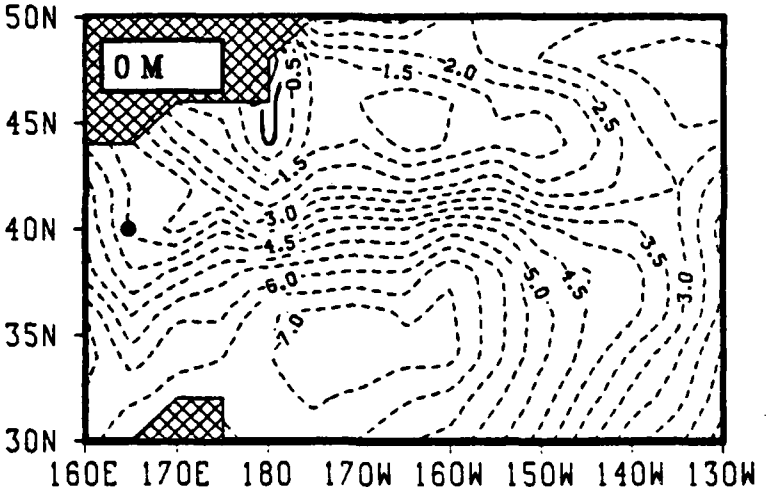

Figure 48. Model temperature (°C) anomaly at the surface during August 1976. No surface heat flux correction was applied in the model.

D. REVISED HEAT FLUX CORRECTION

CA 1 occurs during a period of ocean warming ($\Delta H > 0$) and net downward (but less than expected from climatology) surface heat flux ($Q_T > 0$) which produces excessive warming ($\Delta H - Q_T > 0$). Elsberry et al. (1982) determined that this type of error would occur 26.8% of the time using the corrected total heat flux. The heat flux correction fields for the June-to-August period as determined by Elsberry et al. (1982) are based on only three years. Their basic assumption is that the error in the surface heat flux is systematic and that an average over the three years will give a stable estimate of the required correction. However, it was shown above that the changes in heat content during 1976 were markedly different. Therefore a new heat flux correction field is derived specifically for the 15 June to 18 August 1976 period. The purpose is to determine if the model can predict the correct vertical distribution of the heat if an improved estimate of the total surface heat flux is provided.

The change in oceanic heat content relative to 200 m is

$$\Delta H = H(t + \Delta t) - H(t), \qquad (3)$$

where Δt = two months (June - August 1976) and H relative to 200 m is given by

$$H = \rho_o C_p \int_{-200}^{0} (T(z) - T(200))\, dz\ . \qquad (4)$$

It is expected that ΔH will be positive during this period of net downward heat flux (roughly between April and September). A two-month interval was used to be consistent with the heat correction field derived by Elsberry et al. (1982). They found that bimonthly correction fields were simple to apply and representative of the seasonal variation. This two-month interval is also the time during which CA 1 reached maximum intensity and spatial extent.

The following budget equation is assumed:

$$\Delta H = \int_0^{\Delta t} Q dt + \text{Residual} = Q_T \Delta t + \text{Residual} . \quad (5)$$

The integral sign indicates that the air-sea flux is summed over the same time interval that ΔH is evaluated. Q_T is defined as the total surface heat flux and can be expressed as the time integral of:

$$Q_T = Q_s - (Q_b + Q_h + Q_l) = Q_s - Q_{sfc} , \quad (6)$$

where the subscripts s, b, h and l refer to solar, back, sensible and latent heat fluxes through the sea surface. Q_{sfc} is surface heat flux. The residual term includes non-local physical effects (especially horizontal advection) and the errors in estimating the heat content changes and the surface fluxes. This budget equation assumes that vertical processes dominate the horizontal, and for the space and

time scales in this study, that the local change in heat content over the given period should be balanced by the vertical flux of heat at the air-sea interface.

The analyzed temperature fields and the model physics were assumed correct. Using predicted temperature fields for August 1976 determined without any heat corrections and the analyzed temperature fields for August 1976, a new bimonthly surface heat flux correction relative to 200 m at each grid point is

$$\begin{aligned} \text{correction} &= (\Delta H_{\text{mod(Aug)}} - \Delta H_{\text{anal(Aug)}})/\Delta t \\ &= (H_{\text{mod(Aug)}} - H_{\text{anal(Aug)}})/\Delta t \end{aligned} \quad . \qquad (7)$$

The correction field (Fig. 49) with units of cal/cm^2/h was added to the FNOC surface heat flux each hour in the model integration. The solar radiation fields are assumed to be correct. Negative values in the resulting correction field (Fig. 49) indicate that the upward heat flux is to be reduced by the amount shown. It can be seen that H_{mod} and H_{anal} are approximately equal at the central point (40°N, 165°E), so that only a small correction is required.

The model was initialized with the 15 June 1976 analysis and integrated through 18 August 1976 (Fig. 50). The intensity of CA 1 is correctly hindcast, although the gradients around the anomaly are too large. There is also a warm anomaly along 170°E which is not present in the analyzed anomaly field (Fig. 38A). The shape of the

anomalous warm region in the mid-southern section of the ADS domain is in agreement with that analyzed, albeit with much too high temperatures. It may also be seen in Fig. 50 that there is some weakening of the anomalous features through the middle of the ADS domain. The model does hindcast the eastern region as cold, which agrees with the analysis.

At the central point of CA 1 (Fig. 51), there is very good agreement between the monthly objective analyzed mixed layer temperature and the temperature corresponding to the daily maximum mixed layer depth. The good agreement at this point was expected from Fig. 47 since the new correction is almost zero. Major improvements due to the new correction field relative to either the original (Fig. 45) or no (Fig. 48) correction are found through most of the domain.

To determine if further improvements in the surface anomaly field could be made, two other correction fields were derived. As the summer mixed layer is shallow and warm, the local atmospheric effects are only felt in the upper 100 m. Thus a correction field based on the heat content changes relative to 100 m was produced (Fig. 52). The model was then initialized with the 15 June analysis and integrated with this correction field added to the FNOC surface heat flux fields through 18 August 1976. The resulting surface anomaly field (Fig. 53) is less representative of that analyzed than in Fig. 50. The eastern, middle

and southern sections were not hindcast well. In the region of CA 1, the temperature of the predicted anomaly is too low and the anomaly center is displaced northward.

Since the anomaly in August 1976 is present above 60 m, it is possible that the heat flux correction field should be based on the heat content changes in the upper 50 m. Therefore, a correction field relative to 50 m (Fig. 54) was also produced. The model was then integrated over the same time period as previously. The resulting surface anomaly field (Fig. 55) is a much poorer representation of the analyzed field (Fig. 38A) than the predicted fields with surface heat flux correction fields relative to 100 and 200 m. One region of improvement in Fig. 55 is in the eastern section, although the improvement is small relative to Fig. 50.

The pattern correlation was calculated between the analyzed and predicted temperature changes between 15 June and 15 August 1976. These calculations are over an area bounded by 34°N, 44°N, 170°E and 135°W. The pattern correlation for the model integration with the surface heat flux correction relative to 200 m was 0.49, while the pattern correlation for the model integration with the correction field relative to 100 m was -0.05. Based on these and the previous results, the new correction field relative to 200 m was judged to be better. The improved results with the larger depth suggest that this calculation is more effective in removing some of the effects of horizontal advection and changes in heat content due to vertical

displacements of the thermocline. Making the corrections relative to 50 and 100 m may intertwine these effects with the effects of local atmospheric forcing.

In summary, if the best possible estimate of the surface heat flux is provided, the model predictions were improved, although they were only a fair representation of the analyzed August 1976 fields. One possible source of error is the assumption that the total correction should be applied to the surface heat flux. Perhaps a fraction of the correction field should be applied to the solar heat flux. The areas of erroneous high temperatures in the model predictions may also be due to the absence of shear production due to the mean current. It is possible that non-local atmospheric forcing and events may contribute to the poor model performance. Given the available data, it is not possible to separate the effects of three-dimensional processes, poor forcing, inaccurate ocean analyses and incomplete model physics and parameterizations.

The very strong anomalous conditions associated with CA 1 are at least partly due to the anomalous atmospheric forcing during the period. Unfortunately, the magnitude of the anomalous forcing appears to be of the same order of magnitude as the bias in the FNOC surface heat flux fields. When the uncertainties in the heat correction field are large, the ability of the model to predict anomalous ocean conditions cannot be satisfactorily tested. These tests

with a single case would suggest that improvements in the FNOC surface heat flux are required. It is hoped that the new Navy Operational Global Atmospheric Prediction System will provide these improved fields.

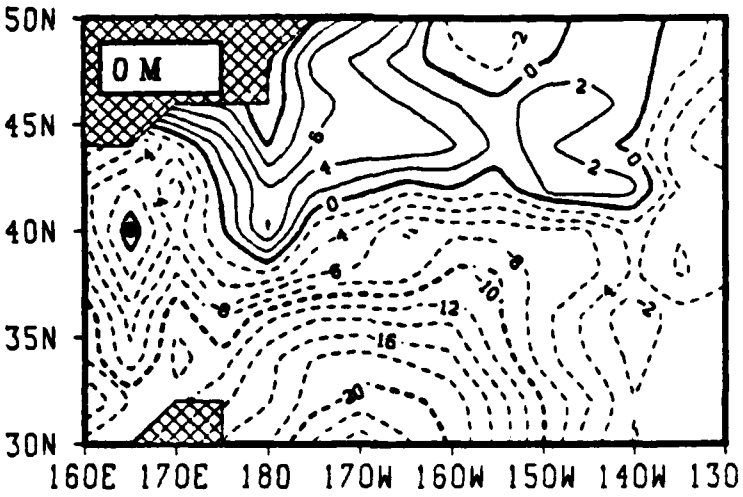

Figure 49. Correction field (cal/cm^2/h) relative to 200 m for 15 June to 18 August 1976 to be applied to the FNOC surface heat flux fields. Negative values indicate that the upward heat flux is to be reduced by the amount shown.

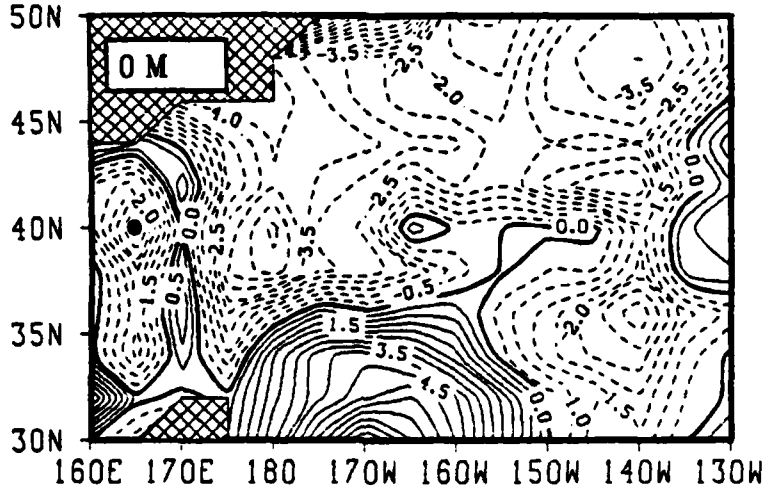

Figure 50. Model temperature (°C) anomaly at the surface during August 1976 resulting from the correction field relative to 200 m being applied to the FNOC surface heat flux fields.

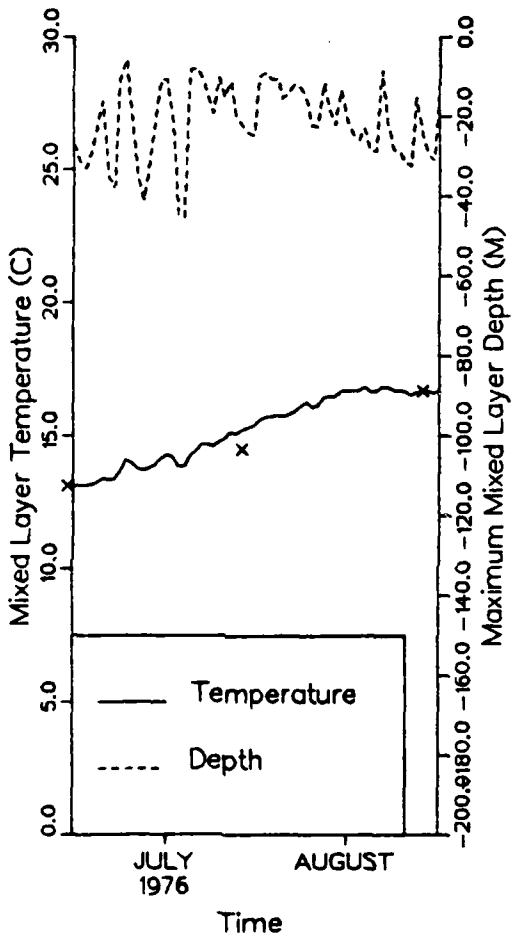

Figure 51. Daily maximum model mixed layer depth and corresponding model mixed layer temperature (MLT) resulting from the new correction field relative to 200 m being applied, compared to objectively analyzed MLT (denoted by x on the 15th of each month) at the center of CA 1 40.0°N, 165°E from 15 June to 18 August 1976.

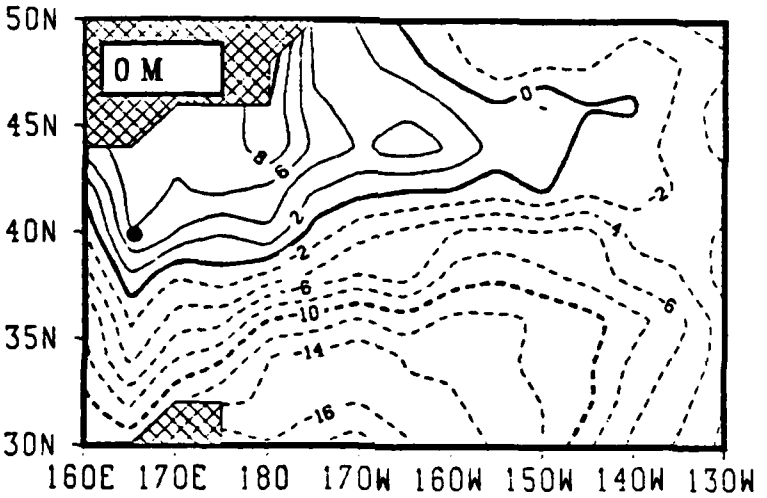

Figure 52. Similar to Fig. 49 except for correction field relative to 100 m.

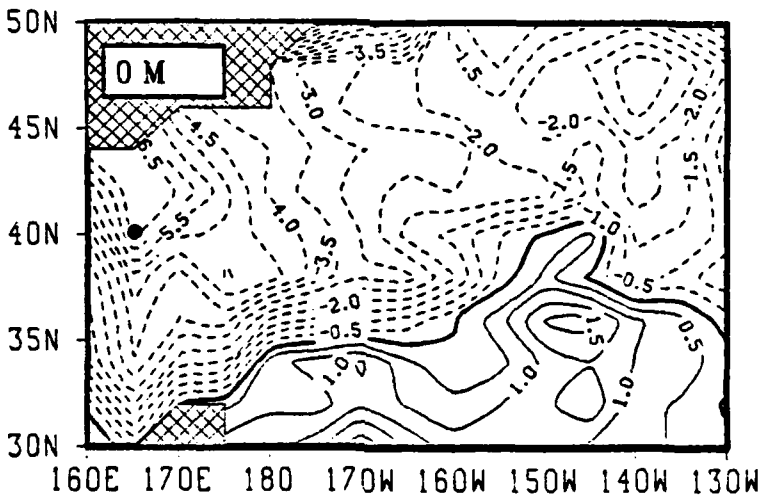

Figure 53. Similar to Fig. 50 except for the application of the correction field relative to 100 m.

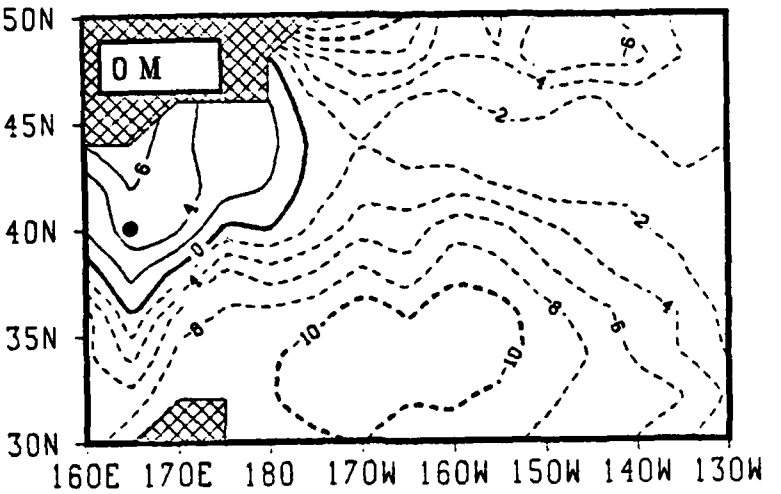

Figure 54. Similar to Fig. 49 except for correction field relative to 50 m.

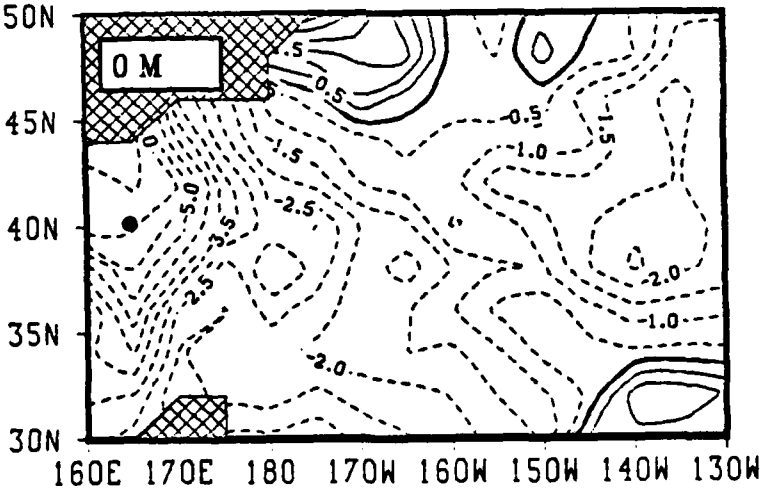

Figure 55. Similar to Fig. 50 except for the application of the correction field relative to 50m.

V. CONCLUSIONS

The Garwood model does a very commendable job of hindcasting the large-scale long duration anomaly CA 12 through the autumn of 1977 and winter of 1978. Errors in the model prediction increased substantially in the spring, following the analyzed spring transition between 15 March and 15 April 1978. It was found that an additional downward surface heat flux of 5 cal/cm^2/h during this period produced improved predictions. With the additional heat flux correction the model spring transition occurred during the same period as the analysis. For March and April 1978, the improvements of model features, the presence of a warm anomaly along the eastern ADS region boundary and the reduction in relative heat content errors, suggest that the most likely cause of errors at the central point for these two months is inaccurate atmospheric forcing. However, the additional downward surface heat flux did not improve the horizontal temperature anomaly structure for May and June 1978. Those fields had much too strong thermal anomalies which did not resemble the analyzed horizontal structure, although the relative errors in heat content were decreased substantially. This suggests that a correction of about 5 cal/cm^2/h of heat should be added, but not entirely as a surface heat flux. In May and June 1978, there was anomalous anticyclonic flow

over the region of CA 1. Thus, either an additional downward solar heat flux and/or Ekman transport of warm water could be the process by which the additional heat needs to be distributed in the model.

These results verify the hypothesis that CA 12 was primarily generated by the vertical mixing processes during the autumn of 1977 and the winter of 1978. That is, the mixed layer temperature change is related to one-dimensional processes to the first order. The usefulness of the heat flux correction fields, derived by Elsberry et al. (1982), for FNOC surface heat flux estimates in North Pacific Ocean predictions was demonstrated during the autumn of 1977 and the winter of 1978. The model results for CA 12 in the spring suggested that in periods of rapid change (i.e., spring transition) a better estimate of the surface heat flux is required. The results for CA 1 emphasized this.

It was found from the hindcast of CA 1 that the heat flux correction fields derived by Elsberry et al. (1982) were not satisfactory for June to August 1976. A new surface heat flux correction field was derived specifically for 15 June to 18 August 1976. This new heat flux correction exactly accounts for the difference in the predicted (without correction) and analyzed temperature profile heat content relative to 200 m. With this more correct estimate of the surface heat flux, the model did produce an improved result

which was a fair representation of that analyzed for August 1976. However, there were still errors in the model results. Perhaps some of the heat flux correction needs to be applied to the solar heat flux. There is also the possibility of model physics being the source of error. The Garwood model may benefit from the inclusion of entrainment shear production. This entrainment may reduce the sensitivity of the model by preventing overly shallow mixed layers from persisting during the spring and summer.

The uncertainties in the heat flux correction fields are fairly large in the spring and summer. This limits tests of the ability of the model to predict anomalous ocean conditions during the spring and summer. It is recommended that the model's capability for spring and summer predictions be further examined.

The results of this study are generally encouraging. The most encouraging aspect is that a one-dimensional mixed layer model, such as the Garwood model, has the capability to predict anomalous conditions over long integration periods. The validity of a vertical mixing hypothesis for the formation and maintenance of cold anomalies in the North Pacific Ocean is also demonstrated. However, these predictions illustrate the crucial role of the surface heat and momentum fluxes in predicting the ocean mixed layer characteristics. The FNOC surface heat fluxes from the

hemispheric, primitive-equation model need to be improved, especially during the spring and summer. It is hoped that the new NOGAPS model at FNOC will provide these improved fields.

APPENDIX

GARWOOD MODEL

The Garwood (1977) model is a bulk or vertically integrated model for the oceanic planetary boundary layer (OPBL) or mixed layer. It is comprised of a closed system of seven equations.

The entrainment buoyancy flux equation,

$$-bw(-h) = \frac{m_4 \langle \overline{w^2} \rangle^{1/2} \langle \bar{E} \rangle}{h} \quad ; \qquad (1)$$

the horizontal component of turbulent kinetic energy,

$$\frac{1}{2} \frac{\partial}{\partial t} \left(h \langle \overline{u^2+v^2} \rangle \right) = m_3 u_* - \frac{bw(-h) |\Delta C|^2}{2\Delta B}$$

$$- m_2 (\langle \bar{E} \rangle - 3\langle \overline{w^2} \rangle) (\bar{E})^{1/2} - \frac{2m_1}{3} (\langle \bar{E} \rangle^{1/2} + \frac{m_5}{m_1} \overline{fh}) \langle \bar{E} \rangle ; \qquad (2)$$

the vertical component of turbulent kinetic energy,

$$\frac{1}{2} \frac{\partial}{\partial t} \left(h \langle \overline{w^2} \rangle \right) = \frac{1}{2} hbw(-h) - \frac{1}{2} hu_* b_*$$

$$+ m_2 (\langle \bar{E} \rangle^{1/2} - 3\langle \overline{w^2} \rangle) \langle \bar{E} \rangle^{1/2}$$

$$- \frac{m_1}{3} (\langle \bar{E} \rangle^{1/2} + \frac{m_5}{m_1} \overline{fh}) \langle \bar{E} \rangle \quad ; \qquad (3)$$

the mean buoyancy and mean momentum equations

$$h \frac{\partial \langle B \rangle}{\partial t} = \overline{bw}(-h) - \overline{bw}(0) + \frac{\alpha q}{\rho_o C_p} Q_o \quad , \tag{4}$$

$$h \frac{\partial \langle C \rangle}{\partial t} = \overline{cw}(-h) - \overline{cw}(0) + \text{if} \langle C \rangle h \quad ; \tag{5}$$

and the jump conditions at the bottom of the mixed layer (relating entrainment fluxes to the rate of deepending, and the changes in mean momentum and buoyancy at the base of the mixed layer),

$$-\overline{cw}(-h) = \Delta C \frac{\partial h}{\partial t} \quad , \qquad \text{and} \tag{6}$$

$$-\overline{bw}(-h) = \Delta B \frac{\partial h}{\partial t} \quad . \tag{7}$$

The time-dependent model forcing consists of the surface fluxes of momentum and buoyancy. In the present experiments, the contribution to the buoyancy due to salinity is neglected due to the lack of salinity data. Thus, the surface boundary conditions required to compute these fluxes are the total heat flux (Q_t), the solar radiation (Q_s) and the wind speed. Model outputs are the entrainment fluxes, turbulent kinetic energy, mixed layer depth and mixed layer temperature.

The mechanism Garwood (1977) envisioned in the initial destabilization of the interface (between the mixed layer

and the denser water beneath) and the resulting entrainment is a "local" Kevin-Helmholtz instability (also known as a Benjamin (1963) class C instability). This instability is triggered by shear across the interface provided by the local turbulent eddies. The shear due to mean flow only is assumed to make a minor contribution to the achievement of this critical shear value; thus (5) can be neglected. By using the equation for the flux Richardson number evaluated at $z = -h$,

$$Rf = \frac{\overline{bw}}{(\overline{uw}\,\frac{\partial U}{\partial t} - \overline{vw}\,\frac{\partial V}{\partial z})} \quad , \qquad (8)$$

and the jump conditions (6) and (7), one can find that shear production is a fixed fraction of buoyant damping in the entrainment zone. This zone may have a flux Richardson number greater than 1.0 and still possess enough turbulent kinetic energy for mixing to continue. In the Garwood model the shear production is only a secondary energy source for mixing, which can only be made available by entrainment initiated by another source. According to Garwood (1977), the most significant source of energy for mixing within an active entrainment zone is the convergence of flux of turbulent energy,

$$-\left(\frac{\partial}{\partial z}\right)\left[\,\overline{w\left(\frac{E}{2} - \frac{P}{\rho_o}\right)}\,\right] \quad .$$

Thus, the critical parameter to determine the entrainment rate is not Rf but the ratio, P, of buoyancy flux to the convergence of energy flux:

$$P = \frac{\overline{bw}}{\frac{\partial}{\partial z}\left[w \left(\frac{\bar{E}}{2} + \frac{p}{\rho_o}\right) \right]} \quad . \qquad (9)$$

The Garwood model uses separate vertical and horizontal equations (2) and (3) for the turbulent kinetic energy. This allows the convergence of turbulent kinetic energy flux to be included in the model. Mixed layer retreat occurs when the vertical component of turbulence is inadequate to transport heat, momentum and turbulence to the earlier depth of mixing.

As explained by Tennekes and Lumley (1972), the dissipation rate can be estimated from the rate at which large scale eddies supply energy to the smaller scale eddies. This gives rise to a dissipative time scale

$$t_\varepsilon = \frac{\langle \bar{E} \rangle}{\langle \varepsilon \rangle} \quad . \qquad (10)$$

Where the vertically integrated averaged turbulent kinetic energy is defined as

$$\langle \bar{E} \rangle = \frac{\overline{\langle u^2 \rangle}}{2} + \frac{\overline{\langle v^2 \rangle}}{2} + \frac{\overline{\langle w^2 \rangle}}{2} \quad , \qquad (11)$$

and the net rate of dissipation is

$$\langle \varepsilon \rangle = \int_{-h}^{0} \varepsilon \, dz = \int_{-h}^{0} \nu \frac{\partial u_i}{\partial x_j} \frac{\partial u_i}{\partial x_j} dz \quad . \qquad (12)$$

There are two time scales in the oceanic mixed layer. The first is a convective time scale formed from the turbulent velocity and the length scale of the large scale turbulent flow, $t_1 = h/u_*$. This scale can be thought of as the time required for a large turbulent eddy to overturn. The second scale is imposed by planetary rotation, $t_2 = 1/f$. In deeper boundary layers, planetary rotation turns the mean shear direction with depth and t_2 is the characteristic time scale of the resulting vortex stretching. In Garwood's model, both of these time scales are incorporated into the parameterization of the dissipation time scale, which is defined as

$$t_\varepsilon = t_1^{-1} + t_2^{-2} \quad . \qquad (13)$$

The parameterization of the absorption of solar radiation used in the Garwood model is described by Gallacher et al. (1983) as a double exponential model for which one of the extinction depths approaches zero. Computationally, this reduces to absorbing a fixed fraction (1-r) of the flux of solar radiation, Q_s, in the first

meter, and exponential absorption for depths greater than one meter.

Due to the process of Reynolds averaging in the turbulence equations and the subsequent formation of correlations (moments) of the fluctuating variables, there are more unknowns than equations. This problem can not be corrected at a fundamental level with additional equations since each new equation for a higher order of moment introduces additional yet higher order moments. To close the system of equations, the chosen highest moments must be parameterized in terms of lower order moments and mean values. The Garwood model employs a second order closure scheme; thus the triple correlations (second order moments) are parameterized in terms of zeroth order moments (mean values) and first order moments (autocorrelations and cross correlations).

The process of parameterizing the high order moments generates constants of proportionality. In the set (1)-(3), m_1 through m_5 are constants of proportionality which must be determined from geophysical data. The values used in this study were $m_3 = 2.0$, $p_1 = m_4/m_1 = 1.0$, $p_2 = m_2/m_1 = 1.0$, $p_3 = m_5/m_1 = 0.5$, $r = 0.5$ and $\gamma = 0.001$. The critical constants are m_3, p_3, r and γ. In order for the model to produce accurate forecasts it must be able to simulate the fall deepening, which is particularly sensitive to m_3; the winter maximum mixed layer depth, which is sensitive to p_3; the spring transition, which depends on the interaction of

m_3 and the surface heat fluxes; and the summer maximum mixed layer temperature, which depends on r and γ. The values of the critical constants listed above were empirically determined by Gallacher et al. (1983) to be as consistent as possible with the atmospheric forcing used in this study.

LIST OF REFERENCES

Barnett, T.P., and J.D. Ott, 1976: Average features of the subsurface thermal field in the Central Pacific. Scripps Institute of Oceanography Reference Series 76-20, 13 pp.

Benjamin, T.B., 1963: The threefold classification of unstable disturbances in flexible surfaces bounding inviscid flows. J. Fluid Mech., 16, 435-450.

Bernstein, R.L., and W.B. White, 1977: Zonal variability in the baroclinic eddy field of the mid-latitude North Pacific. J. Phys. Oceanogr. 7, 123-126.

Budd, B.W., 1980: Prediction of the spring transition and related sea-surface temperature anomalies. M.S. Thesis, Naval Postgraduate School, 95 pp.

Elbsberry, R.L., 1983: A synoptic case study analysis of the ocean temperature anomalies in the Central Pacific region during 1976-79. Unpublished manuscript, Naval Postgraduate School Tech. Rep. NPS 63-83-00, 50 pp.

_____, P.C. Gallacher, A.A. Bird, and R.W. Garwood, Jr., 1982: Deriving corrections to FNOC surface heat flux estimates for use in North Pacific Ocean predictions. Naval Postgraduate School Tech. Rep. NPS 63-82-005, 67 pp.

_____, P.C. Gallacher, and R.W. Garwood, Jr., 1979: One-dimensional model predictions of ocean temperature anomalies during fall 1976. Naval Postgraduate School Tech. Rep. NPS 63-79-003, 30 pp.

_____, and R.W. Garwood, Jr., 1978: Sea-surface temperature anomaly generation in relation to atmospheric storms. Bull. Amer. Meteor. Soc., 59, 786-789.

_____, and R.W. Garwood, Jr., 1980: Numerical ocean prediction models--goal for the 1980's. Bull. Amer. Meteor. Soc., 61, 1556-1566.

_____, and S.D. Raney, 1978: Sea-surface temperature response to variations in atmospheric wind forcing. J. Phys. Oceanogr., 8, 881-887.

Gallacher, P.C., 1979: Preparation of ocean model forcing parameters from FNWC atmospheric analysis and model predictions. Naval Postgraduate School Tech. Rep. NPS 63-79-005, 24 pp.

_____, A.A. Bird, R.W. Garwood, Jr. and R.L. Elsberry, 1983: A determination of the constants for a second order closure turbulence model from geophysical data. Naval Postgraduate School Tech. Rep. NPS 63-83-004, 35 pp.

Garwood, R.W. Jr., 1977: An oceanic mixed layer model capable of simulating cyclic states. J. Phys. Oceanogr., 7, 455-468.

Haney, R.L., 1980: A numerical case study of the development of large-scale thermal anomalies in the central North Pacific Ocean. J. Phys. Oceanogr., 10, 541-556.

Kraus, W., 1981: The erosion of a thermocline. J. Phys. Oceanogr., 11, 415-433.

Martin, P.J., 1982: Mixed-layer stimulation of bouy observations taken during Hurricane Eloise. J. Geophys. Res., 87, 409-427.

Martin, P.J., 1983: Simulation of the mixed layer at OWS November and Papa with several models. Unpublished manuscript, Navy Oceanographic Research and Development Activity, 46 pp.

Price, J.F., 1981: On the upper ocean response to a moving hurricane. J. Phys. Oceanogr., 11, 153-175.

Steiner, E.F., 1981: One-dimensional model predictions of upper ocean temperature changes between San Francisco and Hawaii. M.S. Thesis, Naval Postgraduate School, 79 pp.

Tennekes, H., and J.L. Lumley, 1972: A First Course in Turbulence. MIT Press, Cambridge, Massachusetts, 300 pp.

Tully, J.P., and L.F. Giovando, 1963: Seasonal temperature structure in the eastern subarctic Pacific Ocean. Roy. Soc. Can. Spec. Publ., 5, 10-36.

White, W.B., and R.L. Bernstein, 1979: Design of an oceanographic network in the midlatitude North Pacific. J. Phys. Oceanogr., 9, 592-606.

_____, R. Bernstein, G. McNally, S. Pazen and R. Dickenson, 1980: The thermocline response to transient atmospheric forcing in the interior North Pacific 1976-78. J. Phys. Oceanogr., 10, 372-384.

INITIAL DISTRIBUTION LIST

		No. Copies
1.	Defense Technical Information Center Cameron Station Alexandria, VA 22314	2
2.	Library, Code 0142 Naval Postgraduate School Monterey, CA 93943	2
3.	Professor Robert J. Renard, Code 63Rd Department of Meteorology Naval Postgraduate School Monterey, CA 93943	1
4.	Professor Christopher N. K. Mooers, Code 68Mr Department of Oceanography Naval Postgraduate School Monterey, CA 93943	1
5.	Professor Russell L. Elsberry, Code 63Es Department of Meteorology Naval Postgraduate School Monterey, CA 93943	5
6.	Mr. Patrick C. Gallacher, Code 63 Department of Meteorology Naval Postgraduate School Monterey, CA 93943	1
7.	Professor Roland W. Garwood, Code 68Gd Department of Oceanography Naval Postgraduate School Monterey, CA 93943	1
8.	LCDR Gary L. Stringer U.S. Navy Oceanography Command Center Box 12, COMNAVMARIANAS FPO San Francisco, CA 96630	2
9.	Directory Naval Oceanography Division Naval Observatory 34th and Massachusetts Avenue NW Washington, D.C. 20390	1
10.	Commander Naval Oceanography Command NSTL Station Bay St. Louis, MS 39522	1

11. Commanding Officer 1
Naval Oceanographic Office
NSTL Station
Bay St. Louis, MS 39522

12. Commanding Officer 1
Fleet Numerical Oceanography Center
Monterey, CA 93943

13. Commanding Officer 1
Naval Ocean Research and Development Activity
NSTL Station
Bay St. Louis, MS 39522

14. Commanding Officer 1
Naval Environmental Prediction Research
Facility
Monterey, CA 93943

15. Chairman, Oceanography Department 1
U.S. Naval Academy
Annapolis, MD 21402

16. Chief of Naval Research 1
800 N. Quincy Street
Arlington, VA 22217

17. Office of Naval Research (Code 420) 1
Naval Ocean Research and Development Activity
800 N. Quincy Street
Arlington, VA 22217

18. Scientific Liaison Office 1
Office of Naval Research
Scripps Institution of Oceanography
La Jolla, CA 92037

19. Library 1
Scripps Institution of Oceanography
P.O. Box 2367
La Jolla, CA 92037

20. Professor Robert L. Haney, Code 63Hy 1
Department of Meteorology
Naval Postgraduate School
Monterey, CA 93943

21. Library 1
Department of Oceanography
University of Washington
Seattle, WA 98105

22. Library 1
School of Oceanography
Oregon State University
Corvallis, OR 97331

23. Commander 1
Oceanographic Systems Pacific
Box 1390
Pearl Harbor, HI 96860